EPFL

Thèse n° 10 531

Bootstrapping amplitudes of scalar particles

Présentée le 4 mars 2024

Faculté des sciences de base
Laboratoire de théorie des champs et des cordes
Programme doctoral en physique

pour l'obtention du grade de Docteur ès Sciences

par

Jan Krzysztof MARUCHA

Acceptée sur proposition du jury

Prof. F. Mila, président du jury
Prof. J. M. Augusto Penedones Fernandes, directeur de thèse
Dr A. Zhiboedov, rapporteur
Prof. F. Riva, rapporteur
Prof. V. Gorbenko, rapporteur

École
polytechnique
fédérale
de Lausanne

2024

Abstract

Quantum Field Theories are a central object of interest of modern physics, describing fundamental interactions of matter. However, current methods give limited insight into strongly coupling theories. S-matrix bootstrap program, described in this thesis, aims to provide insight into these strongly coupled theories, by mapping the space of consistent scattering amplitudes that obey properties imposed by unitarity, Lorentz invariance and causality. This thesis aims to outline the basic principles of the program, along with steps to construct numerical S-matrix bootstrap experiment, presents the `Wolfram Mathematica` library developed by author to automatize parts of the procedure that are shared among experiments, and finally discusses the research on 4d conformal field theories, which, by relevant deformation, can be turned into interacting QFTs, in which bootstrapping the scattering amplitudes allowed finding lower bounds on a-anomaly coefficient in the investigated cases.

Abstrakt

Quantenfeldtheorien sind ein zentraler Gegenstand des Interesses der modernen Physik und beschreiben grundlegende Wechselwirkungen der Materie. Aktuelle Methoden geben jedoch nur begrenzte Einblicke in stark koppelnde Theorien. Das in dieser Arbeit beschriebene S-Matrix-Bootstrap-Programm soll Einblick in diese stark gekoppelten Theorien geben, indem es den Raum konsistenter Streuamplituden abbildet, die den durch Unitarität, Lorentz-Invarianz und Kausalität auferlegten Eigenschaften gehorchen. Ziel dieser Arbeit ist es, die Grundprinzipien des Programms zusammen mit Schritten zum Aufbau eines numerischen S-Matrix-Bootstrap-Experiments zu skizzieren, die vom Autor entwickelte `Wolfram Mathematica`-Bibliothek vorzustellen, um Teile des Verfahrens zu automatisieren, die von Experimenten gemeinsam genutzt werden, und schließlich diskutiert die Forschung zu 4d-konformen Feldtheorien, die durch relevante Verformung in interagierende QFTs umgewandelt werden können, wobei das Bootstrapping der Streuamplituden es ermöglichte, in den untersuchten Fällen Untergrenzen für den a-Anomaliekoeffizienten zu finden.

Contents

Chapter 1

Introduction

As the introductions of PhD theses are usually overly poetic, I'd like to start with the least original phrase – since the beginning of the civilization understanding the nature was not only beneficial to our survival as a species, but for some weird specimens of *H. sapiens var sapiens* it was interesting on its own.

With such set of features given to me by socio-genetic roulette/the higher power of preference[1], I discovered that some people before me tried to explore the rules of nature[1, 2], some have been quite successful[3], and most of them were inspiring.

My favorite part of all the giants and dwarves standing on giants, and other people standing at each other (named later *the scientific community*), were human beings that thought mathematics is the promising way of describing the universe around. With inevitable realization that the complex stuff like humans or fungi is a bit too complicated for now, *physics* was born, a science that uses maths to predict future of (mostly) inanimate things.

Via smashing things with other things[2], scientists unveiled more and more fundamental building blocks for the reality, with progressively weirder and weirder maths behind them, to finally realize the reality is not really made of building blocks (quanta), but rather quantum fields, which could be thought as a fabric of the reality, and all what we considered particles is in fact this very fabric of reality vibrating in quantum excitations. Nevertheless, the name "particle physics" stuck. The (even more weird) mathematical toolkit to describe the quantum fields is named Quantum Field Theory (QFT) and is quite important part of the modern physics, and a very important part of the thesis presented.

QFT, in its all mathematical complexity, answers some questions, and creates even more questions. While quite neatly predicting many experimental results, like 'if I smash electron with another electron, what is the stuff that falls out', or 'why the gyromagnetic ratio is $-2.002319\ldots$, while the first look suggests it's -2'[3], it is also full of numbers that are unknown to have a particular reason to have such values (Standard Model has 19 free parameters, that can

[1] Reader shall choose relevant, based on metaphysical beliefs.

[2] Only smashing inanimate things is considered science, smashing animate things is called 'violence' and shall be avoided.

[3] The semiclassical computation provides $g_e = -2$, but the 1-loop perturbation theory provides $g_e = -2(1 + \alpha/\pi) = -2.002319\ldots$

only be found experimentally, and the relation between this fundamental theory and the effective interaction for emerging particles, like pions and protons introduces much more stuff to measure), full of numbers that have no meaning with respect to experiments (non-observable quantities, like ones occurring in renormalization), and quite rich in problems with high energy (UV) completion (where above some scale the physical predictions behave like a glitchy video game[4]).

As a final touch, the firmest way of doing QFT prediction is perturbation theory, which provide results for some small[4] range of parameters around simple "free theories" that the humankind knows how to solve, with a rather limited insight into "strong coupling", where the parameters are considered large.

With a rather complicated relation between strongly coupling theories and our ability to compute anything in them, the scattering theory was born, where the complicated mathematics of Quantum Field Theory was replaced by complex[5] mathematics of scattering amplitudes, quantities that represent the outcome of a scattering experiment (smashing things with things, mankind's most established way of understanding fundamental physics). With a scattering amplitude $\mathcal{S}_{ab\to cd}$ being the probability amplitude of transition between the state ab and cd ("we smashed a with b and noted c and d came out"), not only this is the most observable of all observable quantities, without any nasty 'renormalization scales' and other decoys, but also it doesn't introduce any problems with strong coupling (in perturbative QFT $\mathcal{S}_{ab\to cd}$ is proportional to a small coupling parameter α in some power, here it's just a number), but it doesn't possess any inherent problems with high energies (the initial state are still particles, just smashed harder at each other).

The collective smartness of many scientists allowed to establish several analytic properties of amplitude $\mathcal{S}$. Merging very fundamental properties expected from the theory describing our world, like causality (which means events are only influenced by past events that were close enough for light signal to reach former), unitarity (the probabilities are not negative and better if they would sum up to 1), and Lorentz invariance (the laws of physics are independent of frame of reference) provides the analytic structure of quantity $\mathcal{S}$ if the variables used to describe it are taken to be complex numbers[6]. A review of these properties will be given in the next chapter, however, this moment desperately calls for a (very unmotivated for now) example.

Considering a general physical theory of a single scalar field of mass m, and no additional assumption, it may be concluded that

- The scattering amplitude of 2-to-2 particles $\mathcal{S}$ is dependent on Mandelstam invariants s, t, with $s = -(p_1^\mu + p_2^\mu)^2$, $t = -(p_1^\mu - p_3^\mu)^2$
- This rather weird distributional quantity may be decomposed into $\mathcal{S} = \mathbb{1} + i(2\pi)^4\delta^{(4)}(p_1 + p_2 - p_3 - p_4)T(s,t)$
- $T(s,t)$ is a function. Moreover, it's a real and analytic function in upper complex plane, both in s and t, with $T^*(s + i\epsilon, t + i\epsilon) = T(s - i\epsilon, t - i\epsilon)$

[4]The range of convergence of such perturbative series is exactly 0, which makes the author scratch his head quite hard.

[5]$c = a + bi$

[6]So long, "it's all physical"

- $T(s,t)$ has a number of branch cuts, corresponding to energies required to produce $n \geq 2$ outgoing particles, starting at $s = 4m^2$, $s = 9m^2$, $s = 16m^2$ and so on.
- $T(s,t)$ may have a pole at m^2, which exist due to 1-particle state of energy m.
- If the theory describing this physical system obeys LSZ reduction formula (relating scattering amplitude to 4-point function), crossing relation $T(s,t) = T(t,u) = T(4m^2 - s - t, t)$ holds. Therefore, the analytic structure in t is similar.[7]

Summarizing these, now very unfounded, claims one gets a picture of analytic structure of T in the complex plane

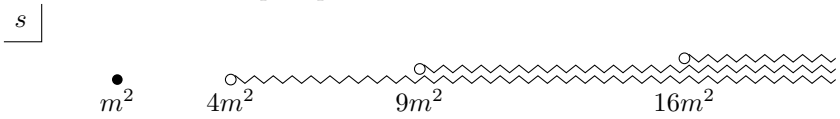

One can ask now "what is the space of functions that have this analytic structure". This is exactly the question asked by $\mathcal{S}$-matrix bootstrap program.

With a minimal amount of the assumptions, so analyticity, as described above, and unitarity (the conservation of non-negative probabilities), one can create an ansatz (a parametrized educated guess) for the function $T(s,t)$, and explore the space of the parameters that do not violate these assumptions. That leads to a beautiful dream, a *dream of the bootstrapper*, in which all physical quantities are like they are because *they are the only logical choice*, with others leading to inconsistent results.

Quite a few projects has shown power of this approach, from bootstrapping pion scattering by imposing real-world resonances and chiral zeroes [5], effective field theories resulting from large N_c QFTs [6, 7], photon-like particles [8], particles to probe a-anomaly [9, 10] (presented in this thesis), or c-anomaly [11], or supersymmetric theories [12].

Obviously, creating an amplitude ansatz with couple hundreds of free parameters and checking for which combinations obey unitarity is a rather tedious task, however, for the tedious tasks humanity has created the devices that know no tiredness nor boredom[8], but are absolutely dumb and do only exactly what they are exactly told to[9].

Computers, which massively accelerated the research, productivity and the spread of conspiracy theories, can now be used to give $\mathcal{S}$-matrix bootstrap program a boost which was unthinkable (by both scientists and computers alike) 60 years ago, when analytic properties of scattering amplitudes grabbed the attention the first time[13].

The research presented here is in great part done for computers and done with the help of computers. The first chapter outlines the first principles of S-matrix as created by biological brains, from the initial step of thinking 'there are particles' (Wigner construction of $ISO(1,3)$ representations), to 'there were two particles in the past, how to say that there will be two (maybe different)

[7] It's not obvious if crossing relations can be derived from QFT axioms. Rigorous texts often postulate crossing as an axiom.

[8] Unlike PhD candidates

[9] Sometimes like PhD candidates

particles later?' (construction of scattering operators and amplitudes), via 'each particle pair is pretty much colliding head on' (Center of Mass frame), through 'this weird diagram above is actually a good idea' (analyticity and crossing), then back to 'angular momentum is conserved, and that pretty much ends the topic how to write unitarity' (Partial Waves and Unitarity), 'how to guess the amplitude, at least up to several hundred free parameters' and 'how to write that into a form our dear computer-savvy[14] friends know how to solve'.

The second chapter is a bit more personal, as it describes my beloved child[10], the SMatrixToolkit, which facilitates setting up S-matrix numerical computations, via using symbolic programming software `Wolfram Mathematica`, to go through as many steps of chapter 2 as it is possible to do by a machine. Derivation of partial waves, construction of ansatze from standard building blocks, putting the precomputed integrals together – these steps have been programmatically solved for scattering scalar particles in 4 dimensions, and with additional efforts can be expended to cover the cases of $d \geq 3$ and spinning particles. It comes with an example to reproduce a classic S-matrix bootstrap experiment[15], and more examples are provided in the repository.

The third chapter describes effects of unholy union of the man and the machine. There I describe how I and my collaborators used S-matrix bootstrap to probe the landscape of 4d conformal field theories (CFTs). The numerical experiments introduced bounds on a-anomaly coefficient of CFTs containing at least a real scalar field. These results suggest existence of unknown $a \leq \frac{1}{5760\pi^2}$ CFTs, with different lower, non-zero bounds on a depending on the symmetries of the problem.

[10] Now orphaned and waiting for adoption.

Chapter 2

S-matrix bootstrap

In this paper the author adapts convention of mostly positive Minkowski metric $\eta_{\mu\nu} = \text{diag}\{-1, 1, 1, 1\}$ and Hermitian generators of Lie groups, in particular Poincaré group $ISO(1, 3)$

2.1 States and amplitudes

In general flat-space QFT a general state can be decomposed into irreducible representations of Poincaré group, with a basis of

$$|c, \vec{p}; \ell, \lambda; \gamma\rangle \tag{2.1}$$

with c being 'center of mass energy', $\vec{p}$ being representations weight under spatial translation (with weight under the time translation being p_0, $p_0^2 = m^2 + \vec{p}^2$), and ℓ, λ being representations of corresponding Lorentz little group (after fixing weights under translations). γ is a theory-dependent set of labels describing the state (e.g. electric charge, particle flavor).

In such basis, the arbitrary state can be described as a transformation of 'zero-momentum state', using boosts (generated by K_i) and rotations (generated by J_i).

$$|c, \vec{p}; \ell, \lambda; \gamma\rangle = e^{-i\phi J_3} e^{-i\theta J_2} e^{+i\phi J_3} e^{i\eta K_3} \left|m, \vec{0}; \ell, \lambda; \gamma\right\rangle \tag{2.2}$$

That results in overall momentum

$$\vec{p} = (p \sin\theta \cos\phi, p \sin\theta \sin\phi, p \cos\theta)\,, \quad p = m^2 \sinh\eta \tag{2.3}$$

In this paper, the underlying QFT will consist only on scalar particles $\phi_1, \phi_2, \ldots$, which give raise to 1 Particle States (1-PS), that are characterized by 'mass'[1], $c = m_i$, and zero spin (that's the 'scalar' part), $\ell = 0$ and $\lambda = 0$. To describe 1-PS, a shorthand is used

$$|\phi_i, \vec{p}\rangle \equiv |m_i, \vec{p}; 0, 0, \gamma_i\rangle \tag{2.4}$$

with (conventional) relativistic normalization of

$$\langle \phi_a, \vec{p}_i | \phi_b, \vec{p}_j \rangle = 2\sqrt{m_a^2 + \vec{p}_i^2}\,(2\pi)^2\,\delta^{(3)}(\vec{p}_i - \vec{p}_j)\delta_{ab} \tag{2.5}$$

[1] Related to Casimir of the Poincaré algebra, $m^2 = -P^\mu P_\mu$

One defines 2 particle states (2-PS) as tensor product of two 1-PS, which is

$$|\phi_a, \phi_b\rangle = |\phi_a, \vec{p}_a\rangle \otimes |\phi_b, \vec{p}_b\rangle \tag{2.6}$$

if the particles are different, or

$$|\phi_a, \phi_a\rangle = \frac{1}{\sqrt{2}}\big(|\phi_a, \vec{p}_a\rangle \otimes |\phi_b, \vec{p}_b\rangle + |\phi_s, \vec{p}_b\rangle \otimes |\phi_a, \vec{p}_a\rangle \big) \tag{2.7}$$

if the particles are the same, to account for Bose symmetry.

The weights under spatial translation

$$\vec{P}\,|\phi_a, \phi_b\rangle = (\vec{p}_a + \vec{p}_b)\,|\phi_a, \phi_b\rangle \tag{2.8}$$

and energy

$$H\,|\phi_a, \phi_b\rangle = \left(\sqrt{m_a^2 + p_a^2} + \sqrt{m_b^2 + p_b^2}\right)|\phi_a, \phi_b\rangle \tag{2.9}$$

simply follow from Abelian nature of $\mathbb{R}^{1,3}$ subgroup, and the normalization is inherited from normalization of 1-PS

$$\begin{aligned}\langle \phi_a, \phi_b | \phi_c, \phi_d\rangle &= 4\,(2\pi)^6 \sqrt{(m_a^2 + p_a^2)(m_b^2 + p_b^2)}\ \times \\ \times \left(\delta^{(3)}(\vec{p}_a - \vec{p}_c)\delta^{(3)}(\vec{p}_b - \vec{p}_d)\delta_{ac}\delta_{bd} + \delta^{(3)}(\vec{p}_a - \vec{p}_d)\delta^{(3)}(\vec{p}_b - \vec{p}_c)\delta_{ad}\delta_{bc}\right)\end{aligned} \tag{2.10}$$

To describe scattering, two different 2-PS are considered, so called *in-state*, before scattering event, at time $t = -\infty$:

$$|\phi_a, \phi_b\rangle_{\text{in}} \tag{2.11}$$

and *out-state*, after the event, at time $t = +\infty$

$$|\phi_c, \phi_d\rangle_{\text{out}} \tag{2.12}$$

where operator translating one to the other can be written as

$$\hat{\mathcal{S}}\,|\phi_a, \phi_b\rangle_{\text{in}} = |\Phi\rangle_{\text{out}} \tag{2.13}$$

where $|\Phi\rangle_{\text{out}}$ is a general out-state that may consist of many-particle states.

The main focus, however, will be the $2 \to 2$ particle scattering. The related matrix elements are

$$\mathcal{S}_{ab\to cd} \times (2\pi)^4\,\delta^{(4)}\Big((p_a + p_b) - (p_c + p_d)\Big) \equiv {}_{\text{out}}\langle \phi_c, \phi_d | \phi_a, \phi_b\rangle_{\text{in}} \tag{2.14}$$

with four-vectors momenta 4-vectors defined as $p_a^\mu = (\sqrt{m_a^2 + |\vec{p}_a|^2},\ \vec{p}_a)$, and the delta function resulting from (2.8)(2.9)

2.2 Mandelstam invariants

Poincare invariance implies, that the matrix element (2.14) stays the same after Lorentz transformations, in particular

$$\begin{aligned} |\phi'_a, \phi'_b\rangle_{\text{in}} &= e^{i\eta_i K_i} |\phi_a, \phi_b\rangle_{\text{in}} \\ |\phi'_c, \phi'_c\rangle_{\text{out}} &= e^{i\eta_i K_i} |\phi_c, \phi_c\rangle_{\text{out}} \ . \end{aligned} \tag{2.15}$$

This invariance,

$${}_{\text{out}}\langle\phi_c, \phi_d|\phi_a, \phi_b\rangle_{\text{in}} = {}_{\text{out}}\langle\phi'_c, \phi'_d|\phi'_a, \phi'_b\rangle_{\text{in}} \tag{2.16}$$

implies the $\mathcal{S}$-matrix, which, first, could be thought as a general function of ingoing and out-going momenta, (along with some labels), depends only on some combinations of these.

For small values of η_i (introducing them as vector $\vec{\eta}$) the resulting in/out-going momenta may be computed to be

$$(p'_i)^\mu = \begin{pmatrix} p_i^0 \\ \vec{p}_i \end{pmatrix} + \begin{pmatrix} \vec{\eta}\cdot\vec{p}_i \\ \vec{\eta}\ p_i^0 \end{pmatrix} + \mathcal{O}(\vec{\eta}^2) \tag{2.17}$$

With these in mind, one sees that may be computed to be

$$\left((p'_i)^\mu - (p'_j)^\mu\right) = \begin{pmatrix} p_i^0 - p_j^0 \\ \vec{p}_i - \vec{p}_j \end{pmatrix} + \begin{pmatrix} \vec{\eta}\cdot(\vec{p}_i - \vec{p}_j) \\ \vec{\eta}\ \ (p_i^0 - p_j^0) \end{pmatrix} + \mathcal{O}(\vec{\eta}^2) \tag{2.18}$$

It makes it not very difficult to observe that values

$$\left((p'_i)^\mu - (p'_j)^\mu\right)^2 = \begin{pmatrix} p_i^0 - p_j^0 \\ \vec{p}_i - \vec{p}_j \end{pmatrix}^2 + \mathcal{O}(\vec{\eta}^2) \tag{2.19}$$

are invariant under this Lorentz boost.

Keeping in mind the momentum conservation encapsulated in (2.14), one can form invariants

$$\begin{aligned} t &= -\left(p_a^\mu - p_c^\mu\right)^2 = -\left(p_b^\mu - p_d^\mu\right)^2 \\ u &= -\left(p_a^\mu - p_d^\mu\right)^2 = -\left(p_b^\mu - p_c^\mu\right)^2 \end{aligned} \tag{2.20}$$

and

$$\begin{aligned} . &= -\left(p_a^\mu - p_b^\mu\right)^2 \\ . &= -\left(p_c^\mu - p_d^\mu\right)^2 \end{aligned} \tag{2.21}$$

where these two are so useless they never even deserved to be named by the scientific community.

With simple argument of counting, one can conclude, that, while 4 3-momenta have $4 \cdot 3 = 12$ free variables (p_0 is fixed by 1PS Casimir), the conservation of 4-momentum brings that down to 8.

Then, by using Lorentz boosts ($e^{i\eta_i K_i}$) one can get rid of 3 (via boosting the system to *zero momentum frame*), bringing number of parameters down to 5.

With leftover rotations ($e^{i\eta_i J_i}$), one can fix in-momenta (to be described in the next section), and some part of out-momenta, and therefore, a scattering event needs only two numbers ($5 - 3 = 2$) to be defined.

Therefore, the values t and u are enough degrees of freedom for parametrizing $2 \to 2$ particle scattering[2].

However, it's useful to introduce another quantity[3]

$$s = -\left(p_a^\mu + p_b^\mu\right)^2 = -\left(p_c^\mu + p_d^\mu\right)^2 \tag{2.22}$$

which may be easily computed to be

$$s = m_a^2 + m_b^2 + m_c^2 + m_d^2 - t - u \tag{2.23}$$

From now on, the $\mathcal{S}$-matrix will be described in terms of variables s, t, u (keeping in mind one of these is redundant via $s + t + u = \sum m_i^2$).

2.3 Center of mass frame

Keeping in mind the construction (2.2), one can similarly invert the relation to put 2-PS instate into *zero-momentum frame*, more often called Center of Mass (CoM) frame, due to its classical mechanics origin. The state, constructed by this transformation, can be described in terms of 4-momenta

$$\begin{aligned} p_a^\mu &= \left\{\sqrt{|p|^2 + m_a^2}, +|p|\sin\theta'\cos\varphi', +|p|\sin\theta'\sin\varphi', +|p|\cos\theta'\right\} \\ p_b^\mu &= \left\{\sqrt{|p|^2 + m_b^2}, -|p|\sin\theta'\cos\varphi', -|p|\sin\theta'\sin\varphi', -|p|\cos\theta'\right\} \end{aligned} \tag{2.24}$$

The 2-PS state of these momenta can still be rotated by

$$|\phi_a, \phi_b\rangle_{\text{in}}^{\text{COM}} = e^{-i\theta' J_2} e^{-i\phi' J_3} |\phi_a, \phi_b\rangle_{\text{in}} \tag{2.25}$$

resulting in very simple in-momenta

$$\begin{aligned} p_a^\mu &= \left\{\sqrt{|p|^2 + m_a^2}, 0, 0, +|p|\right\} \\ p_b^\mu &= \left\{\sqrt{|p|^2 + m_b^2}, 0, 0, -|p|\right\} \end{aligned} \tag{2.26}$$

and the state is still invariant under J_3 rotations. Using this leftover rotation, the general CoM out-state

$$\begin{aligned} p_c^\mu &= \left\{\sqrt{|p'|^2 + m_c^2}, +|p'|\sin\theta\cos\varphi, +|p'|\sin\theta\sin\varphi, +|p'|\cos\theta\right\} \\ p_d^\mu &= \left\{\sqrt{|p'|^2 + m_d^2}, -|p'|\sin\theta\cos\varphi, -|p'|\sin\theta\sin\varphi, -|p'|\cos\theta\right\} \end{aligned} \tag{2.27}$$

can be fixed to almost as simple

$$\begin{aligned} p_c^\mu &= \left\{\sqrt{|p'|^2 + m_c^2}, 0, +|p'|\sin\theta, +|p'|\cos\theta\right\} \\ p_d^\mu &= \left\{\sqrt{|p'|^2 + m_d^2}, 0, -|p'|\sin\theta, -|p'|\cos\theta\right\} \end{aligned} \tag{2.28}$$

[2]One can try to form another invariants to describe scattering of more particles. This is difficult. For $\mathcal{S}$-matrix bootstrap it means 'impractical'. And for computers it means 'impossible'

[3]Note that s depends on in-state or out-state only.

Note that via rotation by π in J_3 the sign of $\sin\theta$ may be flipped, and the in and out momenta are related by

$$s = -\left(\sqrt{|p|^2 + m_a^2} + \sqrt{|p|^2 + m_b^2}\right)^2 = -\left(\sqrt{|p'|^2 + m_c^2} + \sqrt{|p'|^2 + m_d^2}\right)^2 \tag{2.29}$$

Which allows to argue that $\mathcal{S}$-matrix is sufficiently defined as a function of in-momentum $|p|$ and scattering angle $\cos\theta$.

Introducing shorthand for zeroth components of 4-momentuma

$$\begin{aligned} E_a &= \sqrt{m_a^2 + |p|^2} \quad E_b = \sqrt{m_b^2 + |p|^2} \\ E_c &= \sqrt{m_c^2 + |p'|^2} \quad E_d = \sqrt{m_d^2 + |p'|^2} \end{aligned} \tag{2.30}$$

one can relate COM momentum and angle to Mandelstam invariants

$$\begin{aligned} &s \equiv (E_a + E_b)^2 = (E_c + E_d)^2 \ , \\ &t \equiv m_a^2 + m_c^2 - 2E_aE_c + 2|p||p'|\cos\theta \ , \\ &u \equiv m_a^2 + m_d^2 - 2E_aE_d - 2|p||p'|\cos\theta \end{aligned} \tag{2.31}$$

To complete the picture, one can use s and $\cos\theta$ to parametrize scattering[4], with momenta being dependent as

$$|p| = \frac{\mathcal{L}_{ab}(s)}{2\sqrt{s}}, \quad |p'| = \frac{\mathcal{L}_{cd}(s)}{2\sqrt{s}} \tag{2.32}$$

where quantity

$$\mathcal{L}_{ij} = \sqrt{\left(s - (m_i - m_j)^2\right)\left(s - (m_i + m_j)^2\right)} \tag{2.33}$$

will be useful shorthand not only here, but also in the later sections.

To conclude that section, one can express the Mandelstam variables t and u from (2.31) in terms of s and $\cos\theta$. As the details are tedious, just stating the answer shall be enough[5]:

$$\begin{aligned} t &= \frac{1}{2s}\left(\Omega^2 - s^2 + \cos\theta\mathcal{L}_{ab}\mathcal{L}_{cd} - \Delta\right) \\ u &= \frac{1}{2s}\left(\Omega^2 - s^2 - \cos\theta\mathcal{L}_{ab}\mathcal{L}_{cd} + \Delta\right) \\ &\text{with} \quad \Omega^2 = s + t + u = m_a^2 + m_b^2 + m_c^2 + m_d^2 \\ &\qquad \Delta = (m_a^2 - m_b^2)(m_c^2 - m_d^2) \end{aligned} \tag{2.34}$$

2.4 Analyticity and crossing

As shown previously, the S-matrix can be described using so-called Mandelstam invariants:

$$s \equiv -(p_a + p_b)^2 \,, \quad t \equiv -(p_a - p_c)^2 \,, \quad u \equiv -(p_a - p_d)^2 \tag{2.35}$$

[4]Careful reader may think "what about $|p|$ that doesn't correspond to any $|p'|$" – yes, this is the exciting part and foreshadowing of the next chapter.

[5]With $E_a = \frac{s - m_a^2 + m_b^2}{2\sqrt{s}}$ and a bit of symbolic programming it can be done with tolerable amount of suffering.

where the third one is dependent on the previous two via

$$s + t + u = m_a^2 + m_b^2 + m_c^2 + m_d^2 \tag{2.36}$$

Therefore, the definition in (2.14) shall rather be presented as

$$\begin{aligned} \mathcal{S}_{ab\to cd}(s,t) \times (2\pi)^4 \delta^{(4)}(p) &\equiv {}_{\text{out}}\langle \phi_c, \phi_d | \phi_a, \phi_b \rangle_{\text{in}} \\ &= \langle \phi_c, \phi_d | \hat{S} | \phi_a, \phi_b \rangle \end{aligned} \tag{2.37}$$

with $\delta^{(4)}(p)$ being shorthand for 4-momentum conservation.

It's useful to separate the trivial part of scattering from the rest. For matrix elements it is

$$\begin{aligned} i\mathcal{T}_{ab\to cd}(s,t) \times (2\pi)^4 \delta^{(4)}(p) &\equiv {}_{\text{out}}\langle \phi_c, \phi_d | \phi_a, \phi_b \rangle_{\text{in}} - {}_{\text{in}}\langle \phi_c, \phi_d | \phi_a, \phi_b \rangle_{\text{in}} \\ &= \langle \phi_c, \phi_d | \hat{S} - \mathbb{1} | \phi_a, \phi_b \rangle \end{aligned} \tag{2.38}$$

with $\hat{S} = \mathbb{1} + i\hat{T}$.

This section would present analytic properties of function $\mathcal{T}_{ab\to cd}(s,t)$ needed for S-matrix bootstrap. The reader should be aware that properties presented in this section barely scratch the surface of the topic of analyticity, with many papers[16–18] and even books[13] written.

For numerical S-matrix bootstrap program, two properties are needed, real analyticity

$$\mathcal{T}_{ab\to cd}(s^*, t^*) = \mathcal{T}^*_{cd\to ab}(s,t) \tag{2.39}$$

and crossing property [19]

$$\mathcal{T}_{ab\to cd}(s,t) = \mathcal{T}_{\bar{c}b\to\bar{a}d}(t,s) \tag{2.40}$$

Note that this relation, and fact that in-states or out-states may be relabeled

$$\mathcal{T}_{ab\to cd}(s,t) = \mathcal{T}_{ba\to cd}(s,u) = \mathcal{T}_{ab\to dc}(s,u) \tag{2.41}$$

implies

$$\mathcal{T}_{ab\to cd}(s,t) = \mathcal{T}_{\bar{c}\bar{d}\to\bar{a}\bar{b}}(s,t) \tag{2.42}$$

This can be thought as a consequence of CPT invariance. In case of elastic scattering, it follows from Lorentz invariance that

$$\mathcal{T}_{ab\to ab}(s,t) = \langle p_a, p_b | \hat{T} | p'_a, p'_b \rangle = \langle p'_a, p'_b | \hat{T} | p_a, p_b \rangle \tag{2.43}$$

as Mandelstam invariant s and t are same for both equations. Moreover, for two-particle states $\langle i|$, $|i\rangle$ which are invariant under charge conjunction, similar property follows straight from (2.42)

$$\langle i | \hat{T} | f \rangle = \langle f | \hat{T} | i \rangle \tag{2.44}$$

With these properties, one can expand on unitarity condition

$$\hat{S}^\dagger \hat{S} = \mathbb{1} \tag{2.45}$$

Inserting $\hat{S} = \mathbb{1} + i\hat{T}$ gives

$$-i\left(\hat{T} - \hat{T}^\dagger\right) = \hat{T}^\dagger \hat{T} \tag{2.46}$$

Sandwiching this expression between states $\langle f|$ and $|i\rangle$ following (2.44) gives

$$\begin{aligned} -i\Big(\langle f|\hat{T}|i\rangle - \langle f|\hat{T}^\dagger|i\rangle\Big) &= \langle f|\hat{T}^\dagger\hat{T}|i\rangle \\ -i\Big(\langle f|\hat{T}|i\rangle - (\langle f|\hat{T}|i\rangle)^*\Big) &= \langle f|\hat{T}^\dagger\hat{T}|i\rangle \\ (2\pi)^4 2\delta^{(4)}(\sum p) Im\{\mathcal{T}_{i\to f}(s,t)\} &= \sum\!\!\!\!\!\!\int_X \langle f|\hat{T}^\dagger|X\rangle \langle X|\hat{T}|i\rangle \end{aligned} \tag{2.47}$$

where X is a complete set of states and sum-integral is carried over with suitable measure.

Note that for $|i\rangle = |f\rangle$ the relation gives well-known optical theorem

$$2\,\mathrm{Im}\,\{\mathcal{T}_{i\to i}(s,0)\} = \sum\!\!\!\!\!\!\int_X |\mathcal{T}_{i\to X}|^2 \tag{2.48}$$

and for any elastic scattering there exist a weaker positivity bound

$$\mathrm{Im}\,\{\mathcal{T}_{i\to i}(s,t)\} \geq 0 \tag{2.49}$$

The equation (2.47) can be separated into number of particles in

$$\begin{aligned} 2\,\mathrm{Im}\,\{\mathcal{T}_{i\to f}(s,t)\} = &\sum\!\!\!\!\!\!\int_{X\in\{1\mathrm{PS}\}} \langle f|\hat{T}^\dagger|X\rangle \langle X|\hat{T}|i\rangle \\ &+ \sum\!\!\!\!\!\!\int_{X\in\{2\mathrm{PS}\}} \langle f|\hat{T}^\dagger|X\rangle \langle X|\hat{T}|i\rangle + \dots \end{aligned} \tag{2.50}$$

The many (two or more) intermediate states (if scattering from $|i\rangle$ to $|X\rangle$ and from $|X\rangle$ to $|f\rangle$ is not prohibited) imply existence of discontinuity in $T(s,t)$, starting at $s = (\sum m_i)^2$, where $m_1, m_2, \dots$ are the masses of particles in the lightest ($n \geq 2$)-particle state. In fully general theory, this will correspond to $s = 4m^2$ where m is the mass of the lightest stable particle (lightest 2PS state).

Note that the discontinuity[6] in s starts at first $s = (\sum m_i)^2$, however each n particle state would correspond to branch point at particular value of s, with branch cuts along the real axis, stacked on top of each other. These branch points are called *normal thresholds*. However, for numerical S-matrix bootstrap considerations, the lowest of these thresholds is important, as this is the point when $\mathcal{T}(s,t)$ starts having imaginary part.

The intermediate 1PS behave slightly different. Let's consider scalar intermediate particle ξ of mass m_ξ. Via conservation of 4-momentum the interesting matrix elements have to be

$$\begin{aligned} \langle f|\hat{T}^\dagger|\xi\rangle &= (2\pi)^4\delta^{(4)}(k - p'_a + p'_b) g_f^* \\ \langle \xi|\hat{T}|i\rangle &= (2\pi)^4\delta^{(4)}(p_a + p_b - k) g_i \end{aligned} \tag{2.51}$$

where g_i and g_f depend only on particle content of the respective in-states and out-states, and k is 4-momentum of the particle. The integral over intermediate states is limited to $k^2 = -m^2$, therefore (2.47) below normal threshold will become

$$2\,\mathrm{Im}\,\{\mathcal{T}_{i\to f}(s,t)\} = \begin{cases} g_f^* g_i & \text{if} \quad s = m_\xi^2 \\ 0 & \text{otherwise} \end{cases} \tag{2.52}$$

[6] $\mathrm{Disc}()_s \mathcal{T}(s,t) = 2i\,\mathrm{Im}\,\{\mathcal{T}(s,t)\}$ is implied by analytic unitarity.

This 'bump' in imaginary value of $\mathcal{T}(s,t)$ implies existence of a pole in amplitude, and via dispersive arguments (skipped here), it may be inferred that

$$\mathcal{T}_{i\to f}(s,t) = \frac{ig_f^* g_i}{s-m_\xi^2} + \dots \tag{2.53}$$

Therefore, from analyticity and unitarity it may be inferred that, for transfer amplitude $\mathcal{T}(s,t)$

- One particle intermediate states create poles in s at locations corresponding to m^2 of these particles.
- Many particle states create branch cuts in s, starting at branch point $(\sum m_i)^2$.

Using crossing

- Different scattering amplitudes may be related by exchanging in-particles and out-particles
- Non-analyticities created at s-channel in one amplitude are non-analyticities in t or u channel in other amplitudes.

For example, having theory of real scalar particle a of mass m_a, analyticity implies that amplitude $\mathcal{T}_{aa\to aa}(s,t)$ has pole at $s=m_a^2$ and discontinuity starting at $s=4m_a^2$, however, via crossing property, also poles at $t=m_a^2$ and $s+t=3m^2$ (u-channel poles), and discontinuities starting at $t=4m_a^2$ and $u=4m_a^2$.

2.5 Partial waves

2-PS states don't form irreducible representations of Poincaré group, but can be written as linear combinations of such, with

$$|\phi_a\phi_b\rangle = \sum_{\ell,\lambda} \mathcal{C}_\lambda^\ell(\vec{p}_a,\vec{p}_b)\left|\sqrt{s},\vec{p};\ell,\lambda\right\rangle^{ab} \tag{2.54}$$

where $\vec{p}=\vec{p_a}+\vec{p_b}$ due to momentum conservation. Norm of $|\sqrt{s},\vec{p};\ell,\lambda\rangle^{ab}$ is up to choice, however, convenient option is to set up

$$\left\langle\sqrt{s},\vec{p'};\ell,\lambda\middle|\sqrt{s},\vec{p};\ell,\lambda\right\rangle^{ab} = (2\pi)^4\delta^4(p^\mu-p'^\mu) \tag{2.55}$$

Without loss of generality, one may consider general state in center of mass, with momenta as in (2.24)

$$|p,\theta,\varphi\rangle^{ab} = |m_a,\vec{p}\rangle\otimes|m_b,-\vec{p}\rangle \tag{2.56}$$

for different particles, and (following (2.7))

$$|p,\theta,\varphi\rangle^{aa} = \frac{1}{\sqrt{2}}\left(|m_a,\vec{p}\rangle\otimes|m_a,-\vec{p}\rangle + \left|m_a,-\vec{p}\right\rangle\otimes|m_a,\vec{p}\rangle\right) \tag{2.57}$$

These two particle states inherit normalization from (2.10), giving (for different particles)

$$\langle p,\theta,\varphi|p',0,0\rangle^{ab} = (2\pi)^4\delta(p^0-p'^0)\delta^3(0)\frac{16\pi^2\sqrt{s}}{\sqrt{\vec{p}\vec{p}'}\sin\theta}\delta(\theta)\delta(\varphi) \tag{2.58}$$

and for same particles

$$\begin{aligned}\langle p,\theta,\varphi|p',0,0\rangle^{ab} &= (2\pi)^4\delta(p^0-p'^0)\delta^3(0)\\ &\frac{16\pi^2\sqrt{s}}{\sqrt{\vec{p}\vec{p}'}\sin\theta}\left[\delta(\theta)\delta(\varphi)+\delta(\pi-\theta)\delta(\pi-\varphi)\right]\end{aligned} \tag{2.59}$$

Note that $\delta^3(0)$ comes from conservation of total momenta, which in COM frame is automatic. Let's start by considering a case $a \neq b$. Writing expression (2.54) in the rest frame gives

$$|p,\theta,\varphi\rangle^{ab} = \sum_{\ell,\lambda}\mathcal{C}^\ell_\lambda(p,\theta,\varphi)\left|\sqrt{s},0,\ell,\lambda\right\rangle^{ab} \tag{2.60}$$

Multiplying it with ${}^{ab}\langle\sqrt{s},0,\ell,\lambda|$ gets rid of the sum and provides

$$\mathcal{C}^\ell_\lambda(p,\theta,\varphi)(2\pi)^4\delta^{(4)}(0) = \left\langle\sqrt{s},0,\ell,\lambda\middle|p,\theta,\varphi\right\rangle \tag{2.61}$$

However, the state $|p,\theta,\varphi\rangle^{ab}$ can be constructed via rotations, with

$$|p,\theta,\varphi\rangle^{ab} = e^{-i\varphi J_3}e^{-i\theta J_2}e^{-i\alpha J_3}\,|p,0,0\rangle^{ab} \tag{2.62}$$

where the rightmost rotation acts trivially.

Therefore,

$$\left\langle\sqrt{s},0,\ell,\lambda\middle|p,\theta,\varphi\right\rangle = \left\langle\sqrt{s},0,\ell,\lambda\middle|e^{-i\varphi J_3}e^{-i\theta J_2}e^{-i\alpha J_3}\middle|p,0,0\right\rangle^{ab} \tag{2.63}$$

As the bra here is irreducible representation of $ISO(1,3)$, the effect of rotations on it can be expressed as

$$\begin{aligned}&\left\langle\sqrt{s},0,\ell,\lambda\right|e^{-i\varphi J_3}e^{-i\theta J_2}e^{-i\alpha J_3} =\\ &\sum_{\lambda'}\left\langle\sqrt{s},0,\ell,\lambda'\right|e^{-i\varphi\lambda}d^{(\ell)}_{\lambda'\lambda}(-\theta)e^{-i\alpha\lambda'}\end{aligned} \tag{2.64}$$

which assembles to elegant

$$\mathcal{C}^\ell_\lambda(p,\theta,\varphi)(2\pi)^4\delta^{(4)}(0) = \sum_{\lambda'}e^{-i\varphi\lambda}d^{(\ell)}_{\lambda'\lambda}(-\theta)e^{-i\alpha\lambda'}\left\langle\sqrt{s},0,\ell,\lambda'\middle|p,0,0\right\rangle \tag{2.65}$$

As the left-hand side is independent of α, the terms with $\lambda' \neq 0$ must vanish:

$$\left\langle\sqrt{s},0,\ell,\lambda'\middle|p,0,0\right\rangle = 0 \quad \text{if} \quad \lambda' \neq 0 \tag{2.66}$$

the result is

$$\mathcal{C}^\ell_\lambda(p,\theta,\varphi)(2\pi)^4\delta^{(4)}(0) = e^{-i\varphi\lambda}d^{(\ell)}_{0\lambda}(-\theta)\left\langle\sqrt{s},0,\ell,0\middle|p,0,0\right\rangle \tag{2.67}$$

As the braket on the right is constant, coefficient is defined up to a prefactor

$$\mathcal{C}^{\ell}_{\lambda}(p,\theta,\varphi) = C_\ell(p) e^{-i\varphi\lambda} d^{(\ell)}_{\lambda 0}(\theta) \tag{2.68}$$

This results in rather familiar

$$|p,\theta,\varphi\rangle^{ab} = \sum_{\ell,\lambda} C_\ell(p) e^{-i\varphi\lambda} d^{(\ell)}_{\lambda 0}(\theta) \left|\sqrt{s},0,\ell,\lambda\right\rangle^{ab} \tag{2.69}$$

To determine the prefactor $C_\ell(p)$ it's enough to bra the result with $\langle p,0,0|$, giving

$$\begin{aligned}\langle p,0,0|p,\theta,\varphi\rangle =& \sum_{\ell,\lambda} C_\ell(p) e^{-i\varphi\lambda} d^{(\ell)}_{\lambda 0}(\theta) \left\langle p,0,0\middle|\sqrt{s},0,\ell,\lambda\right\rangle^{ab} = \\ =& \sum_{\ell} C_\ell(p) d^{(\ell)}_{00}(\theta) (2\pi)^4 \delta^{(4)}(0) C^*_\ell(p)\end{aligned} \tag{2.70}$$

where the last equation was obtained by inserting (2.67) with $\theta = 0, \varphi = 0$. Now, by expanding the Wigner matrix $d^{(\ell)}_{00} = P_\ell(\cos\theta)$ and applying the (2.58), one gets

$$\frac{16\pi^2\sqrt{s}}{p\sin\theta}\delta(\theta)\delta(\varphi) = \sum_{\ell} |C_\ell(p)|^2 P_\ell(\cos\theta) \tag{2.71}$$

Multiplying both sides by $P_{\ell'}(\cos\theta)\sin\theta$ and integrating over $\mathrm{d}\varphi$ and $\mathrm{d}\theta$ gives

$$16\pi^2\frac{\sqrt{s}}{p} P_\ell(1) = \frac{4\pi}{2\ell+1}|C_\ell(p)|^2 \tag{2.72}$$

which, as $P_\ell(1) = 1$, simply gives

$$C_\ell(p) = \sqrt{4\pi(2\ell+1)\frac{\sqrt{s}}{p}} \tag{2.73}$$

Note that this is the result for two different particles. For two identical ones, inserting the norm (2.58) gives

$$\frac{16\pi^2\sqrt{s}}{p\sin\theta}\left(\delta(\theta)\delta(\varphi) + \delta(\pi-\theta)\delta(\pi+\varphi)\right) = \sum_{\ell} |C_\ell(p)|^2 P_\ell(\cos\theta) \tag{2.74}$$

which is integrated to

$$16\pi^2\frac{\sqrt{s}}{p}\left(P_\ell(1) + P_\ell(-1)\right) = \frac{4\pi}{2\ell+1}|C_\ell(p)|^2 \tag{2.75}$$

This is absolutely delightful result. With $P_\ell(-1) = (-1)^\ell P_\ell(1)$ one gets only 0 for each odd spin. **Identical scalars form only spin-even partial waves.** This is important, it very often cuts down number of computations by two.

To summarize this rather long computation, each two particle state in center of mass can be decomposed into irreducible representations of $ISO(1,3)$, and this decomposition is given by

$$|p,\theta,\varphi\rangle^{ab} = \sum_{\ell,\lambda} C^{ab}_\ell(p) e^{-i\lambda\varphi} d^{(\ell)}_{\lambda 0}(\theta) \left|\sqrt{s},0,\ell,\lambda\right\rangle^{ab} \tag{2.76}$$

where

$$\begin{aligned} C_\ell^{ab}(p) &= \sqrt{4\pi(2\ell+1)\frac{\sqrt{s}}{p}} \qquad \text{if} \quad a \neq b \\ C_\ell^{aa}(p) &= \sqrt{8\pi(2\ell+1)\frac{\sqrt{s}}{p}} \qquad \text{if} \quad \ell = 2n \\ C_\ell^{aa}(p) &= 0 \qquad\qquad\qquad\qquad \text{if} \quad \ell = 2n+1 \end{aligned} \tag{2.77}$$

It also shall come to no surprise, that equation (2.76) can be readily inverted

$$\left|\sqrt{s},0,\ell,\lambda\right\rangle^{ab} = \frac{2\ell+1}{4\pi C_\ell(p)}\int_0^{2\pi}\mathrm{d}\varphi\int_0^{\pi}\mathrm{d}\theta\sin\theta e^{-i\lambda\varphi}d_{0\lambda}^{(\ell)}(\theta)\left|p,\theta,\varphi\right\rangle^{ab} \tag{2.78}$$

Let's define scattering operator for partial waves

$$(2\pi)^4\delta^4(0)\mathcal{S}_{ab\to cd}^{(\ell,\lambda)}(s) = {}_{\text{out}}^{cd}\left\langle\sqrt{s},\vec{0},\ell,\lambda\right|\left.\sqrt{s},\vec{0},\ell,\lambda\right\rangle_{\text{in}}^{ab} \tag{2.79}$$

Considering the states in COM frame,

$$\left|\phi_a\phi_b\right\rangle_{\text{in}} = \left|p,0,0\right\rangle_{\text{in}}^{ab} \tag{2.80}$$

$$\left|\phi_c\phi_d\right\rangle_{\text{out}} = \left|p,\theta,\varphi\right\rangle_{\text{out}}^{cd} \tag{2.81}$$

and their decomposition into irreducible representations

$$\left|\phi_a\phi_b\right\rangle_{\text{in}} = \sum_{\ell,\lambda}C_\ell^{ab}\left(p\right)e^{-i\lambda\varphi}d_{\lambda0}^{(\ell)}\left(\theta\right)\left|\sqrt{s},\vec{0};\ell,\lambda\right\rangle_{\text{in}}^{ab} \tag{2.82}$$

$$\left|\phi_c\phi_d\right\rangle_{\text{out}} = \sum_{\ell,\lambda}C_\ell^{ab}\left(p\right)e^{-i\lambda\varphi}d_{\lambda0}^{(\ell)}\left(\theta\right)\left|\sqrt{s},\vec{0};\ell,\lambda\right\rangle_{\text{out}}^{cd} \tag{2.83}$$

one can expand the matrix element

$$\begin{aligned} {}_{\text{in}}\left\langle\phi_a,\phi_b|\phi_c,\phi_d\right\rangle_{\text{out}} = \sum_{\ell,\lambda}C_\ell^{ab}\left(p\right)C_\ell^{cd}\left(p'\right)d_{\lambda0}^{(\ell)}\left(\theta\right)e^{-i\lambda\varphi}\times \\ \times\,{}_{\text{in}}^{ab}\left\langle\sqrt{s},\vec{0};\ell,\lambda\right|\left.\sqrt{s},\vec{0};\ell,\lambda\right\rangle_{\text{out}}^{cd} \end{aligned} \tag{2.84}$$

to get

$$S_{ab\to cd}(s,\cos\theta) = \sum_{\ell,\lambda}C_\ell^{ab}\left(p\right)C_\ell^{cd}\left(p'\right)d_{\lambda0}^{(\ell)}\left(\theta\right)e^{-i\lambda\varphi}S_{ab\to cd}^{(\ell)}(s) \tag{2.85}$$

This can be readily inverted to

$$\mathcal{S}_{ab\to cd}^{(\ell,\lambda)}(s) = \frac{2\ell+1}{4\pi C_\ell^{ab}C_\ell^{cd}}\int_0^{\pi}\mathrm{d}\theta\sin\theta\int_0^{2\pi}\mathrm{d}\varphi\,e^{i\lambda\varphi}d_{\lambda0}^{(\ell)}(\theta)\mathcal{S}_{ab\to cd}(s,\cos\theta) \tag{2.86}$$

As the scattering amplitude does not depend on φ angle, the integral over φ is trivial and

$$\mathcal{S}_{ab\to cd}^{(\ell,\lambda)}(s) = 0 \quad \text{if} \quad \lambda \neq 0\ . \tag{2.87}$$

For the rest of this paper the superscript λ will be dropped, and lack of it will implicitly denote $\lambda = 0$ element, with

$$\mathcal{S}_{ab\to cd}^{(\ell)}(s) = \frac{2\ell+1}{2C_\ell^{ab}\left(p\right)C_\ell^{cd}\left(p'\right)}\int_0^{\pi}\sin\theta\,\mathrm{d}\theta\,d_{00}^{(\ell)}(\theta)\mathcal{S}_{ab\to cd}(s,\cos\theta) \tag{2.88}$$

which is further simplified by expanding $d^{(\ell)}_{00}(\theta) = P_\ell(\cos\theta)$. Inserting values for C^{ab}_ℓ, C^{cd}_ℓ, one gets a practical expression

$$\mathcal{S}^{(\ell)}_{ab\to cd}(s) = \frac{\sqrt{pp'}}{8\pi\kappa\sqrt{s}} \int_0^\pi \sin\theta \,\mathrm{d}\theta \, P_\ell(\cos\theta)(\theta)\mathcal{S}_{ab\to cd}(s,\cos\theta) \tag{2.89}$$

with $\kappa = \sqrt{1+\delta_{ab}}\sqrt{1+\delta_{cd}}$ to account for symmetry factors. However, it's still important to keep in mind that if either $a = b$ or $c = d$, the partial amplitudes for odd values of ℓ all vanish. Per analogia to general frame, a nontrivial part of amplitude (transfer amplitude) may be defined as

$$i(2\pi)^4\delta^4(0)\mathcal{T}^{(\ell)}_{ab\to cd}(s) = {}^{cd}_{\text{out}}\left\langle\sqrt{s},\vec{0},\ell,\lambda\middle|\sqrt{s},\vec{0},\ell,\lambda\right\rangle^{ab}_{\text{in}} - {}^{cd}_{\text{in}}\left\langle\sqrt{s},\vec{0},\ell,\lambda\middle|\sqrt{s},\vec{0},\ell,\lambda\right\rangle^{ab}_{\text{in}} \tag{2.90}$$

This seems to exactly the same at the first glance to previously defined scattering and transfer amplitudes, however, assembling the included pieces gives

$$\mathcal{S}^{(\ell)}_{ab\to ab}(s) = 1 + i\mathcal{T}^{(\ell)}_{ab\to ab}(s) \tag{2.91}$$

$$\mathcal{S}^{(\ell)}_{ab\to cd}(s) = 0 + i\mathcal{T}^{(\ell)}_{ab\to cd}(s) \quad \text{if} \quad ab \neq cd \tag{2.92}$$

Careful reader should notice a big difference to (2.90), namely 1 occurring there. Not $\mathbb{1}$.

$$1 \quad \text{(a number.)}$$

Therefore, when dealing with partial amplitudes, the relationship between transfer amplitude and scattering amplitude does not consist of any distributional properties, just a number. A number 1.

The nontrivial step is relating $\mathcal{T}^{(\ell)}_{ab\to cd}$ to $\mathcal{T}_{ab\to ab}$. The relationship (2.92) is simple, as both the scattering amplitude and the partial amplitude are related just by prefactor of i. Let's show the relation between $\mathcal{T}^{(\ell)}_{ab\to ab}$ and $\mathcal{T}_{ab\to ab}$.

In center of mass frame the defining equation (2.38) is

$$i\mathcal{T}_{ab\to ab}(s,\cos\theta)\times(2\pi)^4\delta^{(4)}(0) = {}_{\text{out}}\langle\phi_a,\phi_b|\phi_a,\phi_b\rangle_{\text{in}} - {}_{\text{in}}\langle\phi_a,\phi_b|\phi_a,\phi_b\rangle_{\text{in}} \tag{2.93}$$

which, when inserting the definition (2.14) and normalization (2.58) or (2.58), becomes

$$\begin{aligned} i\mathcal{T}_{ab\to ab}(s,\cos\theta)\times(2\pi)^4\delta^{(4)}(0) = \mathcal{S}_{ab\to ab}(s,\cos\theta)\times(2\pi)^4\,\delta^{(4)}(0) + \\ -(2\pi)^4\delta^4(0)\frac{16\pi^2\sqrt{s}}{\sqrt{\vec{p}\vec{p}'}\sin\theta}\left(\delta(\theta)\delta(\varphi)+\delta_{ab}\delta(\pi-\theta)\delta(\pi+\varphi)\right) \end{aligned} \tag{2.94}$$

Factoring out delta functions and projecting using partial wave projector

$$\Pi_\ell = \frac{1}{16\pi^2\kappa}\frac{\sqrt{pp'}}{\sqrt{s}}\int_0^{2\pi}\mathrm{d}\varphi\int_0^\pi \sin\theta\,\mathrm{d}\theta\,P_\ell(\cos\theta) \tag{2.95}$$

one gets

$$\frac{i}{8\pi\kappa}\frac{\sqrt{pp'}}{\sqrt{s}}\int_0^{2\pi}\mathrm{d}\varphi\int_0^{\pi}\sin\theta\,\mathrm{d}\theta\,P_\ell(\cos\theta)\mathcal{T}_{ab\to ab}(s,\cos\theta) =$$
$$\frac{1}{8\pi\kappa}\frac{\sqrt{pp'}}{\sqrt{s}}\int_0^{2\pi}\mathrm{d}\varphi\int_0^{\pi}\sin\theta\,\mathrm{d}\theta\,P_\ell(\cos\theta)\mathcal{S}_{ab\to cd}(s,\cos\theta)+$$
$$-\frac{1}{8\pi\kappa}\frac{\sqrt{pp'}}{\sqrt{s}}\int_0^{2\pi}\mathrm{d}\varphi\int_0^{\pi}\sin\theta\,\mathrm{d}\theta\,P_\ell(\cos\theta)\frac{16\pi^2\sqrt{s}}{\sqrt{\vec{p}\vec{p'}}\sin\theta}\left(\delta(\theta)\delta(\varphi)+\delta_{ab}\delta(\pi-\theta)\delta(\pi+\varphi)\right) \tag{2.96}$$

The first term in the sum is obviously $S^{(\ell)}_{ab\to ab}(s)$. The second part needs a bit more love. The integration over φ is not terribly difficult[7], via $\int_0^{2\pi}\mathrm{d}\phi\delta(\varphi)=1$ and via $\int_0^{2\pi}\mathrm{d}\phi\delta(\pi+\varphi)=1$. However, the integral over $\cos\theta$ is slightly more complex, with Dirac delta giving a factor of half:

$$\int_0^{\pi}\mathrm{d}\theta P_\ell(\cos\theta)\frac{16\pi^2\sqrt{s}}{\sqrt{\vec{p}\vec{p'}}}\left(\delta(\theta)+\delta(\pi-\theta)\right)=\left(P_\ell(1)+\delta_{ab}P_\ell(-1)\right)\frac{8\pi^2\sqrt{s}}{\sqrt{\vec{p}\vec{p'}}} \tag{2.97}$$

For $a\neq b$ the symmetry factor κ is 1, and everything gathered together gives

$$\begin{aligned}\frac{i}{8\pi\kappa}\frac{\sqrt{s}}{\sqrt{pp'}}\int_0^{\pi}\sin\theta\,\mathrm{d}\theta\,P_\ell(\cos\theta)\mathcal{T}_{ab\to ab}(s,\cos\theta) &= \mathcal{S}^{(\ell)}_{ab\to ab}-1\\ &= i\mathcal{T}^{(\ell)}_{ab\to ab}\end{aligned} \tag{2.98}$$

In case of identical particles, for even spins, the additional factor of 2 coming from two Dirac deltas exactly cancels with prefactor of $\frac{1}{\kappa}=\frac{1}{2}$, making the equation (2.99) valid again, and for odd spins, the identity $0=0$ is obtained, with no surprise, keeping in mind the previous results.

Merging this and the earlier case $ab\neq cd$, and, as a final touch, expressing the prefactor using (2.33) gives the elegant formula

$$i\mathcal{T}^{(\ell)}_{ab\to cd}=\frac{i\sqrt{\mathcal{L}_{ab}\mathcal{L}_{cd}}}{16\pi\kappa s}\int_0^{2\pi}\mathrm{d}\varphi\int_0^{\pi}\sin\theta\,\mathrm{d}\theta\,P_\ell(\cos\theta)\mathcal{T}_{ab\to cd}(s,\cos\theta) \tag{2.99}$$

2.6 Unitarity

In unitary QFT, every state has non-negative norm, e.g. $\forall\,|\psi\rangle:\langle\psi|\psi\rangle\geq 0$. Let's enlist all the in-states

$$V_{\text{in}}\equiv\bigoplus|\phi_a,\phi_b\rangle_{\text{in}} \tag{2.100}$$

and all the out-states

$$V_{\text{out}}\equiv\bigoplus|\phi_a,\phi_b\rangle_{\text{out}} \tag{2.101}$$

As in- and out- states are related by scattering operator, one can write a norm of any $|v\rangle\in V_{\text{in}}\oplus V_{out}$, as following

$$\langle v|v\rangle=\left(\langle v_{\text{in}}|\oplus\langle v_{\text{out}}|\right)\left(|v_{\text{in}}\rangle\oplus|v_{\text{out}}\rangle\right)\geq 0 \tag{2.102}$$

[7] At the first glance it looks like it shall be $\frac{1}{2}$, because one integrates $\delta\varphi$ from 0 to something, effectively taking half of it. However, the integration from $2\pi-\epsilon$ to 2π is providing another half of integration range.

However, both Hilbert spaces are related by $\mathcal{S}$ matrix, with $|v_{\text{out}}\rangle = \mathcal{S}\,|v'_{\text{in}}\rangle$, and similarly for bras[8].

Therefore, the inner product is

$$\langle v|v\rangle = \left(\langle v_{\text{in}}| \oplus \langle v'_{\text{in}}|\,\mathcal{S}^\dagger\right)\left(|v_{\text{in}}\rangle \oplus \mathcal{S}\,|v'_{\text{in}}\rangle\right) \geq 0\ . \tag{2.103}$$

Defining $|w\rangle = |v\rangle \oplus |v'\rangle$, one can write

$$\langle w| \begin{pmatrix} \mathbb{1} & \mathcal{S} \\ \mathcal{S}^\dagger & \mathbb{1} \end{pmatrix} |w\rangle \geq 0 \tag{2.104}$$

Therefore, unitarity implies semidefinitness of the matrix

$$\mathcal{M} = \begin{pmatrix} \mathbb{1} & \mathcal{S} \\ \mathcal{S}^\dagger & \mathbb{1} \end{pmatrix} \succeq 0 \tag{2.105}$$

where $\mathcal{S}$ describes scattering of states.

This is rather difficult to tackle in such form. However, one can consider a subspace, constructed from 2PS partial waves

$$W_{\text{in}} \equiv \bigoplus_{\ell} \bigoplus_{s} \bigoplus_{a,b} \left|\sqrt{s}, 0, \ell, 0\right\rangle_{\text{in}}^{ab} \tag{2.106}$$

$$W_{\text{out}} \equiv \bigoplus_{\ell} \bigoplus_{s} \bigoplus_{a,b} \left|\sqrt{s}, 0, \ell, 0\right\rangle_{\text{out}}^{ab} \tag{2.107}$$

This allows to express a matrix of inner product as a direct sum of unitarity matrices of partial waves,

$$\mathcal{M}^\ell(s) = \begin{pmatrix} \mathbb{1} & \mathcal{S}^{(\ell)}(s) \\ (S^{(\ell)})^\dagger(s) & \mathbb{1} \end{pmatrix} \tag{2.108}$$

where the matrix $S^{(\ell)}$ is formed over all two particle content forming in-states, and out-states.

$$\underset{\text{out}}{{}^{cd}}\left\langle \sqrt{s}, 0, \ell, 0\middle|\mathcal{S}^{(\ell)}(s)\middle|\sqrt{s}, 0, \ell, 0\right\rangle_{\text{in}}^{ab} = (2\pi)^4\delta^{(4)}(0)\mathcal{S}^{(\ell)}(s)_{ab\to cd} \tag{2.109}$$

To give some example, if a theory has in-states and out-states composed of particles ϕ_a, ϕ_b, $\S^{(\ell)}$ is very concretely

$$\mathcal{S}^{(\ell)}(s) = \begin{pmatrix} \mathcal{S}^{(\ell)}(s)_{aa\to aa} & \mathcal{S}^{(\ell)}(s)_{aa\to ab} & \mathcal{S}^{(\ell)}(s)_{aa\to bb} \\ \mathcal{S}^{(\ell)}(s)_{ab\to aa} & \mathcal{S}^{(\ell)}(s)_{ab\to ab} & \mathcal{S}^{(\ell)}(s)_{ab\to bb} \\ \mathcal{S}^{(\ell)}(s)_{bb\to aa} & \mathcal{S}^{(\ell)}(s)_{bb\to ab} & \mathcal{S}^{(\ell)}(s)_{bb\to bb} \end{pmatrix} \tag{2.110}$$

and $\mathbb{1}$ is again, quite concretely,

$$\mathbb{1} = \begin{pmatrix} 1 & 0 & 0 \\ 0 & 1 & 0 \\ 0 & 0 & 1 \end{pmatrix} \tag{2.111}$$

The general unitarity constraint is therefore, if put in terms of single matrix, is

$$\mathcal{M} = \bigoplus_{\ell,s} \mathcal{M}^\ell(s) \succeq 0 \tag{2.112}$$

[8]If the Hilbert space doesn't lose dimensionality with the flow of time. I hope it doesn't.

However, this is equivalent to imposing unitarity on each component of the direct sum.

$$\mathcal{M}^\ell(s) = \begin{pmatrix} \mathbb{1} & \mathcal{S}^\ell(s) \\ (\mathcal{S}^\ell)^\dagger(s) & \mathbb{1} \end{pmatrix} \succeq 0 \quad \text{for} \quad \forall s, \ell \tag{2.113}$$

Of course, one may try to express the unitarity condition in terms of transfer amplitudes

$$\mathcal{M}^\ell(s) = \begin{pmatrix} \mathbb{1} & \mathbb{1} + i\mathcal{T}^\ell(s) \\ \mathbb{1} - i(\mathcal{T}^\ell)^\dagger(s) & \mathbb{1} \end{pmatrix} \succeq 0 \quad \text{for} \quad \forall s, \ell \tag{2.114}$$

This is not very practical formula, as (potentially small) transfer amplitude may occur next to 1 from trivial part, introducing round-off errors in practical computations.

However, with an invertible matrix

$$\mathcal{A} = \begin{pmatrix} 1 & 1 \\ 0 & i \end{pmatrix} \tag{2.115}$$

an equivalent condition can be written

$$\mathcal{A}^\dagger \mathcal{M}^\ell(s) \mathcal{A} = \begin{pmatrix} \mathbb{1} & (\mathcal{T}^\ell)^\dagger(s) \\ \mathcal{T}^\ell(s) & 2\,\mathrm{Im}(T) \end{pmatrix} \succeq 0 \tag{2.116}$$

So, having answered numerical stability problems, and running out of good letters for matrices, let's use the name $\mathcal{M}$ for this ultimate unitarity matrix

$$\mathcal{M}^\ell(s) = \begin{pmatrix} \mathbb{1} & (\mathcal{T}^\ell)^\dagger(s) \\ \mathcal{T}^\ell(s) & 2\,\mathrm{Im}(\mathcal{T}^\ell(s)) \end{pmatrix} \succeq 0 \quad \text{for} \quad \forall s, \ell \tag{2.117}$$

This is the set of unitarity conditions every set of amplitudes has to obey for physical values of s (above the normal threshold).

2.7 S-matrix bootstrap program

With all properties described in previous sections, one can finally dive into S-matrix bootstrap. The goal is to find the space of amplitudes consistent with unitarity, while having analytic properties described in previous sections.

To account for kinematic non-analyticities one starts with following "building block" (function)

$$\rho_w(z; z_0) = \frac{\sqrt{w - z_0} - \sqrt{w - z}}{\sqrt{w - z_0} + \sqrt{w - z}} \tag{2.118}$$

which is an expression with branch cut starting at $z = w$, and going to infinity.

One can use it to construct a series describing an amplitude with suitable branch cuts

$$\mathcal{T}_{ab\to cd}(s,t,u) = \sum_{a,b,c}^{\infty} \alpha_{abc} \rho_{s_{\text{cut}}}(s; s_0)^a \rho_{t_{\text{cut}}}(t; t_0)^b \rho_{u_{\text{cut}}}(u; u_0)^c + \dots \tag{2.119}$$

This ansatz has a lot of redundancy, as $s + t + u = m_a^2 + m_b^2 + m_c^2 + m_d^2$. This can be crudely mitigated by setting $\alpha_{abc} = 0$ if $abc \neq 0$[9].

[9]Neither it's the most justified way, nor one that makes α_{abc} unique, but when limiting the ansatz size to $a + b + c \leq \texttt{maxN}$, the number of free parameters in bootstrap declines from $O(\texttt{maxN}^3)$ to $O(\texttt{maxN}^2)$. This is enough to jump from "eternity" to "quite long" in terms of computational time.

One can and should expand the ansatz to account for other non-analyticities encountered in the problem, for example the poles

$$\mathcal{T}_{ab\to cd}(s,t,u) = \cdots + \frac{g}{s-m_X^2} + \dots \tag{2.120}$$

or threshold bound states

$$\mathcal{T}_{ab\to cd}(s,t,u) = \cdots + \frac{\xi}{\rho_{s_{\text{cut}}}(s;s_0)^a - 1} + \dots \tag{2.121}$$

Although second of these non-analyticities can be reproduced by a suitable linear combination in (2.119), the number of terms in series for the numerical computations must be limited, by introducing truncation

$$\alpha_{abc} = 0 \quad \text{if} \quad a+b+c > \texttt{maxN} \tag{2.122}$$

and the convergence is greatly improved by adding (2.121). Expanding the ansatz by suitable 'improvement terms' for a particular problem is a bit of physics, a bit of art and a bit of trial and error. For example, the logarithmic terms coming from 1-loop perturbation theory[20], proportional to $\log(-s)$ or $\log^2\left(\frac{t}{u}\right)$ may be used to expand the ansatz.

2.8 Numerical bootstrap

Given set of unitarity constraints

$$\mathcal{M}^\ell(s) = \begin{pmatrix} \mathbb{1} & (\mathcal{T}^\ell)^\dagger(s) \\ \mathcal{T}^\ell(s) & 2\,\text{Im}(T) \end{pmatrix} \succeq 0 \quad \text{for} \quad \forall s, \ell \tag{2.123}$$

one already formulated the problem in terms of already well-known convex optimization task:

> For a set of i free parameters, and $i*j$ 'building blocks' $[M_j]_0$ and $[M_j]_i$ find the space of parameters α_i such that matrices $M_j = [M_j]_0 + \sum_i \alpha_i \cdot [M_j]_i$ are all positive semidefinite.

with, in this case, M_j is set of matrices $\mathcal{M}^{(\ell)}(s)$ for chosen finite subset of values of s and ℓ.

This family of tasks is named Semifdefinite Problems (SDP), and optimized interior-point method solvers like SDPB are available and used.

In practice mapping the entire space of functions is impossible, but the solutions that, consistently with unitarity, maximize or minimize some interesting parameters, can be computed, and indeed, solvers such as SDPB[10], are computing optimization tasks:

> For a set of i free parameters α_i, goal vector b_i, and $i*j$ 'building blocks' $[M_j]_0$ and $[M_j]_i$find the vector α_i such that matrices $M_j = [M_j]_0 + \sum_i \alpha_i \cdot [M_j]_i$ are all positive semidefinite, and value $c = \alpha_i \cdot b_i$ is maximized.

For example goal vector $b_i = \{1,0,0,0,\dots\}$ describes a task to maximize α_1 parameter, and $b_i = \{-1,0,0,0,\dots\}$ creates a task to minimize it.

[10] There are many solvers available, but sparsity optimizations in SDPB make it especially efficient in numerical S-Matrix problems.

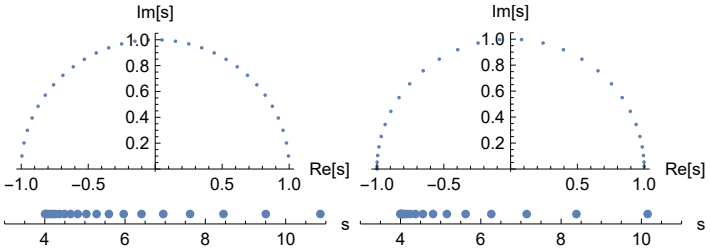

Figure 2.1: Regular grid vs Chebyshev grid, of 30 points each.

Except the finite grid of values of s, and an ansatz (2.119) truncated to some value `maxN`, the set of spins ℓ must also be limited (by limiting $\ell \leq$ `maxJ`). The nature of these computational constraints is rather annoying, as with denser grid of s, and larger `maxJ` the grid becomes stricter (one's adding additional constraints, approaching the 'true' unitarity bound), and looser with increasing `maxN` (as the amplitude ansatz is getting more degrees of freedom).

In practice, one has to experiment with number of grid points in s, and their distribution. Again, with it being a bit of art and a bit of physics, a good grid has a lot of points in s near the normal threshold, and reasonably spaced points up to an infinity. The decent guess is spacing the grid in φ such that $\rho_{s_{\rm cut}}(s;s_0) = e^{i\varphi}$ for the range $\varphi \in (0,\pi)$.

In most papers, either equally spaced grid of N points $\varphi_k = \frac{k}{N}\pi$ is used, or, given by slightly more involved expression, 'Chebyshev grid', consisting of $x_k = \cos\left(\frac{\pi(k+1/2)}{N}\right)$, $\varphi_k = \pi(1+x_k)/2$. The nodes of Chebyshev polynomials, x_k, are often used in integration methods, however, this reason is irrelevant in case of S-matrix bootstrap, but such grid is slightly denser in s's near the threshold (see fig. 2.8), and in high energies (which has rather vague meaning in this case), resulting in better convergence in similar grid sizes[11]. Throughout this paper, 'Chebyshev grid' is universally used. Note that

$$\varphi = \arg \rho_{s_{\rm cut}}(s;s_0) \tag{2.124}$$

is a handy way variable to plot entire amplitude, as it maps the region $[s_{\rm cut};\infty)$ onto $[0,\pi]$ range.

The last technicality is getting rid of complex numbers, as the solvers are made for real and symmetric matrices, not complex and hermitian. However, it may be addressed using row-doubling

$$\mathcal{M} \succcurlyeq 0 \iff \begin{pmatrix} \operatorname{Re}\mathcal{M} & \operatorname{Im}\mathcal{M} \\ \operatorname{Im}\mathcal{M} & \operatorname{Re}\mathcal{M} \end{pmatrix} \succcurlyeq 0 \tag{2.125}$$

This is easily proven, as the matrix on the right is just $\begin{pmatrix} \mathcal{M} & 0 \\ 0 & \mathcal{M}^* \end{pmatrix}$ in different basis. For (2.117), this gives

$$\begin{pmatrix} \mathbb{1} & \operatorname{Re}\mathcal{T}^\ell(s) & 0 & \operatorname{Im}\mathcal{T}^\ell(s) \\ \operatorname{Re}\mathcal{T}^\ell(s) & 2\operatorname{Im}\mathcal{T}^\ell(s) & -\operatorname{Im}\mathcal{T}^\ell(s) & 0 \\ 0 & -\operatorname{Im}\mathcal{T}^\ell(s) & \mathbb{1} & \operatorname{Re}\mathcal{T}^\ell(s) \\ \operatorname{Im}\mathcal{T}^\ell(s) & 0 & \operatorname{Re}\mathcal{T}^\ell(s) & 2\operatorname{Im}\mathcal{T}^\ell(s) \end{pmatrix} \succeq 0 \tag{2.126}$$

[11] And as the time is money, smaller grids are better, if the result is the same.

and is the commonly implemented matrix for practical computations.

This concludes the chapter about setup. The next part presents how the numerical experiment described above may be set up using `SMatrixToolkit`, a package made for facilitating the steps of partial waves computation, generation of actual input for solver, and parsing the results.

Chapter 3

The Toolkit

The previous section introduced the concept of scattering amplitudes, their analytic properties, and the unitarity constraints.

Setting up the numerical S-matrix bootstrap experiment follows a series of steps

1. Constructing the amplitude ansatz/ansatze – a linear combination of building blocks $a_i \cdot \texttt{fn[s,t,u]}_i$

2. Imposing further constraints on the ansatze. These may include soft conditions, extra symmetries, etc.

3. Expanding the ansatze with 'improvement terms', that are redundant building blocks improving convergence in practical computations.

4. Setting up partial integrals using (2.95). For every building block $\texttt{fn[s,t,u]}_i$ the partial integral $\texttt{int[s, } \ell\texttt{]}_i = \Pi_\ell \texttt{fn[s,t,u]}_i$ shall be found. In practice lots of time can be saved by factoring out as large part dependent only on s from $\texttt{fn[s,t,u]}_i$, as then many integrals can be reused.

5. Set up a grid of values of s, for which partial amplitudes shall be computed (and on which unitarity constraints shall be imposed).

6. Perform "precomputation" – create a table of $\texttt{int[s, } \ell\texttt{]}_i$ (or objects to construct them) for set all the building blocks, all values of s from the grid and set of spins ℓ.

7. Create 'unitarity matrix' from amplitudes, as in (2.117).

8. By plugging in the objects $\texttt{int[s, } \ell\texttt{]}_i$ into unitarity matrix for each s and ℓ, construct a semidefinite problem (SDP), which, can be optimized for some goal $g_i \cdot a_i$. Usually the goal is to maximize or minimize a parameter (which corresponds to goal vector of $g = 0, \cdots, \pm 1, \cdots$).

9. Use the dedicated solver to solve the SDP.

10. Analyze the data, publish a paper, earn Nobel Prize, etc.

One can notice that only three of these steps require physics, and the rest is just following the recipe.

The author noticed that, and created a package that tries to automatize as much of these steps as possible, creating[1] the `SMatrixToolkit`, Wolfram Mathematica package.

The toolkit is fully Free and Open Source Software, and the repository is publicly available at `https://github.com/jmarucha/SMatrixToolkit`. This chapter aims to describe the usage and inner workings of the project, showing the room for further possible development.

3.1 Setting up

The first step of constructing amplitude is defining the particles involved. Declaring particle is as simple as

```
p1 = Particle[name, mass]
```

where name is arbitrary string, and mass is particle's mass[2]. For particles in particular scattering process one shall define

```
particles = ParticleContent[
  {inparticle1, inparticle2},
  {outparticle1, outparticle2}
]
```

The core building block for amplitude anzatz is the ρ series (2.119), constructed out of ρ variables. They are available using

```
RhoVariable[z, Cut-> w, Center -> z0]
```

The branch cuts are chosen in such a way $\mathrm{Im}\,(\rho_w(z;z_0)) > 0$ for $z > w$, unlike with default `Mathematica` branch cuts resulting from `Sqrt[]`. There is no need to define separate variables for $z > w$ and $z < w$.

The (truncated) rho ansatz described in (2.119) is constructed with dedicated function

```
RhoSeries[
  particles, (* ParticleContent[] described before *)
  alpha, (* coefficients are named alpha[a,b,c] *)
  RhoVariable[s, ...],
  RhoVariable[t, ...],
  RhoVariable[u, ...],
  maxN (* terms with a+b+c > maxN are set to 0 *)
]
```

The crossing symmetries will be inferred from particle content, however it can be overridden with option `Symmetry -> "none"` or `"ST"`, `"SU"`, `"TU"` and `"STU"`. Similarly, poles can be declared by

[1] Ideas for the better name are welcome.

[2] Particles are considered same or different on the basis of name. Having particles of same name, but different properties lead to unpredictable behavior

```
Pole[
  particles, (* ParticleContent[] again *)
  g, (* name of residue coefficient *)
  s, (* channel, shall be s, t, or u *)
  1 (* pole location *)
]
```

This is in fact just a shorthand for more general option, allowing to add arbitrary coefficients:

```
ExtraParam[
  particles, (* ParticleContent[] again and again *)
  weirdthing, (* name of associated coefficient *)
  Log[t/u]^2 (* some arbitrary function of s,t,u *)
]
```

In case of building blocks other than `RhoSeries` and `Pole`, `Symmetry` option may become really handy. An example of improvement term explicitly braking *stu* symmetry (but still useful) will be given in case of bootstrapping a-anomaly. The ansatze are joint using standard addition:

```
amplitude = RhoSeries[particles, alpha,
RhoS, RhoT, RhoU, maxN] + Pole[particles, g, s, 1]
```

which also allows to use `Sum` for example for constructing amplitude with multiple poles

```
manyPoles = Sum[
  Pole[particles, g[location], s, location],
  {location, 2, 3, 1/10}
]
(* resonances at 20/10, 21/10, ..., 30/10 *)
```

For constructing amplitude ansatze related by crossing, one uses the function

```
amplitudeABtoAB = Crossing[amplitudeAAtoBB, "I2"<->"O1"]
```

The shorthand in second arguments is describing crossing between second in-particle (`"I2"`) and first out-particle (`"O1"`). `"I2"` and `"O2"` are other available options.

To fix a particular coefficient in amplitude, a function `FixCoefficient` is available

```
newAmplitude = FixCoefficient[amplitude, g == 4]
```

and to impose value of the entire ansatz expression at given point s_0, t_0, u_0 the function `Reshape` shall be used

```
amplitude = Pole[particles, g, s, 1, Symmetry -> "none"] +
  ExtraParam[particles, x, 2, Symmetry -> "none"]
  (* Creates ansatz g * 1/(1-s) + x * 2 *)

Reshape[amplitude == 2 a, {s -> 0, t -> 0, u -> 0}]
  (* ansatz of a*(1-1/s-1) + x* (2 + 2/(s-1) *)

Reshape[amplitude == 2 a, {s -> 0, t -> 0, u -> 0},
 KeepCoefficients -> g]
 (* ansatz of a*(1-1/s-1) + g* (-1 - 1/(s-1) *)
```

Unfortunately it requires numerical prefactor different to 1 in front of the new coefficient (to be fixed). In conjunction with `FixCoefficient` it is very handy tool for imposing some soft conditions.

3.2 Partial waves and precomputation

The precomputation step needs integrals, which are obtained from each amplitude

```
integrals = amplitude["PartialIntegrals"]
```

This is an association, the key corresponds to a building block (with as many factors of s or $\rho(s)$ factored out), and the value is (inactivated) integral, that has prefactor from (2.99) applied, along with (2.31) expanding t and u inside the integral. Creating list of integrals from many amplitudes can be achieved with Mathematica built-in functions

```
amplitudes = {amplitude1, amplitude2, amplitude3}
integrals = Union[Through[amplitudes["PartialIntegrals"]]]
```

The second secret ingredient is grid of values of s, and there are two options already implemented.

The function `RegularGrid` creates a list of points where `RhoVariable[s] = Exp[ii Pi n/N]`, so grid points are regularly spaced in argument of `RhoVariable[s]`, and the function `ChebyshevGrid` creates list of points that have arguments of `RhoVariable[s]` in roots of Chebyshev polynomials $T_i(\cos\phi) = 0$. It's useful, as it is way denser next to brunch cut of ρ, and in large values of s. This is where exciting things happen, so in practice `ChebyshevGrid` is a go-to grid generator.

At the most basic level, constructing grid is as simple as inserting `RhoVariable` and number of points.

```
rho1 = RhoVariable[s, Cut->4, Center->4/3]
grid = ChebyshevGrid[rho1, 250]
```

However, the `RhoVariable`s have to be precomputed as well (for performance reasons, when constructing the problem, having these values precomputed massively reduce memory footprint and construction time). This is done with option

`ExtraObjects`. The second allowed option is `WorkingPrecision`, which is quite self-explanatory[3]. The example (as later used in a-anomaly computations)

```
rho1 = RhoVariable[s, Cut->4, Center->0]
rho2 = RhoVariable[s, Cut->4, Center->4/3]
rho3 = RhoVariable[s, Cut->4, Center->1]
grid = ChebyshevGrid[rho2, 250,
  ExtraObjects->{rho1, rho3},
  WorkingPrecision->110
  ]
```

bases the grid on `rho2`, however also precomputes values of `rho1` and `rho3` at grid points.

These two are enough for precomputation, and to pull the trigger one shall use command `PrecomputeGrid`, which, along with previously mentioned s grid and integrals needs output directory and list of spins. For example,

```
directory = "/home/marucha/grid";
spins = Range[0, 40];
PrecomputeGrid[directory, integrals, grid, spins]
```

The last command takes the same options as `NIntegrate`, e. g. `AccuracyGoal`, `WorkingPrecision` or `MaxRecursion`. This command takes a while and is paralelized by separate spins (however, on home computers the program seems to be limited by memory bandwidth, so the gains are relatively small, especially in comparison to octa-channel server boards).

The effect of this computation is a bunch of files in `grid` directory:

```
grid/
  integralObjectsMap.m
  spin=0.mx
  spin=1.mx
  ...
  spin=40.mx
```

The first one maps each integrand onto `integralObject###`, and the rest of files contain associations mapping each `integralObject###` into a precomputed value on each grid point. That allows to do computationally-heavy integrand matching only once when constructing the SDPB problem.

Note that, for precomputation one needs only integrals and grid, so to launch precomputation on the remote server, it's enough to

```
(* on local machine *)
Export["precomputeTask.m", {integrals, grid}]

(* on remote machine *)
```

[3]Setting this to number higher than `WorkingPrecision` of `NIntegrate` allows getting way less annoying errors about integrand precision.

```
Get["SMatrix`"];
{integrals, grid} = Import["precomputeTask.m"];
directory = "/home/marucha/grid";
spins = Range[0, 40];
PrecomputeGrid[directory, integrals, grid, spins]
```

Note that to use multiple cores on Slurm clusters one needs to launch script requesting multiple cores for process, for example for 41 spins

```
srun -c 41 wolframscript -f precomputeScript.wls
```

3.3 Creating problems

With amplitude ansatze constructed, and integrals precomputed one can finally construct S-matrix problem.

To load the data one uses

```
data = LoadData["path/to/grid"]
```

To define S-matrix one declares a (linear) function from amplitudes to matrix, for example, for one amplitude, using (2.126)

```
matrixFunct = {
  {    1,  Re[#],      0,  Im[#]},
  {Re[#], 2Im[#], -Im[#],      0},
  {    0, -Im[#],      1,  Re[#]},
  {Im[#],      0,  Re[#], 2Im[#]}
}&
```

or, using the simplified unitarity condition from [15] (not generalizable beyond one amplitude)

```
matrixFunct = {
  {1+Re[#], 1-Im[#]},
  {1-Im[#], 1-Re[#]}
}&
```

With such function, and amplitude ansatz `amplitude`, one declares unitarity matrix

```
uMatrix = UnitarityMatrix[matrixFunct, amplitude]
```

which correspond to expanding the `amplitude` using its partial wave into matrix generated by `matrixFunct`.

For unitarity matrices containing more than one amplitude, a function of many variables shall be defined, and all the ansatze shall be passed to `UnitarityMatrix`:

```
matrixFunct = {amp1, amp2, ...} |-> {
  {1, Re[amp1], Re[amp2], ...},
  ...
}
uMatrix = UnitarityMatrix[
  matrixFunct,
  {amplitude1, amplitude2, ...}
]
```

Of course, in more complex problems, many unitarity matrices may need to be defined.

Now, a problem template can be constructed. This is an object containing amplitude ansatze in terms of precomputed `integralObject`.

This is done by using function `CreateProblemTemplate`.

```
template = CreateProblemTemplate[{uMatrix}, data]
```

or for multiple unitarity matrices

```
template = CreateProblemTemplate[{uMatrix1, umatrix2,...}, data]
```

However, sometimes, despite the best effort, automatic resolution of symbolic expression into integral objects fail. The option `ExplicitBindings` is a rather ugly last resort into solving that.

The option syntax

```
ExplicitBindings->{weirdCoefficient->{0,0,s*integralObject2137}}
```

means "the coefficient `weirdCoefficient` resolves to 0 for the first and second amplitude, but to `s*integralObject2137` for the third amplitude". Second available option is `MaxN`, which limits the rho series to `maxN` terms.

Now, the final step is actually constructing the SDPB input via function `BuildSMatrix`. The basic syntax is

```
BuildSMatrix[template, goal, data]
```

where `goal` is one of `Maximal[coeff]`, `Minimal[coeff]` or `Manual[...]`. The first two are pretty self-explanatory, asking to minimize or maximize coefficient of given name.

The last one is a definition of goal vector $\vec{b}$, as described in [14], with syntax

```
Manual[{coeff1->weight1, coeff2->weight2,..., _->0}]
```

meaning "construct such $\vec{b}$ that $\vec{b}_i \cdot$ `coeff`$_i$ = `coeff1 * weight1 + coeff2 * weight2 + ...`". The goal `Maximal[coeff]` is equivalent to `Manual[{coeff->1,_->0}]`, and `Minimal[coeff]` to `Manual[{coeff->-1,_->0}]`.

The additional options are `MaxN` and `MaxJ`, to limit `maxN` and `maxJ` of constructed problems. The set of spins and s values for each `UnitarityMatrix` is limited automatically based on Bose symmetry and branch cuts.

The user can pass additional semi-definite constraints using option `AdditionalConstraints`, which takes a list of matrices of coefficients. For example

```
AdditionalConstraints->{
  {{a[0,0,0]}},
  {{a[0,0,1]}}
}
```

would force inequalities $\mathtt{a}[0,0,0] \geq 0$, $\mathtt{a}[0,0,1] \geq 0$, and

```
AdditionalConstraints->{
  {
    {g1, g2},
    {g2, g3}
  }
}
```

would add constraint

$$\begin{pmatrix} \mathtt{g1} & \mathtt{g2} \\ \mathtt{g2} & \mathtt{g3} \end{pmatrix} \succcurlyeq 0 \tag{3.1}$$

This allows to add analytic high-energy constraints (for example $\sum \alpha_{abc}(-1)^{a+b+c} a \geq 0$, as described in [15]), or relationships between residues of the poles (as later seen in (4.114)).

The result of function `BuildSMatrix` is a Mathematica input for SDPB, conforming to [21],

```
SDP[objective, normalization, {
  PositiveMatrixWithPrefactor[1, ...],
  PositiveMatrixWithPrefactor[1, ...],
  ...
}]
```

ready to be exported and processed by `sdp2input` and `sdpb`.

Last, it is very useful to save the relation between coefficient names and parameters of SDPB problem (as `SDP[...]` operates on unnamed list of parameters), using

```
template["Keys"]
template["Keys", maxN]
```

These arrays will allow to decode the parameter names from output file `y.txt` of SDPB.

Having constructed and exported the problem and keys

```
Export["sdpbInput.m", CreateProblemTemplate[...]]
Export["sdpbInput.key.m", template["Keys", maxN]]
```

one finally does processing using SDPB, and, although running it is very dependent on machine one works with, the author feels in duty to provide at least one example of starting the task on Slurm cluster.

```
srun sdp2input -i sdpbInput.m -o sdpbInput.gz --precision 512 #
↪  binary digits
# run on 24 cores for 12 hours
srun -n 24 -t 12:00:00 sdpb \
  -s sdpbInput.gz \
  --procsPerNode 24 \
  --writeSolution y \
  --precision 512
```

This will generate the directory `sdpbInput.gz_out`, containing the result of the numerical experiment.

To load the data into the notebook, the function `LoadSDPBOutput` is available, with usage of

```
LoadSDPBOutput[directory, keyfile]
```

which in the example given shall be

```
LoadSDPBOutput[sdpbInput.gz_out, sdpbInput.key.m]
```

This results in association, of all status fields of `out.txt`, like `terminateReason` or `primaryGoal`, along with `vector` column, which contains the association of coefficients and their respective optimized values. The route from now on is entirely in hands of scientist that wants to understand the data, and the author wishes all the best to the readers with their papers.

3.4 Example: ϕ^4 theory

The example presented below replicates part of the experiment presented in [15]. The full code of this example is available as a part of ***SMatrixToolkit*** *repository in the notebook* ***pionScattering.nb****.*

3.4.1 Particles and amplitudes

Starting with definition of massive pion

```
pion = Particle["π0", 1]
```

and input and output particles for scattering amplitude

```
particles = ParticleContent[{pion, pion}, {pion, pion}]
```

Now, let's set up ρ variable

```
Rho[x]:= RhoVariable[x, Cut -> 4, Center -> 4/3]
```

and build up the ansatz

```
amplitude = RhoSeries[
  particles, α,
  Rho[s], Rho[t], Rho[u],
  $MaxN
]
```

Output of the last command should be displayed as fancy table with list of free coefficients `α[a, b, c]` and the amplitude ansatz. The correct crossing symmetry is inferred from particle content.

Adding poles and improvement terms is simply done by summation

```
amplitude += Pole[particles, g, s, 1]
amplitude += ExtraParam[particles, xi, 1/(1-Rho[s])]
```

3.4.2 Precomputation

Let's generate a list of integrals using constructed amplitude ansatz:

```
integrals = amplitudes["PartialIntegrals"]
```

and grid of s values

```
grid = ChebyshevGrid[$GridSize, Rho[s], WorkingPrecision->80]
```

At this point it maybe handy to export precomputation task (the variables `{integrals, grid}` are sufficient), and run it on remote machine. Launching the task is done by

```
PrecomputeGrid[
  $GridDirectory,
  integrals,
  grid,
  Range[0,$MaxSpin],
  options
]
```

where `options` can be any set of parameters passed to `NIntergate`, for example

```
options = Sequence[
  WorkingPrecision->80,
  AccuracyGoal->60,
  PrecisionGoal->60
]
```

After computation, the catalog `$GridDirectory` will contain text file `integralObjectsMap.m` along with binary files `spin=N.mx` for each spin; the

first one contains a dictionary that translate symbolic expressions to names, and second is populated with actual partial wave integrals.

To load,

```
data = LoadData[$GridDirectory]
```

3.4.3 Constructing problems

The general form of unitarity matrix as a function of amplitude is

$$\texttt{matrixFunct} = \begin{pmatrix} 1+\texttt{Re}[\#] & 1-\texttt{Im}[\#] \\ 1-\texttt{Im}[\#] & 1-\texttt{Re}[\#] \end{pmatrix} \texttt{\&} \ ;$$

In one go, one can modify existing amplitudes for:

- Experiments on quartic coupling

```
uMatrixQuartic =
  UnitarityMatrix[matrixFunct, amplitude ~
    FixCoefficient ~ (g == 0) ~
    FixCoefficient ~ (xi == 0)]
(* without improvement term *)
uMatrixQuarticImprov =
  UnitarityMatrix[matrixFunct, amplitude ~
    FixCoefficient ~ (g == 0)]
(* with improvement term *)
```

- Experiments with cubic coupling

```
uMatrixCubic = UnitarityMatrix[matrixFunct, amplitude ~
  FixCoefficient ~ (xi == 0)]
```

3.4.4 Creating tasks

One needs to match declared amplitude with precomputed integral table, for example

```
template = CreateProblemTemplate[{uMatrixQuartic}, data]
```

and with that, constructs SDPB input tasks with

```
Table[
  baseName="amplitude"<>
    "_n_"<>ToString[maxN]<>
    "_j_"<>ToString[maxN+deltaJ];
  (* the names for parameters *)
  Export[$OutputDir<>baseName<>".key.m",
    LimitKeys[template[[1,"keys"]],maxN]];
```

```
  (* the SDPB input *)
  Export[$OutputDir<>baseName<>".m",
    BuildSMatrix[
      template,
      Maximize[α[0,0,0]],
      data,
      MaxN->maxN,
      MaxJ->maxN+deltaJ
    ]
  ],
  {deltaJ, {8,12}}, (* maxJ = maxN+deltaJ *)
  {maxN, 10, 20, 2}
]
```

3.4.5 Computing

This heavily depends on infrastructure used, however

```
srun sdp2input \
  -i amplitude_n_22_j_30.m\
  -o amplitude_n_22_j_30.gz\
  --precision 256
srun -n 72 sdpb \
  -s amplitude_n_22_j_30.gz\
  --procsPerNode 72
```

shall do the trick for slurm-based clusters (switch 72 for suitable core count).

3.4.6 Results

For the sake of demonstration, example computations were done for the following problem. Both raw data, and the notebook to generate the plots is presented in pionScatteringResult directory of the repository. To provide at least some eye-candy diagrams, the figures 3.1 and 3.2 are attached.

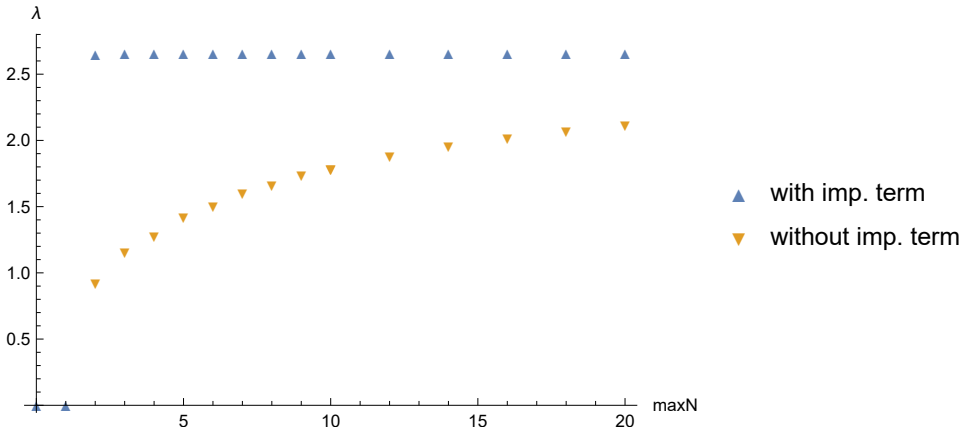

Figure 3.1: Upper bound of λ – comparison between ansatz with and without the improvement terms.

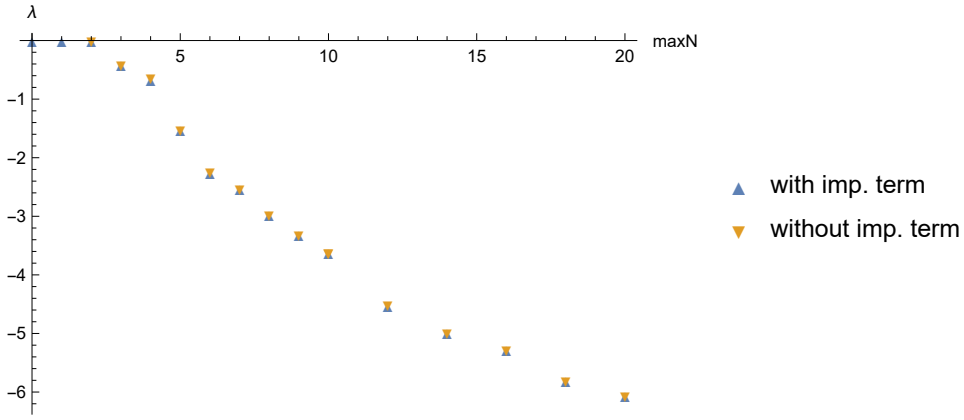

Figure 3.2: Lower bound of λ – the improvement term doesn't make any difference in this case.

Chapter 4

Bootstrapping a-anomaly

This chapter contains the work of the author with Dr. D. Karateev, Dr. Biswajit Sahoo and Prof. João Penedones, published in [9], along with the continuation of this work in [10]. The author also wants to acknowledge the work of Sébastien Reymond in his master thesis[22], which gave the foundations the author's paper[10] builds upon.

As mentioned in the introduction, the eventual goal of the bootstrap program is mapping out the space of consistent Quantum Field Theories.

To make the question bit more manageable, one can define a Quantum Field Theory non-perturbatively, as a renormalization group (RG) flow from the UV to the IR fixed points. These fixed points are assumed to have conformal invariance, and are described by Conformal Field Theories (CFTs). These CFT endpoints have parameters, which do not increase along the RG flow, giving the natural 'axis' along which these theories can be mapped[1].

In case of 2d CFTs such quantity is central charge c, related to Operator Product Expansion (OPE) of stress-energy tensor

$$\langle T(z)T(0)\rangle = \frac{c}{2z^4} \tag{4.1}$$

The full classification of 2d CFTs has been done for unitary theories between $c = 0$ and $c = 1$, via Minimal Models, explicitly constructed CFTs with finite number of primary operators and $c = 1 - \frac{6}{p(p-1)}$. Some explicit relevant deformations are known to trigger RG flow from one theory to another. This map of 2d CFT space is presented on the figure 4, along the map of 4d CFTs with respect to trace anomaly a.

This trace anomaly has a slightly more involved definition, which involves putting the CFT onto the curved background.

$$\langle T^{\mu}{}_{\mu}(x)\rangle_g = \ -a \times E_4 + c \times W^2, \tag{4.2}$$

The relation of this quantity to purely CFT expected value of three-point function of the stress tensor will be discussed in the next section, along with a review of the proof of monotonicity of a along the RG flow.

[1] These theories are not uniquely defined by aforementioned parameters. In 2D tetracritical Ising model and 3-state Potts model share same central charge, and in 4D a theory of 62 massless scalar fields have same a as a massless vector field.

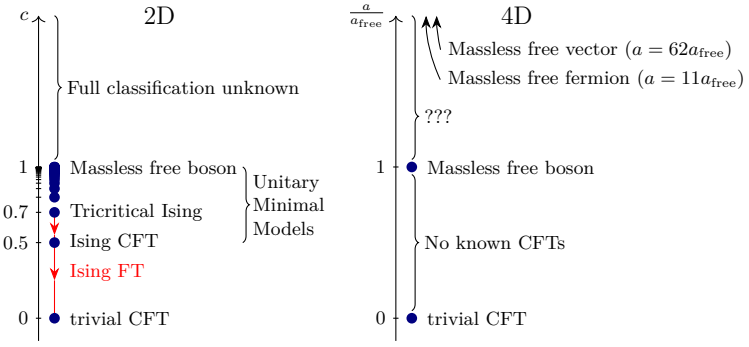

Figure 4.1: Sketch of the space of 2d and 4d CFTs[23].

One may ask where is the place of S-matrix bootstrap. As proven by [24], in 4d, the anomaly coefficients of UV CFT may be probed by taking QFT along the renormalization group flow, and couple it to compensator field φ, schematically

$$A_{QFT} \longrightarrow A_{QFT} + \int \mathrm{d}^4x\, \varphi(x) T^{\mu}_{\mu}(x) + \int \mathrm{d}^4x\, f^2 (\partial\varphi(x))^2 \tag{4.3}$$

If the theory A_{QFT} is gapped, RG flow would result in some effective field theory for field φ in IR. This EFT allows to probe the a_{UV} via dilaton scattering amplitude

$$\mathcal{T}_{BB\to BB} = \frac{a_{\mathrm{UV}}}{2f^4}\left(s^2+t^2+u^2\right) + \mathcal{O}\left(s^3\right) \tag{4.4}$$

The numerical experiments described in this chapter aim to find a lower bound of a-anomaly using S-matrix bootstrap. A QFT with single real scalar will be put under the scrutinizing glass of bootstrap method.

As a result of S-matrix bootstrap computations, bounds are found on a_{UV}, presented in the table below:

Theory	a-anomaly	Annotations
Single **free** scalar	$a_{\mathrm{free}} = \frac{1}{5760\pi^2}$	Derived analyticaly in [25], confirm to saturate unitarity bounds.
Single stable $\mathbb{Z}_2$-odd scalar	$\gtrsim 0.32 \cdot a_{\mathrm{free}}$	
Single stable scalar	$\gtrsim 0.15 \cdot a_{\mathrm{free}}$	No resonances at $s < 4m_A^2$, with m_A the mass of the lightest particle.
Two stable scalars	$\gtrsim 0.034 \cdot a_{\mathrm{free}}$	The minimal a-anomaly occurs for $m_X^2 \approx (2.5 \pm 0.1)\, m_A^2$.
Many stable scalars	$\gtrsim 0.036 \cdot a_{\mathrm{free}}$	The data comes only from preliminary investigations, which explains why the extrapolated bound is slightly inconsistent with the previous case.

4.1 Review of classic results

All the quantum field theories have a very special operator called the stress-tensor $T^{\mu\nu}(x)$. It is symmetric in its two Lorentz indices and obeys the conservation law, namely

$$T^{\mu\nu}(x) = T^{\nu\mu}(x), \qquad \partial_\mu T^{\mu\nu}(x) = 0. \tag{4.5}$$

4.1.1 Stress tensor and trace anomaly in CFTs

Let us start the discussion by considering conformally invariant quantum field theory. The conformal symmetry puts severe constraints on the form of correlation functions. In [25] it was shown that the most general two- and three-point functions of the stress tensor in CFTs have the following form

$$\langle 0|T^{\mu\nu}(x_1)T^{\rho\sigma}(x_2)|0\rangle = \frac{C_T}{x_{12}^8} \times \mathbf{T}_0^{\mu\nu;\rho\sigma}, \tag{4.6}$$

$$\langle 0|T^{\mu\nu}(x_1)T^{\rho\sigma}(x_2)T^{\alpha\beta}(x_3)|0\rangle = \frac{1}{x_{12}^4 x_{23}^4 x_{31}^4}\Big(\mathbb{A}\mathbf{T}_1^{\mu\nu;\rho\sigma;\alpha\beta} + \mathbb{B}\mathbf{T}_2^{\mu\nu;\rho\sigma;\alpha\beta} + \mathbb{C}\mathbf{T}_3^{\mu\nu;\rho\sigma;\alpha\beta}\Big). \tag{4.7}$$

Here the objects $\mathbf{T}_0$, $\mathbf{T}_1$, $\mathbf{T}_2$ and $\mathbf{T}_3$ take care of the correct behaviour of the correlation functions under conformal transformations. They are called tensor structures. The standard basis for these tensor structures is defined in appendix 4.A. The coefficient $C_T \geq 0$ is usually referred to as the central charge. The coefficients $\mathbb{A}$, $\mathbb{B}$ and $\mathbb{C}$ are called the OPE coefficients since they appear in the OPE expansion of the stress-tensor with itself. All of them are real quantities. Due to the conformal Ward identities[2] the following relation holds

$$C_T \;=\; \frac{\pi^2}{3}\Big(14\mathbb{A} - 2\mathbb{B} - 5\mathbb{C}\Big). \tag{4.8}$$

Summarizing, there are three independent parameters describing the 2- and the 3-point function of the stress-tensor. One can choose these three parameters to be for example $\{C_T,\ \mathbb{A},\ \mathbb{B}\}$. It is standard to also define the following quantities

$$a \equiv \frac{\pi^4}{64\times 90}\Big(9\mathbb{A} - 2\mathbb{B} - 10\mathbb{C}\Big), \qquad c \equiv \frac{\pi^4}{64\times 30}\Big(14\mathbb{A} - 2\mathbb{B} - 5\mathbb{C}\Big) = \frac{\pi^2}{64\times 10}C_T. \tag{4.9}$$

Finally we recall that in CFTs the trace of the stress-tensor vanishes, namely

$$T^{\mu}{}_{\mu}(x) = 0. \tag{4.10}$$

Let us now discuss CFTs on the curved background which is described by the metric $g_{\mu\nu}(x)$. Conformal invariance on a curved background is achieved by requiring diff $\times$ Weyl invariance. We recall that the Weyl transformation is defined as

$$g_{\mu\nu}(x) \to e^{2\sigma(x)}g_{\mu\nu}(x), \qquad \mathcal{O}(x) \to e^{-\Delta_{\mathcal{O}}\sigma(x)}\mathcal{O}(x), \tag{4.11}$$

[2] All the generators of the conformal transformation can be written as certain integral of the stress-tensor, see for example [25]. By performing appropriate integrals over one stress-tensor in (4.7) and using the properties of the generators we effectively obtain the two-point function (4.6).

where $\sigma(x)$ is an arbitrary scalar function, $\mathcal{O}(x)$ is a local scalar operator and $\Delta_{\mathcal{O}}$ is the scaling dimension of the operator $\mathcal{O}(x)$. Contrary to the flat space-time where (4.10) holds, for CFTs on the curved background we instead have

$$\langle 0|T^{\mu}{}_{\mu}(x)|0\rangle_g = \ -a \times E_4 + c \times W^2, \tag{4.12}$$

where E_4 is the Euler density defined in (4.148) and W^2 is the square of Weyl tensor defined in (4.149). The subscript g in the left-hand side of (4.12) indicates that the CFT is on the curved background rather than on the flat one. The coefficients a and c are exactly the ones introduced in (4.9). They are called the Weyl anomalies as well as trace anomalies. The name Weyl anomaly is appropriate because exact Weyl invariance implies $\langle 0|T^{\mu}{}_{\mu}(x)|0\rangle_g = 0$.

4.1.2 Compensator field and the dilaton particle

Let us define a generic quantum field theory as the renormalization group flow from the UV to the IR fixed points which are described by the UV and the IR conformal field theories. Such a theory in curved background can be described by the action

$$A(g, M_i) \equiv A_{\text{UV CFT}}(g) + A_{\text{deformation}}(g, M_i), \tag{4.13}$$

where the deformation of the UV CFT has the form

$$A_{\text{deformation}}(g, M_i) = \sum_i \int d^4x \sqrt{-g} \left(\lambda_i M_i^{4-\Delta_i} \mathcal{O}_i(x)\right). \tag{4.14}$$

Here $\mathcal{O}_i(x)$ are relevant scalar UV CFT operators (operators obeying $\Delta_i < 4$), λ_i are dimensionless coefficients and M_i are the mass scales which control when the deformation due to a particular operator becomes important. The explicit dependence on $g_{\mu\nu}(x)$ indicates that we work on a generic curved background. The QFT in flat space-time is recovered by setting $g_{\mu\nu}(x)$ to the flat metric $\eta_{\mu\nu}$. The determinant of the metric is defined as follows

$$g \equiv \det\, g_{\mu\nu}(x). \tag{4.15}$$

The action (4.14) is diff invariant by construction.

In curved background the stress-tensor is defined as

$$T^{\mu\nu}(x) = \frac{2}{\sqrt{-g}} \frac{\delta A(g, M_i)}{\delta g_{\mu\nu}(x)}. \tag{4.16}$$

Under the Weyl transformation (4.11), the trace of the stress-tensor can be defined as a variation of the action with respect to the infinitesimal Weyl transformation parameter σ in the following way,

$$T^{\mu}_{\mu}(x) \equiv \frac{1}{\sqrt{-g}} \frac{\delta_W A(g, M_i)}{\delta \sigma(x)}. \tag{4.17}$$

Performing the Weyl transformation (4.11) in (4.13) and focusing on flat space-time we obtain the trace of the stress-tensor using the above definition, which reads

$$g_{\mu\nu} = \eta_{\mu\nu}: \qquad T^{\mu}{}_{\mu}(x) = \sum_i \lambda_i (4 - \Delta_i) M_i^{4-\Delta_i} \mathcal{O}_i(x). \tag{4.18}$$

This is the standard result in QFT, namely the trace is proportional to the deforming operators.

The correlation functions of the stress-tensor both in the UV and IR are described by (4.6) and (4.7) where the coefficients C_T, $\mathbb{A}$, $\mathbb{B}$ and $\mathbb{C}$ have an additional label UV and IR respectively. Out of all the above coefficients the a trace anomaly is the most interesting. In [26] it was conjectured that

$$a^{\rm UV} - a^{\rm IR} \geq 0, \tag{4.19}$$

where the equality can hold only if there is no flow and the theory remains conformal, in other words if $A_{\rm deformation} = 0$ in (4.13). The inequality (4.19) is known as the a-theorem. It was shown to hold in perturbation theory in [27, 28]. It was proven non-perturbatively in [29], for further discussion see also [29–31]. The proof of [29] gives also the prescription on how to probe/compute the difference $(a^{\rm UV} - a^{\rm IR})$ in a given QFT. One of the main ingredients of this proof is the compensator field and the associated particle which we call the dilaton. In the rest of this section we will define the compensator field and the dilaton particle.

Let us work with the action (4.13) on a curved background. It is diff invariant but not Weyl invariant. There are two sources which break the Weyl symmetry, namely the trace anomaly of the UV and IR CFTs given by (4.12) and the deformation part of the action $A_{\rm deformation}$ in (4.13) which explicitly depends on the scale. The latter breaking can be compensated for in a modified theory with the following action

$$A'(g, M_i, \Omega) \equiv A(g, M_i\Omega(x)) + A_{\rm dynamics}(g, \Omega), \tag{4.20}$$

where $\Omega(x)$ is a real scalar field called the compensator field and the action A was defined in (4.13). Both the metric $g_{\mu\nu}(x)$ and the compensator field $\Omega(x)$ are non-dynamical fields. We can however promote them to dynamical probe fields by adding a kinetic term $A_{\rm dynamics}(g, \Omega)$. We will discuss possible convenient choices for this term in the end of this subsection. The compensator field $\Omega(x)$ can be represented in the following two ways

$$\Omega(x) = e^{-\tau(x)} = 1 - \frac{\varphi(x)}{\sqrt{2}f}. \tag{4.21}$$

We refer to the real scalar fields $\tau(x)$ and $\varphi(x)$ also as the compensator or the dilaton fields interchangeably. Here f is a new parameter with mass dimension one. The following relation holds

$$\tau(x) = \frac{\varphi(x)}{\sqrt{2}f} + O\left(\frac{1}{f^2}\right). \tag{4.22}$$

Let us now emphasize that the action (4.20) can be made invariant under the Weyl transformation (4.11) given that the dilaton transforms in the following way

$$\tau(x) \to \tau(x) + \sigma(x) \tag{4.23}$$

and that the term $A_{\rm dynamics}$ is chosen appropriately. The particle created by the compensator (or the dilaton) field $\varphi(x)$ from the vacuum is called the dilaton particle. It will be denoted by B throughout this paper.

The simplest[3] choice for $A_{\text{dynamics}}(g,\Omega)$, already used in [29], reads as

$$A_{\text{dynamics}}(g,\Omega)=\frac{1}{6}\,f^2\int d^4x\,\sqrt{-\widehat{g}}\,R(\widehat{g}), \tag{4.24}$$

where we have defined

$$\widehat{g}_{\mu\nu}\equiv e^{-2\tau}g_{\mu\nu}. \tag{4.25}$$

The action (4.24) is Weyl invariant at the classical level but not at the quantum level. One can simply see this for instance by taking the $f\to\infty$ limit and focusing on the flat space. The action (4.24) then reduces to the standard kinetic term describing free massless scalar. Free massless scalar gives a particular example of a CFT with trace anomalies a and c reported in (4.153). The latter break Weyl invariance via (4.12). There are many other possible choices of $A_{\text{dynamics}}(g,\Omega)$. Let us stress, that these choices do not have to be Weyl invariant even classically.

Let us now focus on flat space-time $g_{\mu\nu}=\eta_{\mu\nu}$. Using (4.14), (4.18), (4.21) and (4.24) we can rewrite the modified action (4.20) in the following equivalent way[4]

$$A'(M_i,\varphi)\equiv A(M_i)-\frac{1}{\sqrt{2}f}\int d^4x\,T^{\mu}{}_{\mu}(x)\varphi(x)-\int d^4x\left(\frac{1}{2}\partial_\mu\varphi(x)\partial^\mu\varphi(x)\right)+O\left(\frac{1}{f^2}\right). \tag{4.26}$$

From (4.26) it becomes obvious that in the limit $f\to\infty$ the interaction between the dilaton and the rest of the system disappears and the action (4.20) simply becomes the original one plus the freely propagating dilaton field. The dilaton field $\varphi(x)$ should be seen as a probe for a given QFT which does not disturb it in the limit $f\to\infty$.

4.1.3 a-theorem

Let us now take the UV and IR limits of the action (4.20). They can be written as[5]

$$\begin{aligned} A'_{\text{UV}}(g,\Omega)&\equiv A_{\text{UV CFT}}(g)+A_{\text{dynamics}}(g,\Omega),\\ A'_{\text{IR}}(g,\Omega)&\equiv A_{\text{IR CFT}}(g)+A_{\text{dilaton EFT}}(g,\Omega)+A_{\text{dynamics}}(g,\Omega). \end{aligned} \tag{4.27}$$

Here $A_{\text{dilaton EFT}}$ is the effective field theory (EFT) action describing the dilaton interaction at low energy. In order to obtain it in some explicit QFT model one needs to integrate out all the "massive" degrees of freedom throughout the RG

[3] As it will be shown in section 4.2, the low energy constrains are not influenced by the choice of dynamics term.

[4] If in the UV CFT there exists more than one relevant operator which can be used to deform the theory (i.e. for $i>1$), the neglected terms starting from order $O(f^{-2})$ in equation (4.26) can not be expressed in terms of the trace of the stress-tensor in general. Indeed, the order $O(f^{-2})$ contribution in $A'(M_i)$ turns out to be $\frac{1}{4f^2}\sum_i(4-\Delta_i)(3-\Delta_i)\int d^4x\,\varphi^2(x)\left(\lambda_i M_i^{4-\Delta_i}\mathcal{O}_i(x)\right)$, which is not expressible in terms of the trace of the stress tensor given in equation (4.18) for $i>1$.

[5] Let us emphasize that we have made here a very non-trivial statement that the IR dilaton EFT action completely decouples from the IR CFT even though dilaton self interaction is present. One can argue for this at least in the limit of flat space-time: by construction (4.20), dilaton couples only to mass parameters, IR CFT instead does not have dimensionful parameters.

flow which is almost impossible in practice. Luckily there is a model independent way to compute $A_{\text{dilaton EFT}}$ which we will now review.

Consider the action (4.20). It breaks Weyl invariance in a very special way. The Weyl symmetry breaking is coming only from the UV and IR fixed points (4.27). Taking into account (4.12) we get

$$\begin{aligned}\delta_W A'_{\rm UV}(g,\Omega) = \int d^4x\sqrt{-g}\sigma(x)\Big(&-a^{\rm UV}\times E_4\\ &+c^{\rm UV}\times W^2\Big)+\delta_W A_{\text{dynamics}}(g,\Omega),\\ \delta_W A'_{\rm IR}(g,\Omega) = \int d^4x\sqrt{-g}\sigma(x)\Big(&-a^{\rm IR}\times E_4+c^{\rm IR}\times W^2\Big)\\ &+\delta_W A_{\text{dilaton EFT}}(g,\Omega)+\delta_W A_{\text{dynamics}}(g,\Omega).\end{aligned}\tag{4.28}$$

Here δ_W stands for the infinitesimal Weyl variation.

Let us now assume that the Weyl anomaly in the UV matches the Weyl anomaly in the IR, in other words

$$\delta_W A'_{\rm UV}(g,\Omega)=\delta_W A'_{\rm IR}(g,\Omega).\tag{4.29}$$

Notice that contrary to the 't Hooft anomaly matching, there is no proof for the Weyl anomaly matching (4.29) and it might not be true in general.[6] For further discussion on Weyl anomaly matching and its consequences see [11]. Plugging (4.28) in (4.29) we obtain the following variational equation

$$\begin{aligned}&\delta_W A_{\text{dilaton EFT}}(g,\Omega)=\\ &\qquad\int d^4x\sqrt{-g}\sigma(x)\Big(-\big(a^{\rm UV}-a^{\rm IR}\big)\times E_4+\big(c^{\rm UV}-c^{\rm IR}\big)\times W^2\Big).\end{aligned}\tag{4.30}$$

The most general solution for this equation can be written in the following form

$$\begin{aligned}A_{\text{dilaton EFT}}(g,\Omega) = &-(a^{\rm UV}-a^{\rm IR})\times A_a(g,\Omega)\\ &+(c^{\rm UV}-c^{\rm IR})\times A_c(g,\Omega)\\ &+\ A_{\text{invariant}}(g,\Omega),\end{aligned}\tag{4.31}$$

where the two newly introduced terms $A_a(g,\Omega)$ and $A_c(g,\Omega)$ behave in the following way under the infinitesimal Weyl transformation

$$\delta_W A_a(g,\Omega)=\int d^4x\sqrt{-g}\sigma(x)\,E_4,\qquad \delta_W A_c(g,\Omega)=\int d^4x\sqrt{-g}\sigma(x)\,W^2.\tag{4.32}$$

The term $A_{\text{invariant}}$ instead remains completely invariant. The solution to the above requirement was found in [29, 33], it reads

$$\begin{aligned}A_a(g,\Omega) = \int d^4x\sqrt{-g}\Big(&\tau E_4+4\left(R^{\mu\nu}-\frac{1}{2}g^{\mu\nu}R\right)(\partial_\mu\tau)(\partial_\nu\tau)\\ &-4(\partial\tau)^2(\partial^2\tau)+2(\partial\tau)^4\Big),\\ A_c(g,\Omega) = \int d^4x\sqrt{-g}\tau(x)\,W^2.&\end{aligned}\tag{4.33}$$

[6] In fact the authors of [32] found an apparent mismatch of the c-anomaly on the Higgs branch of $\mathcal{N}=2$ super-conformal field theory where conformal symmetry is spontaneously broken.

This solution is not easy to obtain but it is easy to check that it satisfies (4.32). It is also important to stress that even though (4.29) might not hold for every QFT, the weaker Wess-Zumino consistency condition exists, see [11], which implies that at the very least the first line in (4.33) always holds true.

The most general Weyl invariant action can be parametrized as follows

$$A_{\text{invariant}}(g,\Omega)=\int d^4x\ \sqrt{-\widehat{g}}\Big(M^4\lambda+M^2r_0\widehat{R}\ +\ r_1\widehat{R}^2+r_2\widehat{W}^2+r_3\widehat{E}_4+\dots\Big). \tag{4.34}$$

Here the Ricci scalar, Weyl tensor and the Euler density are built out of the metric (4.25). The real dimensionless parameters λ, r_0, r_1, r_2 and r_3 depend on a particular QFT. The EFT cut-off scale M can be chosen to be the lowest deformation energy scale of the UV CFT. In spontaneously broken QFTs $\lambda=0$, but in generic QFTs $\lambda\neq 0$. However, when defining the action (4.20), if needed, one can fine tune the counterterms in such a way that $\lambda=0$.

In flat space the solution (4.31) together with (4.33) and (4.34) simply leads to

$$\begin{aligned}A_{\text{dilaton EFT}}(\varphi)=\frac{M^4\lambda}{4f^4}\int d^4x\big(\varphi(x)\big)^4\ +\frac{6M^2r_0}{f^2}\int d^4x\Big(-\frac{1}{2}p_\mu\varphi(x)p^\mu\varphi(x)\Big)\\ +36r_1\int d^4x\Big(\frac{1}{2f^2}+\frac{\varphi(x)}{\sqrt{2}f^3}+\frac{3\varphi(x)^2}{4f^4}\Big)(p^2\varphi(x))^2\\ +\frac{a^{\text{UV}}-a^{\text{IR}}}{2f^4}\times\int d^4x\ \big(\partial\varphi(x)\big)^4+\ O\big(f^{-5}p^4\varphi^5\ ,\ f^{-4}p^6\varphi^4\big).\end{aligned} \tag{4.35}$$

The term proportional to r_0 gives an $O(f^{-2})$ correction to the dilaton kinetic term coming from $A_{\text{dynamics}}(g,\Omega)$. In the limit $f\to\infty$ it should be neglected. The interacting part of the dilaton scattering process $B(p_1)B(p_2)\to B(p_3)B(p_4)$ at low energy is described by the effective action (4.35) and has the following form

$$\lim_{f\to\infty}f^4\mathcal{T}_{BB\to BB}(s,t,u)=6M^4\lambda+(a^{\text{UV}}-a^{\text{IR}})\times(s^2+t^2+u^2)+O(s^3). \tag{4.36}$$

where $s=-(p_1+p_2)^2\ ,\ t=-(p_1-p_3)^2\ ,\ u=-(p_1-p_4)^2$ with $s+t+u=0$. Note, that the term proportional to r_1 in (4.35) does not contribute to this scattering amplitude, since it vanishes under the dilaton equation of motion. Using the standard approach one can write the following dispersion relation in the $f\to\infty$ limit

$$\begin{aligned}a^{\text{UV}}-a^{\text{IR}}&=\frac{f^4}{2}\ \frac{1}{2\pi i}\oint_0\frac{ds}{s^3}\ \mathcal{T}_{BB\to BB}(s,0,-s)\\ &=\ \frac{f^4}{\pi}\ \int_0^\infty\frac{ds}{s^3}\ \text{Im}\mathcal{T}_{BB\to BB}(s,0,-s).\end{aligned} \tag{4.37}$$

Since $\text{Im}\mathcal{T}_{BB\to BB}(s,0,-s)=s\ \sigma(s)\geq 0$ where $\sigma(s)$ is the total cross section for the scattering of $BB\to$ anything, $(a^{\text{UV}}-a^{\text{IR}})$ is non-negative. This proves the a-theorem.

Note that the dispersion relation (4.37) conveniently provides the sum rule

$$a^{\text{UV}}-a^{\text{IR}}=\frac{f^4}{2}=16f^4\sum_{\ell=0,2,4\dots}\int_0^\infty\frac{ds}{s^3}\ \text{Im}\mathcal{T}^\ell_{BB\to BB} \tag{4.38}$$

Application in free scalar theory As an application of the a-theorem consider the UV CFT which is generated by the free massless field $\Phi(x)$, namely we have the action

$$A_{\text{UV CFT}} = -\int d^4x \left(\frac{1}{2}\partial_\mu\Phi(x)\partial^\mu\Phi(x)\right). \tag{4.39}$$

It is straightforward to compute then the two- and tree-point correlation functions of the stress-tensor with itself. One obtains (4.6) and (4.7) with

$$C_T^{\text{UV}} = \frac{1}{3\pi^4}, \qquad \mathbb{A}^{\text{UV}} = \frac{1}{27\pi^6}\ , \qquad \mathbb{B}^{\text{UV}} = -\frac{4}{27\pi^6}\ , \qquad \mathbb{C}^{\text{UV}} = -\frac{1}{27\pi^6}. \tag{4.40}$$

Let us now add the following deformation

$$A_{\text{deformation}}(m) = -\frac{1}{2}m^2\Phi(x)^2, \tag{4.41}$$

where m becomes the mass of the field Φ. This triggers the flow to an empty IR fixed point, thus in the deep IR we simply have

$$C_T^{\text{IR}} = 0, \qquad \mathbb{A}^{\text{IR}} = 0, \qquad \mathbb{B}^{\text{IR}} = 0, \qquad \mathbb{C}^{\text{IR}} = 0. \tag{4.42}$$

As a result according to (4.9) we get the following UV an IR a-anomaly

$$a^{\text{UV}} = \frac{1}{5760\pi^2}, \qquad c^{\text{UV}} = \frac{1}{1920\pi^2}, \qquad a^{\text{IR}} = 0, \qquad c^{\text{IR}} = 0. \tag{4.43}$$

Using the the modified action (4.26) we can also compute the dilaton scattering at low energies. We get

$$\lim_{f\to\infty} f^4\mathcal{T}_{BB\to BB}(s,t,u) = \frac{1}{5760\pi^2} \times (s^2+t^2+u^2) + O(s^3). \tag{4.44}$$

The details of the computation are given in appendix 4.B. The result (4.44) is in a perfect agreement with CFT result (4.43).

4.2 Matter - dilaton scattering at low energy

In [29] the authors derived the most general low energy effective action of the dilaton field in a curved background. As reviewed in section 4.1.3 this action is given in (4.31). It is found by solving the 't Hooft anomaly matching conditions which can be written as a system of differential equations (4.32). In flat space this action reduces to (4.35) and leads to the explicit expression of the low energy $BB \to BB$ amplitude given by equation (4.36).

Here we perform a similar analysis for the $AB \to AB$ amplitude. We start in section 4.2.1 by writing the most general low energy effective action in curved background which describes this process. In section 4.2.2 we evaluate it in flat space and derive the resulting scattering amplitude at low energy. The final result turns out to be universal (independent of a particular model) and is given by equation (4.77).

For simplicity, first and a theory where asymptotic particle A obeys $\mathbb{Z}_2$ symmetry. Afterwards the difference introduced by lifting this symmetry will be discussed.

4.2.1 The most general effective action – $\mathbb{Z}_2$-symmetric case

The assumption of this paper is the presence of a single $\mathbb{Z}_2$ asymptotic particle A. Let us denote by $\Phi(x)$ the effective field associated to this particle. We would like to find the most general low energy effective action $A_{\text{eff}}[\Phi, \varphi]$, using which we can compute the S-matrix for the scattering process $AB \to AB$.[7] We remind that the filed $\varphi(x)$ creates the dilaton particle B from the vacuum.

Following the discussion of section 4.1.2 we work with the diff and Weyl invariant action (4.20). We would like to rewrite this action in terms of low energy degrees of freedom $\Phi(x)$ and $\varphi(x)$ using only diff and Weyl symmetry. The main ingredients for doing this are the Weyl invariant metric $\widehat{g}_{\mu\nu}(x)$ and scalar $\widehat{\Phi}(x)$, defined in terms of background metric $g_{\mu\nu}(x)$ and scalar field $\Phi(x)$ in the following way

$$\widehat{g}_{\mu\nu}(x) = e^{-2\tau(x)}\, g_{\mu\nu}(x), \qquad \widehat{\Phi}(x) = e^{\Delta\tau(x)}\Phi(x), \tag{4.45}$$

where $\tau(x)$ is the dilaton field related to $\varphi(x)$ according to (4.21) and Δ is some effective scaling dimension of the field $\Phi(x)$. Now we want to write the most generic form of the effective action $A^g_{\text{eff}}[\Phi, \varphi]$ in the curved background, which should be general coordinate invariant in the metric $\widehat{g}_{\mu\nu}(x)$ and should contain the scalar $\widehat{\Phi}(x)$. Finally, to get the flat space effective action (only perturbed by soft dilaton field φ), we need to substitute $g_{\mu\nu} = \eta_{\mu\nu}$ in $A^g_{\text{eff}}[\Phi, \varphi]$, resulting in $A_{\text{eff}}[\Phi, \varphi]$, which describes the scattering process $AB \to AB$. For the construction of $A^g_{\text{eff}}[\Phi, \varphi]$ we adapt a variation of the covariantization prescription originally developed in [34, 35] for the soft gravitational background.

Let us start from the tangent space with locally flat metric η_{ab}. The connection between the curved and tangent space is provided by the objects $e^a_\mu(x)$ and $E^\mu_a(x)$ called the vierbein and inverse vierbein respectively. They are defined via the relations

$$\widehat{g}_{\mu\nu}(x) = e^a_\mu(x) e^b_\nu(x)\eta_{ab}, \qquad \eta_{ab} = E^\mu_a(x) E^\nu_b(x)\widehat{g}_{\mu\nu}, \tag{4.46}$$

where η_{ab} is the flat Minkowski metric. We start with the quadratic part of the tangent space 1PI effective action for scalar field $\Phi(x)$,

$$A^{\text{tangent}} = \frac{1}{2}\int \mathrm{d}^4x \;\; \Phi(x) K(\partial_a)\Phi(x) \;, \tag{4.47}$$

where we dropped all the terms with cubic and higher powers of Φ since they will not contribute to the scattering process $AB \to AB$ after covariantization. The most general form of the kinetic operator K can be written as[8]

$$K(\partial_a) \equiv \sum_{n=0}^{\infty} c_n^{a_1 a_2 \ldots a_n} \partial_{a_1}\partial_{a_2}\ldots\partial_{a_n}, \tag{4.48}$$

where the coefficients c_n are built out of all possible combinations of η^{ab} with arbitrary numerical coefficients and $c_n^{a_1\ldots a_n}$ is symmetric under the exchange

[7] One can think of the effective action $A_{\text{eff}}[\Phi, \varphi]$ as the Legendre transform of the generating function $W[\zeta, \varphi]$ where $\zeta(x)$ is the source that couples to a local operator $\mathcal{O}_\Delta(x)$ that can create particle A from the vacuum.

[8] The form of the kinetic operator as Taylor series expansion in derivatives is always possible for a EFT where massless particles are absent.

of tangent space indices. Now we would like to first covariantize the tangent space action (4.47). This requires to make the following replacements: $\mathrm{d}^4x \to \mathrm{d}^4x\sqrt{-\widehat{g}}$ together with

$$K(\partial_a) \to \sum_{n=0}^{\infty} c_n^{a_1 a_2 \ldots a_n} E_{a_1}^{\mu_1} E_{a_2}^{\mu_2} \cdots E_{a_n}^{\mu_n} D_{\mu_1} D_{\mu_2} \cdots D_{\mu_n} \ \equiv F. \tag{4.49}$$

Above F is obtained only by minimally covariantizing the kinetic operator. In principle F could contain non-minimal terms involving one or more Riemann tensors and derivatives on them. Since those non-minimal terms contain two or more derivatives of the dilaton field, they start contributing at higher orders in low dilaton momentum expansion of $AB \to AB$ scattering amplitude. Since our interest is to constrain first two terms in low dilaton momentum expansion of the scattering amplitude $AB \to AB$, we are not including those terms under our covariantization process. Now on top of the covariantization we also need to make the action Weyl invariant which is achieved by replacing $\Phi(x) \to \widehat{\Phi}(x)$. Also in $A^g_{\rm eff}[\Phi, \varphi]$ we should include general coordinate invariant scalar term purely constructed out of metric $\widehat{g}_{\mu\nu}(x)$ given in (4.34) as well as the classically Weyl invariant action (4.24) to make the dilaton dynamical. As a result of all these, our curved space effective action becomes

$$A^g_{\rm eff}[\Phi, \varphi] = \frac{1}{2}\int \mathrm{d}^4x\, \sqrt{-\widehat{g}}\, \widehat{\Phi}(x) F \widehat{\Phi}(x) \ + A_{\rm dynamics}(g, \Omega) + A_{\rm invariant}(g, \Omega) + \ \cdots \tag{4.50}$$

We denote by $\ldots$ all the possible non-minimal terms appearing in the covariantization procedure as described earlier. From here on to reduce complexity we ignore $A_{\rm invariant}(g, \Omega)$ part of the above action as it always contribute terms at higher power in f^{-1} compare to similar terms coming from $A_{\rm dynamics}(g, \Omega)$ and won't affect our result later on.

Now to read off the flat space effective action from $A_{\rm eff}[\Phi, \varphi]$ from (4.50) we need to set $g_{\mu\nu}(x) = \eta_{\mu\nu}$ which in turn requires the following substitutions in (4.50)

$$\begin{aligned}
\widehat{g}_{\mu\nu}(x) &= e^{-2\tau(x)}\, \eta_{\mu\nu} = \Big(1 - \frac{\varphi}{\sqrt{2}f}\Big)^2\, \eta_{\mu\nu}, \\
e^a_\mu(x) &= e^{-\tau(x)}\delta^a_\mu = \Big(1 - \frac{\varphi}{\sqrt{2}f}\Big)\, \delta^a_\mu, \\
E^\mu_a(x) &= e^{\tau(x)}\delta^\mu_a = \Big(1 - \frac{\varphi}{\sqrt{2}f}\Big)^{-1} \delta^\mu_a.
\end{aligned} \tag{4.51}$$

With these substitutions the flat space effective action becomes

$$\begin{aligned}
A_{\rm eff}[\Phi, \varphi] \ &= \ \frac{1}{2}\int \mathrm{d}^4x \Big(1 - \frac{\varphi(x)}{\sqrt{2}f}\Big)^{4-\Delta} \Phi(x) \sum_{n=0}^{\infty} c_n^{a_1 a_2 \ldots a_n} \Big(1 - \frac{\varphi(x)}{\sqrt{2}f}\Big)^{-n} \delta^{\mu_1}_{a_1}\delta^{\mu_2}_{a_2}\cdots\delta^{\mu_n}_{a_n} \\
&\quad \times D_{\mu_1} D_{\mu_2} \cdots D_{\mu_n} \Big(1 - \frac{\varphi(x)}{\sqrt{2}f}\Big)^{-\Delta} \Phi(x) \\
&\quad + \int \mathrm{d}^4x \left(-\frac{1}{2}\partial_\mu\varphi(x)\partial^\mu\varphi(x) + \frac{1}{f}O(p^4\varphi^3)\right) \ + \cdots
\end{aligned} \tag{4.52}$$

Now we expand the effective action $A_{\rm eff}$ in power of f to the second order around $f = \infty$. The result can be written in the following form

$$A_{\rm eff} = A^0_{\rm eff} + \ A^1_{\rm eff} + \ A^2_{\rm eff} + \ldots. \tag{4.53}$$

where the superscript n in $A^n_{\rm eff}$ indicates the order in f^{-n} expansion of $A_{\rm eff}$ around $f \to \infty$. The first term in (4.53) reads as

$$A^0_{\rm eff} = \frac{1}{2}\int {\rm d}^4x \sum_{n=0}^{\infty} c_n^{a_1 a_2 \ldots a_n}\Big(\Phi(x) p_{a_1} p_{a_2} \cdots p_{a_n}\Phi(x)\Big) - \frac{1}{2}\int {\rm d}^4x\, \partial_\mu\varphi(x)\partial^\mu\varphi(x). \tag{4.54}$$

In the second term $A^1_{\rm eff}$ we grouped all the contributions proportional to a single dilaton field φ up to one derivative acting on it and also schematically kept the order of three dilaton field interaction term. The result reads

$$\begin{aligned} A^1_{\rm eff} = \frac{1}{2\sqrt{2}f}\int {\rm d}^4x \Bigg(& \sum_{n=0}^{\infty} c_n^{a_1 a_2 \ldots a_n}\Big\{n - (4-2\Delta)\Big\}\varphi(x)\Phi(x) p_{a_1} p_{a_2}\cdots p_{a_n}\Phi(x) \\ & + \sum_{n=2}^{\infty} c_n^{a_1\ldots a_n} \sum_{\substack{i,j=1\\ i<j}}^{n} \Big\{\delta^\nu_{a_i} p_{a_j}\varphi(x) + \delta^\nu_{a_j} p_{a_i}\varphi(x) - \eta_{a_i a_j} p^\nu \varphi(x)\Big\} \\ & \qquad \times \Phi(x) p_{a_1}\cdots p_{a_{i-1}} p_{a_{i+1}}\cdots p_{a_{j-1}} p_{a_{j+1}}\cdots p_{a_n} p_\nu \Phi(x) \\ & + \sum_{n=1}^{\infty} c_n^{a_1\ldots a_n} \sum_{i=1}^{n} \Delta p_{a_i}\varphi(x)\ \Phi(x) p_{a_1}\cdots p_{a_{i-1}} p_{a_{i+1}}\cdots p_{a_n}\Phi(x) \\ & + O(\Phi^2 p^2\varphi,\ p^4\varphi^3)\Bigg)\,. \end{aligned} \tag{4.55}$$

In the above expression the first term is linear in $\varphi(x)$. It is obtained by replacing all the covariant derivatives in (4.52) by ordinary derivatives and commuting $\left(1-\frac{\varphi(x)}{\sqrt{2}f}\right)^{-\Delta}$ through the derivatives (in other words neglecting terms containing derivatives operating on $\varphi(x)$). Expansion of the resulting expression at linear order in $\varphi(x)$ generates the first term. In the second and third terms in (4.55) one derivative operates on $\varphi(x)$. In presence of two covariant derivatives on $\Phi(x)$ in the first term in (4.52), we need to substitute $D_{\mu_i}D_{\mu_j}\Phi(x) = p_{\mu_i}p_{\mu_j}\Phi(x) - \Gamma^\nu_{\mu_i\mu_j}p_\nu\Phi(x)$. Then writing down the Christoffel connection up to linear order in $\varphi(x)$ for any pair of such covariant derivatives and setting $\varphi = 0$ in all other places we get the second term above. On the other hand when any one of the ordinary derivative from the set of covariant derivatives operates on $\left(1-\frac{\varphi(x)}{\sqrt{2}f}\right)^{-\Delta}$ in the first term in (4.52), we get the third term above at the linear order in $\varphi(x)$ from the expansion of the resulting expression. First non-vanishing contribution to three dilaton interaction appears at four derivative order as schematically written as $O(p^4\varphi^3)$ in the above expression.

In the third term of (4.53), we grouped all the contributions involving $\varphi(x)^2$ and no derivative on it, and the result reads

$$\begin{aligned} A^2_{\rm eff} \;=\; & \frac{1}{2}\int {\rm d}^4x \left(\frac{\varphi(x)}{\sqrt{2}f}\right)^2 \Phi(x)\sum_{n=0}^{\infty}\left(\frac{(4-2\Delta)(3-2\Delta)}{2} - (4-2\Delta)\ n + \frac{n(n+1)}{2}\right) \\ & \times\ c_n^{a_1 a_2\cdots a_n} p_{a_1} p_{a_2}\cdots p_{a_n}\Phi(x)\ +\ \frac{1}{f^2}O(\Phi^2\varphi p\varphi). \end{aligned} \tag{4.56}$$

To get the above contribution we first replace all the covariant derivatives in (4.52) by ordinary derivatives and commute $\left(1-\frac{\varphi(x)}{\sqrt{2}f}\right)^{-\Delta}$ through the deriva-

tives neglecting terms containing derivatives operating on $\varphi(x)$. Then we expand the resulting contribution and collect terms at quadratic order in $\varphi(x)$. We do not need to compute $A^n_{\rm eff}$ for $n \geq 3$ as these terms of the effective action do not contribute to $AB \to AB$ scattering amplitude. Another important point is that once the expansion is done in power of f about $f \to \infty$ in (4.53), in the expressions of $A^n_{\rm eff}$ both tangent space indices $a_1, a_2, \cdots$ and curved space indices $\mu_1, \mu_2, \cdots$ can be treated as just flat space Lorentz indices.

Momentum space It is cleaner to present further discussion in momentum space. We would like to rewrite $A^0_{\rm eff}$, $A^1_{\rm eff}$ and $A^2_{\rm eff}$ as integrals in momenta variables. Let us start by Fourier transforming the object in (4.48) in momentum variable q

$$\mathcal{K}(\partial_a) \longrightarrow \mathcal{K}(q) \equiv \sum_{n=0}^{\infty} (i)^n \; c_n^{a_1 a_2 \ldots a_n} q_{a_1} q_{a_2} \ldots q_{a_n}. \tag{4.57}$$

In appendix 4.E we have derived some other important identities under Fourier transformations which we use below.

Using the definition of (4.57) the momenta space expression of (4.54) becomes

$$\begin{aligned} A^0_{\rm eff} &= \frac{1}{2}\int \frac{{\rm d}^4 q_1}{(2\pi)^4}\frac{{\rm d}^4 q_2}{(2\pi)^4}\; (2\pi)^4\delta^{(4)}(q_1+q_2)\; \Phi(q_1)\mathcal{K}(q_2)\Phi(q_2) \\ &\quad -\frac{1}{2}\int \frac{{\rm d}^4 k_1}{(2\pi)^4}\frac{{\rm d}^4 k_2}{(2\pi)^4}\; (2\pi)^4\delta^{(4)}(k_1+k_2)\varphi(k_1)k_2^2\varphi(k_2). \end{aligned} \tag{4.58}$$

The kinetic operator $\mathcal{K}(q)$ should vanish on-shell as follows from the equation of motion. Using the definition (4.57) and equalities from appendix 4.E in momentum space the expression (4.55) can be written as

$$\begin{aligned} A^1_{\rm eff} &= \frac{1}{2\sqrt{2}f}\int \frac{{\rm d}^4 q_1}{(2\pi)^4}\frac{{\rm d}^4 q_2}{(2\pi)^4}\frac{{\rm d}^4 k}{(2\pi)^4}\; (2\pi)^4\delta^{(4)}(q_1+q_2+k)\; \Phi(q_1)\Phi(q_2)\; \varphi(k) \\ &\quad \left(\Big\{ -(4-2\Delta)\mathcal{K}(q_2) + q_2^\mu \frac{p\mathcal{K}(q_2)}{pq_2^\mu}\Big\} + \frac{1}{2}\big\{\delta^\nu_\mu k_\rho + \delta^\nu_\rho k_\mu - \eta_{\mu\rho}k^\nu\big\} \right. \\ &\quad \left. \times q_{2\nu}\frac{p^2\mathcal{K}(q_2)}{pq_{2\mu}pq_{2\rho}} + \Delta\; k^\mu \frac{p\mathcal{K}(q_2)}{pq_2^\mu} + \; O(k^2)\right). \end{aligned} \tag{4.59}$$

In the above expression we are not explicitly writing down the three dilaton interaction part, as this term involves four power of dilaton momenta and will not be important for the computation of $AB \to AB$ scattering amplitude up to the order we are interested in. Using the definition (4.57) and the properties (4.194) and (4.198) the expression (4.56) can be written in momentum space as

$$\begin{aligned} A^2_{\rm eff} &= \frac{1}{4f^2}\int \frac{{\rm d}^4 q_1}{(2\pi)^4}\frac{{\rm d}^4 q_2}{(2\pi)^4}\frac{{\rm d}^4 k_1}{(2\pi)^4}\frac{{\rm d}^4 k_2}{(2\pi)^4}(2\pi)^4\delta^{(4)}(q_1+q_2+k_1+k_2)\Phi(q_1)\Phi(q_2)\varphi(k_1)\varphi(k_2) \\ &\left((2-\Delta)(3-2\Delta)\mathcal{K}(q_2) + (-3+2\Delta)q_2^\mu\frac{p\mathcal{K}(q_2)}{pq_2^\mu} + \frac{1}{2}q_2^\mu q_2^\nu\frac{p^2\mathcal{K}(q_2)}{pq_2^\mu pq_2^\nu} + O(k_1,k_2)\right). \end{aligned} \tag{4.60}$$

4.2.2 Low energy amplitude

Having obtained the low energy effective action components given by (4.58) - (4.60) we can finally compute the scattering amplitude $AB \to AB$. We start by deriving the Feynman rules. The Feynman propagators are defined as

$$(2\pi)^4\delta^{(4)}(q_1+q_2)\times D_F^{-1}(q_1) \equiv -i\frac{\delta^2 A_{\text{eff}}[\Phi,\varphi]}{\delta\Phi(q_1)\delta\Phi(q_2)}\bigg|_{\Phi,\varphi=0}, \qquad D_F(q_1) \equiv$$

(4.61)

$$(2\pi)^4\delta^{(4)}(k_1+k_2)\times \Delta_F^{-1}(k_1) \equiv -i\frac{\delta^2 A_{\text{eff}}[\Phi,\varphi]}{\delta\varphi(k_1)\delta\varphi(k_2)}\bigg|_{\Phi,\varphi=0}, \qquad \Delta_F(k_1) \equiv$$

(4.62)

The cubic effective vertex $\Phi\Phi\varphi$ is defined as

$$(2\pi)^4\delta^{(4)}(q_1+q_2+k)\times\Gamma^{(3)}(q_1,q_2;k) \equiv i\frac{\delta^3 A_{\text{eff}}[\Phi,\varphi]}{\delta\Phi(q_1)\delta\Phi(q_2)\delta\varphi(k)}\bigg|_{\Phi,\varphi=0} \equiv$$

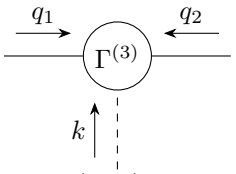

(4.63)

The quartic $\Phi\Phi\varphi\varphi$ vertex is defined as

$$(2\pi)^4\delta^{(4)}(q_1+q_2+k_1+k_2)\times\Gamma^{(4)}(q_1,q_2;k_1,k_2)$$
$$\equiv i\frac{\delta^4 A_{\text{eff}}[\Phi,\varphi]}{\delta\Phi(q_1)\delta\Phi(q_2)\delta\varphi(k_1)\delta\varphi(k_2)}\bigg|_{\Phi,\varphi=0} \equiv$$

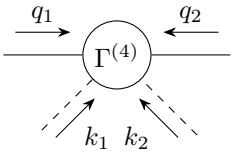

(4.64)

The cubic $\varphi\varphi\varphi$ vertex is defined as

$$(2\pi)^4\delta^{(4)}(k_1+k_2+k_3)\times V^{(3)}(k_1,k_2,k_3)$$
$$\equiv i\frac{\delta^3 A_{\text{eff}}[\Phi,\varphi]}{\delta\varphi(k_1)\delta\varphi(k_2)\delta\varphi(k_3)}\bigg|_{\Phi,\varphi=0} \equiv$$

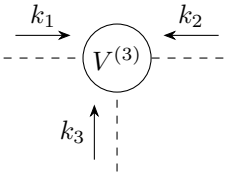

(4.65)

Applying these definitions to (4.58) - (4.60) we conclude that the Feynman propagators read as

$$D_F(q) = i\big(\mathcal{K}(q)\big)^{-1} \equiv \{q^2+m^2-i\epsilon\}^{-1}\Xi(q), \qquad \Delta_F(k) = -i(k^2-i\epsilon)^{-1}. \tag{4.66}$$

where we have introduced for later convenience a new object $\Xi(q)$ which is the

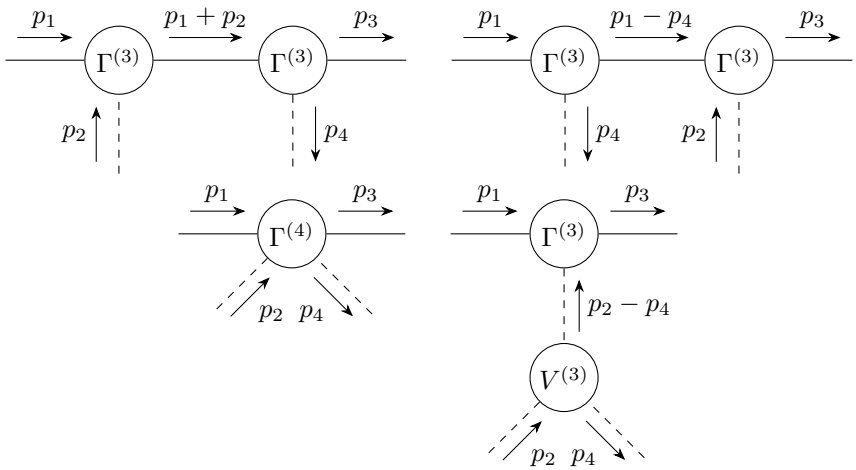

Figure 4.2: The set of diagrams contributing to the $\mathcal{T}_{AB\to AB}$ amplitudes. Here the solid lines represent scalar particles A and dashed lines represent dilatons B.

numerator of the scalar field propagator. The cubic vertex $\Phi\Phi\varphi$ reads

$$\Gamma^{(3)}(q_1,q_2;k) = \frac{i}{2\sqrt{2}f}\Bigg(-(4-2\Delta)\mathcal{K}(q_2) + q_2^\mu \frac{p\mathcal{K}(q_2)}{pq_2^\mu} + \frac{1}{2}\big\{\delta^\nu_\mu k_\rho + \delta^\nu_\rho k_\mu - \eta_{\mu\rho}k^\nu\big\} \times q_{2\nu}\frac{p^2\mathcal{K}(q_2)}{pq_{2\mu}pq_{2\rho}} + \Delta\ k^\mu \frac{p\mathcal{K}(q_2)}{pq_2^\mu} + \ O(k^2)\Bigg) + (q_1 \leftrightarrow q_2), \tag{4.67}$$

where $q_1+q_2+k=0$. In the above expression of $\Gamma^{(3)}$ the terms linear in k actually vanishes when we explicitly write the terms under $q_1 \leftrightarrow q_2$ exchange and substitute $q_2 = -q_1 - k$. The quartic vertex $\Phi\Phi\varphi\varphi$ reads as

$$\Gamma^{(4)}(q_1,q_2;k_1,k_2) = \frac{i}{2f^2}\Bigg((2-\Delta)(3-2\Delta)\mathcal{K}(q_2) - (3-2\Delta)q_2^\mu\frac{p\mathcal{K}(q_2)}{pq_2^\mu} + \frac{1}{2}q_2^\mu q_2^\nu \frac{p^2\mathcal{K}(q_2)}{pq_2^\mu pq_2^\nu} + O(k_1,k_2)\Bigg) + (q_1 \leftrightarrow q_2), \tag{4.68}$$

where $q_1+q_2+k_1+k_2=0$. Three dilaton field interaction vertex $\varphi\varphi\varphi$ reads as

$$V^{(3)}(k_1,k_2,k_3) = \frac{i}{f}\ \mathcal{O}(k_i^4). \tag{4.69}$$

We can now compute the $AB\to AB$ amplitude using the Feynman diagrams depicted in figure 4.2. The total amplitude describing the scattering process $AB\to AB$ becomes

$$\mathcal{T}_{AB\to AB} = \mathcal{T}_1 + \mathcal{T}_2 + \mathcal{T}_3 + \mathcal{T}_4, \tag{4.70}$$

where we have

$$\begin{aligned}
i\mathcal{T}_1 &= \Gamma^{(3)}(p_1, -p_1 - p_2; +p_2) D_F(p_1 + p_2) \Gamma^{(3)}(p_1 + p_2, -p_3; -p_4), \\
i\mathcal{T}_2 &= \Gamma^{(3)}(p_1, -p_1 + p_4; -p_4) D_F(p_1 - p_4) \Gamma^{(3)}(p_1 - p_4, -p_3; +p_2), \\
i\mathcal{T}_3 &= \Gamma^{(4)}(p_1, -p_3; p_2, -p_4), \\
i\mathcal{T}_4 &= \Gamma^{(3)}(p_1, -p_3; p_2 - p_4) \Delta_F(p_2 - p_4) V^{(3)}(-p_2 + p_4, p_2, -p_4).
\end{aligned} \tag{4.71}$$

Plugging the explicit expressions of the Feynman propagators and the effective vertices, expanding around $p_2^\mu = 0$ and $p_4^\mu = 0$ one obtains the following

$$\begin{aligned}
f^2\mathcal{T}_1 &= m^4 (p_1 \cdot p_2)^{-1} - 2m^2(\Delta - 1) - 2im^4 \Xi'(m^2) + O\big((p_1 \cdot p_2), (p_3 \cdot p_4)\big), \\
f^2\mathcal{T}_2 &= -m^4 (p_1 \cdot p_4)^{-1} - 2m^2(\Delta - 1) - 2im^4 \Xi'(m^2) + O\big((p_1 \cdot p_2), (p_3 \cdot p_4)\big), \\
f^2\mathcal{T}_3 &= (4\Delta - 5)m^2 \ + 4im^4 \Xi'(m^2) + O\big((p_1 \cdot p_2), (p_3 \cdot p_4)\big), \\
f^2\mathcal{T}_4 &= 0 \ + O\big((p_1 \cdot p_2), (p_3 \cdot p_4)\big),
\end{aligned} \tag{4.72}$$

where $\Xi'(m^2) \equiv \frac{p\Xi(q)}{pq^2}\Big|_{q^2=-m^2}$.

In deriving these we have used several straightforward relations which follow from the fact that $\mathcal{K}$ is a scalar quantity and thus can depend only on q^2. As a consequence the same is true for Ξ defined in (4.66). These relations read as

$$\mathcal{K}(q) = \mathcal{K}(-q), \quad \Xi(q) = \Xi(-q), \quad \frac{p\mathcal{K}(q)}{pq^\mu} = 2q_\mu \frac{p\mathcal{K}(q)}{pq^2}, \quad \frac{p\Xi(q)}{pq^\mu} = 2q_\mu \frac{p\Xi(q)}{pq^2}, \tag{4.73}$$

together with

$$\begin{aligned}
&\frac{p\mathcal{K}(q)}{pq^\mu}\Xi(q) + \mathcal{K}(q)\frac{p\Xi(q)}{pq^\mu} = 2iq_\mu, \\
&\frac{p^2\mathcal{K}(q)}{pq^\mu pq^\nu}\Xi(q) + \frac{p\mathcal{K}(q)}{pq^\nu}\frac{p\Xi(q)}{pq^\mu} + \frac{p\mathcal{K}(q)}{pq^\mu}\frac{p\Xi(q)}{pq^\nu} + \mathcal{K}(q)\frac{p^2\Xi(q)}{pq^\mu pq^\nu} = 2i\eta_{\mu\nu}.
\end{aligned} \tag{4.74}$$

At the end of the evaluation of the Feynman diagrams we use the following on-shell conditions,

$$\begin{aligned}
&\mathcal{K}(q)\Big|_{q^2=-m^2} = 0 \ , \ \Xi(q)\Big|_{q^2=-m^2} = -i \ , \ \frac{p\mathcal{K}(q)}{pq^\mu}\Big|_{q^2=-m^2} = -2q_\mu, \\
&\frac{p^2\mathcal{K}(q)}{pq^\mu pq^\nu}\Big|_{q^2=-m^2} = -2\eta_{\mu\nu} + 8iq_\mu q_\nu \ \Xi'(m^2).
\end{aligned} \tag{4.75}$$

Plugging (4.72) into (4.70) we obtain

$$f^2\mathcal{T}_{AB\to AB} = \frac{m^4}{(p_1 \cdot p_2)} - \frac{m^4}{(p_1 \cdot p_4)} - m^2 + O\big((p_1 \cdot p_2), (p_3 \cdot p_4)\big). \tag{4.76}$$

Using the definition of the Mandelsatm variables (2.20) and the definition of the tilded amplitudes (4.87) we obtain the final result

$$\widetilde{T}_{AB\to AB}(s,t,u) = \frac{-2m^4}{s - m^2} + \frac{-2m^4}{u - m^2} - m^2 + \ O(u - m^2, s - m^2). \tag{4.77}$$

The above result is independent of Δ, which is not surprising since Δ appears in the definition of $\widehat{\Phi}(x)$ which is nothing but a field redefinition of $\Phi(x)$. Here we

want to emphasize that up to the subleading order in the expansion parameters $s-m^2$ and $u-m^2$, our amplitude $\widetilde{T}_{AB\to AB}(s,t,u)$ is theory independent. In addition, in appendix 4.D we argue for this universal soft behavior by analysing the worldline action of a massive particle in a dilaton background.

At the next order in $O(u-m^2, s-m^2)$ the contribution to (4.77) will depend on $\Xi'(m^2), \Xi''(m^2)$ and the non-minimal interaction strength of the scalar field with the dilaton e.g. flat space interaction follows from $\widehat{R}^{\mu\nu}p_\mu\widehat{\Phi}p_\nu\widehat{\Phi}$.[9] Our derivation is also motivated from the literatures [37–39], where tree level single and double soft dilaton theorems have been studied.

4.2.3 The most general effective action – no $\mathbb{Z}_2$ symmetry

The situation changes only slightly if the symmetry is lifted. Without restriction of $\mathbb{Z}_2$ other terms. Now the odd powers of Φ can appear in the new effective action as well:

$$A'^{g}_{\text{eff}}[\Phi,\varphi] = A^{g}_{\text{eff}}[\Phi,\varphi] + \int \mathrm{d}^4x\sqrt{-\widehat{g}}\Big(\kappa_0\widehat{\Phi}^3 + \kappa_1\widehat{R}\widehat{\Phi}+ \\ + \kappa_2\widehat{R}^2\widehat{\Phi} + \kappa_3\widehat{R}_{\mu\nu}\widehat{R}^{\mu\nu}\widehat{\Phi} + \dots\Big) \tag{4.78}$$

The terms of order $\widehat{\Phi}^3$ will simply provide vertex

$$(2\pi)^4\delta^{(4)}(q_1+q_2+q_3)\times X^{(3)}(q_1,q_2,q_3) \equiv i\frac{\delta^3 A_{\text{eff}}[\Phi,\varphi]}{\delta\Phi(q_1)\delta\Phi(q_2)\delta\Phi q_3}\bigg|_{\Phi,\varphi=0} \equiv$$

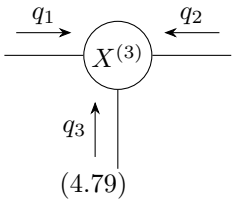

(4.79)

along with contributions to vertices $\Phi\Phi\Phi\varphi$ and so on. These, however, as they do contain higher powers of Φ, don't contribute to low energy effective action.

More of interest are terms with single Φ and curvature scalars[10].

With $\widehat{g} = \left(1-\frac{\phi(x)}{\sqrt{2}f}\right)^2$ one can compute

$$\widehat{R} = \frac{3\sqrt{2}\,\partial^2\varphi}{f\left(1-\frac{\phi(x)}{\sqrt{2}f}\right)^3} \tag{4.80}$$

$$\widehat{R}^2 = \frac{18}{f^2}\big(\partial^2\varphi\big)^2 + \frac{1}{f^3}\mathcal{O}\big(\phi^3\big) \tag{4.81}$$

$$\widehat{R}^{\mu\nu}\widehat{R}_{\mu\nu} = \frac{1}{f^2}\left(6(\partial^2\phi)^2 + 2\partial_\mu\partial_\nu\phi\;\partial^\mu\partial^\nu\phi\right) + \frac{1}{f^3}\mathcal{O}\big(\phi^3\big) \tag{4.82}$$

This implies the term $\left(\kappa_1\widehat{R}\widehat{\Phi}\right) = \frac{3\sqrt{2}\kappa_1}{f}\Phi\partial^2\varphi + \dots$ can be removed via field redefinition, as the kinetic terms always can be made diagonal in fields. The term $\partial^2\varphi$ is proportional to equations of motion, therefore it doesn't contribute

[9] The theory dependence of sub-subleading soft graviton theorem along the same line of derivation has been worked out in [36].

[10] With $R^{\mu\nu\rho\sigma}R_{\mu\nu\rho\sigma} = W^2 + 2R^{\mu\nu}R_{\mu\nu} - \frac{1}{3}R^2$, and Weyl scalar being invariant under Weyl transformation, only two independent quadratic invariants can contribute to the action.

to vertices with dilatons on shell (and dilaton internal lines introduce extra factor of $\frac{1}{f^2}$ to diagram, which makes it vanish in probe limit). Therefore, the vertex factor introduced by quartic curvature-Φ terms

$$(2\pi)^4\delta^{(4)}(k_1+k_2+q)\times Y^{(3)}(k_1,k_2;q) \equiv i\frac{\delta^3 A_{\text{eff}}[\Phi,\varphi]}{\delta\Phi(q_1)\delta\Phi(q_2)\delta\varphi(k)}\bigg|_{\Phi,\varphi=0} \equiv$$

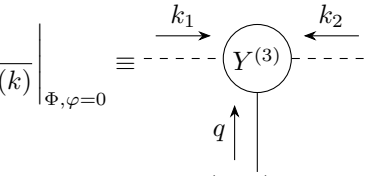

(4.83)

is

$$Y^{(3)}(k_1,k_2;q) = i\frac{4\kappa_3}{f^2}(k_1\cdot k_2)^2 + \mathcal{O}\left(\frac{1}{f^3}\right) \tag{4.84}$$

This term is obviously non-universal, and gives rise to another diagram

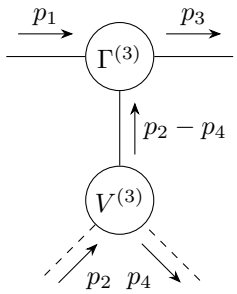

$$= i\frac{4t\kappa_2}{f^2(t-m^2)}X^{(3)}(p_1,p_3,p_1-p_3) + \mathcal{O}\left(\frac{1}{f^3}\right) \tag{4.85}$$

This implies nothing more than existence of pole of non-universal residue in t channel. Note that due to prefactor of t from derivative coupling, the low energy expansion (4.77) holds true for non-$\mathbb{Z}_2$ symmetric theories as well.

4.3 S-matrix bootstrap setup

To *probe* a quantum field theory, one introduces the **dilaton**, a massless scalar particle basically coupled to the trace of the energy-momentum tensor [24]. The S-matrix bootstrap setup containing the lightest stable scalar particle of the theory, called A (and of mass m_A, in practical computations normalized to 1), and dilaton B (of mass $m_B = 0$) contains the following amplitudes:

$$\begin{aligned} &AA\to AA, \quad AA\to AB, \quad AA\to BB,\\ &AB\to BB, \quad BB\to BB, \quad AB\to AB. \end{aligned} \tag{4.86}$$

Note that $AB \to AB$ is s-t crossing of $AA \to BB$, and the other amplitudes are fully crossing symmetric.

As shown in the section before, each vertex with at least p dilaton legs introduces factor of $\frac{1}{f^p}$ into the diagram, allowing to sort amplitudes into leading part (which may be interpreted as diagrams without dilaton internal lines), and

subleading terms, vanishing in probe limit $f \to \infty$:

$$\begin{aligned}
\mathcal{T}_{AA\to AA} &= \tilde{\mathcal{T}}_{AA\to AA} + O(f^{-1}) \\
\mathcal{T}_{AA\to AB} &= \frac{1}{f}\tilde{\mathcal{T}}_{AA\to AB} + O(f^{-2}) \\
\mathcal{T}_{AA\to BB} &= \frac{1}{f^2}\tilde{\mathcal{T}}_{AA\to BB} + O(f^{-3}) \\
\mathcal{T}_{AB\to BB} &= \frac{1}{f^3}\tilde{\mathcal{T}}_{AB\to BB} + O(f^{-4}) \\
\mathcal{T}_{BB\to BB} &= \frac{1}{f^4}\tilde{\mathcal{T}}_{BB\to BB} + O(f^{-5}) \\
\mathcal{T}_{AB\to AB} &= \frac{1}{f^2}\tilde{\mathcal{T}}_{AA\to BB} + O(f^{-3})
\end{aligned} \tag{4.87}$$

The amplitude $\tilde{\mathcal{T}}_{BB\to BB} = a_{\text{UV}}\left(s^2+t^2+u^2\right)$, via [24], relates the a-anomaly of UV CFT to dilaton scattering and is the central point of interest of the numerical experiments described in this paper.

4.3.1 Partial Waves

Following steps described in chapter 2, one shall decompose the amplitudes into partial waves, with

$$\begin{aligned}
\mathcal{T}^{(\ell)}_{AA\to AA} &= \frac{1}{32\pi}\left(1-4m^2/s\right)^{\frac{1}{2}}\int_{-1}^{+1}\mathrm{d}(\cos\theta)\,P_\ell(\cos\theta)\mathcal{T}_{AA\to AA} \\
\mathcal{T}^{(\ell)}_{AA\to AB} &= \frac{\sqrt{2}}{32\pi}\left(1-4m^2/s\right)^{\frac{1}{4}}\left(1-m^2/s\right)^{\frac{1}{4}}\int_{-1}^{+1}\mathrm{d}(\cos\theta)\,P_\ell(\cos\theta)\mathcal{T}_{AA\to AB} \\
\mathcal{T}^{(\ell)}_{AA\to BB} &= \frac{1}{32\pi}\left(1-4m^2/s\right)^{\frac{1}{4}}\int_{-1}^{+1}\mathrm{d}(\cos\theta)\,P_\ell(\cos\theta)\mathcal{T}_{AA\to BB} \\
\mathcal{T}^{(\ell)}_{AB\to BB} &= \frac{\sqrt{2}}{32\pi}\left(1-m^2/s\right)^{\frac{1}{4}}\int_{-1}^{+1}\mathrm{d}(\cos\theta)\,P_\ell(\cos\theta)\mathcal{T}_{AB\to BB} \\
\mathcal{T}^{(\ell)}_{BB\to BB} &= \frac{1}{32\pi}\int_{-1}^{+1}\mathrm{d}(\cos\theta)\,P_\ell(\cos\theta)\mathcal{T}_{BB\to BB} \\
\mathcal{T}^{(\ell)}_{AB\to AB} &= \frac{1}{16\pi}\left(1-m^2/s\right)^{\frac{1}{2}}\int_{-1}^{+1}\mathrm{d}(\cos\theta)\,P_\ell(\cos\theta)\mathcal{T}_{AB\to AB}
\end{aligned} \tag{4.88}$$

Note the suitable prefactors in agreement with (2.99). The expressions for t and u in each case given by (2.31)

4.3.2 Unitarity

Writing out (2.117)

$$\begin{pmatrix} 1 & 0 & 0 & \mathcal{T}^{*\ell}_{AA\to AA} & \mathcal{T}^{*\ell}_{AA\to AB} & \mathcal{T}^{*\ell}_{AA\to BB} \\ 0 & 1 & 0 & \mathcal{T}^{*\ell}_{AB\to AA} & \mathcal{T}^{*\ell}_{AB\to AB} & \mathcal{T}^{*\ell}_{AB\to BB} \\ 0 & 0 & 1 & \mathcal{T}^{*\ell}_{BB\to AA} & \mathcal{T}^{*\ell}_{BB\to AB} & \mathcal{T}^{*\ell}_{BB\to BB} \\ \mathcal{T}^{\ell}_{AA\to AA} & \mathcal{T}^{\ell}_{AB\to AA} & \mathcal{T}^{\ell}_{BB\to AA} & 2\,\mathrm{Im}\,\mathcal{T}^{\ell}_{AA\to AA} & 2\,\mathrm{Im}\,\mathcal{T}^{\ell}_{AA\to AB} & 2\,\mathrm{Im}\,\mathcal{T}^{\ell}_{AA\to BB} \\ \mathcal{T}^{\ell}_{AA\to AB} & \mathcal{T}^{\ell}_{AB\to AB} & \mathcal{T}^{\ell}_{BB\to AB} & 2\,\mathrm{Im}\,\mathcal{T}^{\ell}_{AA\to AB} & 2\,\mathrm{Im}\,\mathcal{T}^{\ell}_{AB\to AB} & 2\,\mathrm{Im}\,\mathcal{T}^{\ell}_{AB\to BB} \\ \mathcal{T}^{\ell}_{AA\to BB} & \mathcal{T}^{\ell}_{AB\to BB} & \mathcal{T}^{\ell}_{BB\to BB} & 2\,\mathrm{Im}\,\mathcal{T}^{\ell}_{AA\to BB} & 2\,\mathrm{Im}\,\mathcal{T}^{\ell}_{AB\to BB} & 2\,\mathrm{Im}\,\mathcal{T}^{\ell}_{BB\to BB} \end{pmatrix} \succcurlyeq 0 \tag{4.89}$$

In probe limit, $f \to 0$, this condition simplifies to

$$\begin{pmatrix} 1 & \tilde{\mathcal{T}}^{*\ell}_{AA\to AA} & \tilde{\mathcal{T}}^{*\ell}_{AA\to AB} & \tilde{\mathcal{T}}^{*\ell}_{AA\to BB} \\ \tilde{\mathcal{T}}^{\ell}_{AA\to AA} & 2\,\mathrm{Im}\,\tilde{\mathcal{T}}^{\ell}_{AA\to AA} & 2\,\mathrm{Im}\,\tilde{\mathcal{T}}^{\ell}_{AA\to AB} & 2\,\mathrm{Im}\,\tilde{\mathcal{T}}^{\ell}_{AA\to BB} \\ \tilde{\mathcal{T}}^{\ell}_{AA\to AB} & 2\,\mathrm{Im}\,\tilde{\mathcal{T}}^{\ell}_{AA\to AB} & 2\,\mathrm{Im}\,\tilde{\mathcal{T}}^{\ell}_{AB\to AB} & 2\,\mathrm{Im}\,\tilde{\mathcal{T}}^{\ell}_{AB\to BB} \\ \tilde{\mathcal{T}}^{\ell}_{AA\to BB} & 2\,\mathrm{Im}\,\tilde{\mathcal{T}}^{\ell}_{AA\to BB} & 2\,\mathrm{Im}\,\tilde{\mathcal{T}}^{\ell}_{AB\to BB} & 2\,\mathrm{Im}\,\tilde{\mathcal{T}}^{\ell}_{BB\to BB} \end{pmatrix} \succcurlyeq 0 \tag{4.90}$$

Introducing this full matrix (4×4 with 5 independent amplitudes) is computationally very expensive. Instead, via Sylvester's criterion, two necessary conditions are investigated numerically:

$$\begin{pmatrix} 1 & \tilde{\mathcal{T}}^{*\ell}_{AA\to AA} & \tilde{\mathcal{T}}^{*\ell}_{AA\to BB} \\ \tilde{\mathcal{T}}^{\ell}_{AA\to AA} & 2\,\mathrm{Im}\,\tilde{\mathcal{T}}^{\ell}_{AA\to AA} & 2\,\mathrm{Im}\,\tilde{\mathcal{T}}^{\ell}_{AA\to BB} \\ \tilde{\mathcal{T}}^{\ell}_{AA\to BB} & 2\,\mathrm{Im}\,\tilde{\mathcal{T}}^{\ell}_{AA\to BB} & 2\,\mathrm{Im}\,\tilde{\mathcal{T}}^{\ell}_{BB\to BB} \end{pmatrix} \succcurlyeq 0, \quad \left(2\,\mathrm{Im}\,\tilde{\mathcal{T}}^{\ell}_{AB\to AB}\right) \succcurlyeq 0, \tag{4.91}$$

Note that these two conditions are sufficient if processes $AA \to AB$ and $AB \to BB$ are forbidden by a $\mathbb{Z}_2$ symmetry of theory as assumed in [9]. Looking at this subset of unitarity conditions reduces problem to three independent amplitudes:

$$AA \to AA, \quad AA \to BB, \quad BB \to BB\ .$$

4.3.3 Analyticity and crossing

The kinematic non-analycities introdued previously2.4 are taking rather unusual form. The existence of masseless state BB suggests branch cuts starting at $s = 0$.

However, as previously shown, the transfer amplitude $\mathcal{T}_{\{x_i\}\to\{x_j\}}$ has prefactor f^{-n} where n is number of dilaton external particles. Therefore, in the equation (2.50) the intermediate states involving dilatons will vanish. To give

an explicit example,

$$\begin{aligned}
&\text{Disc}[\mathcal{T}_{AA\to AA}] = \oint\!\!\!\!\!\!\int \mathcal{T}_{AA\to X}\mathcal{T}_{X\to AA} = \\
&= \oint\!\!\!\!\!\!\int \left(\mathcal{T}_{AA\to AA}\mathcal{T}_{AA\to AA} + \oint\!\!\!\!\!\!\int \mathcal{T}_{AA\to AB}\mathcal{T}_{AB\to AA} + \oint\!\!\!\!\!\!\int \mathcal{T}_{AA\to BB}\mathcal{T}_{BB\to AA} + \dots\right) = \\
&\quad = \oint\!\!\!\!\!\!\int \mathcal{T}_{AA\to AA}\mathcal{T}_{AA\to AA} + \\
&\qquad + \frac{1}{f^2}\oint\!\!\!\!\!\!\int \tilde{\mathcal{T}}_{AA\to AB}\tilde{\mathcal{T}}_{AB\to AA} + \\
&\qquad + \frac{1}{f^4}\oint\!\!\!\!\!\!\int \tilde{\mathcal{T}}_{AA\to BB}\tilde{\mathcal{T}}_{BB\to AA} \to \\
&\quad \to \oint\!\!\!\!\!\!\int \mathcal{T}_{AA\to AA}\mathcal{T}_{AA\to AA}
\end{aligned} \tag{4.92}$$

The similar reasoning applies to other amplitudes – the only contributing intermediate states are ones of A particles only

$$AA, AAA, \dots \tag{4.93}$$

If the process $\mathcal{T}_{X\to AA}$ is allowed, the branch cut starts at $4m^2$. However, if particle A is constrained by $\mathbb{Z}_2$ symmetry, the process $AB \to AA$ is prohibited. The corresponding amplitude $\mathcal{T}_{AB\to AB}$ has a branch cut starting at $9m^2$ then.

To set up respective branch cuts,

$$\rho_1(z; z_0) = \frac{\sqrt{4m_A^2 - s_0} - \sqrt{4m_A^2 - s}}{\sqrt{4m_A^2 - s_0} + \sqrt{4m_A^2 - s}} \tag{4.94a}$$

$$\rho_2(z; z_0) = \frac{\sqrt{9m_A^2 - s_0} - \sqrt{9m_A^2 - s}}{\sqrt{9m_A^2 - s_0} + \sqrt{9m_A^2 - s}} \tag{4.94b}$$

are defined, and the ansatz for (finite part) of the amplitudes is

$$\tilde{\mathcal{T}}_{AA\to AA}(s,t,u) = \sum_{a,b,c} \alpha_{abc}\rho_1^a\left(s;\frac{4}{3}\right)\rho_1^b\left(t;\frac{4}{3}\right)\rho_1^c\left(u;\frac{4}{3}\right) + \dots \tag{4.95a}$$

$$\tilde{\mathcal{T}}_{BB\to BB}(s,t,u) = \sum_{a,b,c} \gamma_{abc}\rho_1^a(s;0)\rho_1^b(t;0)\rho_1^c(u;0) + \dots \tag{4.95b}$$

with the amplitude $AA \to BB$ depending on symmetry of the problem

$$\tilde{\mathcal{T}}^{\mathbf{Z}_2}_{AA\to BB}(s,t,u) = \sum_{a,b,c} \beta_{abc}\rho_1^a(s;0)\rho_2^b(t;1)\rho_2^c(u;1) \tag{4.95c}$$

$$\tilde{\mathcal{T}}_{AA\to BB}(s,t,u) = \sum_{a,b,c} \beta_{abc}\rho_1^a(s;0)\rho_1^b(t;1)\rho_1^c(u;1) \tag{4.95d}$$

The choice for origin points (second argument of rho variables) is made to facilitate imposing soft conditions and residues related to poles

With amplitudes $AA \to AA$ and $BB \to BB$ being fully crossing symmetric, the crossing conditions imply $\alpha_{abc} = \alpha_{bac} = \alpha_{cba}$ and $\gamma_{abc} = \gamma_{bac} = \gamma_{cba}$. The

amplitude $AA \to BB$ is symmetric in tu variables, implying $\beta_{abc} = \beta_{acb}$, is related to amplitude $AB \to AB$ by s-t crossing.

$$\tilde{\mathcal{T}}_{AB\to AB}(s,t,u) = \tilde{\mathcal{T}}_{AA\to BB}(t,s,u) \tag{4.96}$$

As described in previous section, to reduce the redundancy in parametrization of $\tilde{\mathcal{T}}$'s, one imposes $\alpha_{abc} = 0$ if $a \neq 0 \wedge b \neq 0 \wedge c \neq 0$ and similar for other amplitudes.

4.4 Poles and improvement terms

4.4.1 Pole structure and soft conditions

As shown previously, a one-particle intermediate state in (2.50) implies existence of pole in scattering amplitudes. As in previous section, intermediate states of dilaton B are introduced with extra factor of $\frac{1}{f^2}$, so there are no poles due to dilaton exchange. Keeping in mind crossing symmetries, the poles due to exchange of particle A in aforementioned amplitudes are

$\tilde{\mathcal{T}}_{AA\to AA} =$ 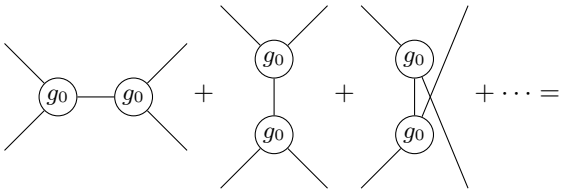 (4.97a)

$$= -|g_0|^2 \left(\frac{1}{s-m_A^2} + \frac{1}{t-m_A^2} + \frac{1}{u-m_A^2} \right) + \dots$$

$\tilde{\mathcal{T}}_{AA\to BB} =$ 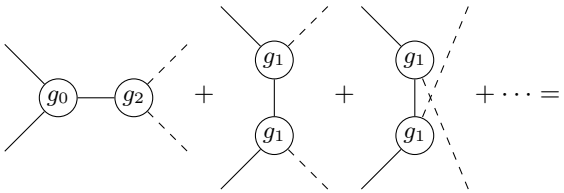 (4.97b)

$$= -\frac{g_0 g_2}{s-m_A^2} - |g_1|^2 \left(\frac{1}{t-m_A^2} + \frac{1}{u-m_A^2} \right) + \dots$$

$\tilde{\mathcal{T}}_{BB\to BB} =$ 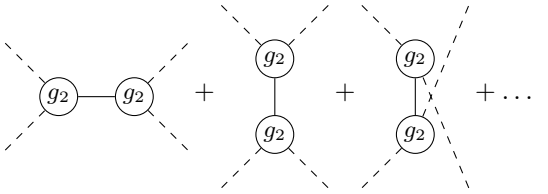 (4.97c)

$$= -|g_2|^2 \left(\frac{1}{s-m_A^2} + \frac{1}{t-m_A^2} + \frac{1}{u-m_A^2} \right) + \dots$$

where solid line is propagation of A and dashed line is propagation of B. At least this is the general case. For particle A constrained by $\mathbb{Z}_2$-symmetry the only occuring pole is

$$\tilde{\mathcal{T}}^{\mathbb{Z}_2}_{AA\to BB} = \quad + \quad + \dots \tag{4.98}$$
$$= -|g_1|^2 \left(\frac{1}{t-m_A^2} + \frac{1}{u-m_A^2} \right) + \dots$$

If one introduces an additional particle X of mass m_X, other poles are introduced due to its exchange:

$$\tilde{\mathcal{T}}_{AA\to AA} = \quad + \quad + \quad \cdots = \tag{4.99a}$$
$$= -|g_0'|^2 \left(\frac{1}{s-m_X^2} + \frac{1}{t-m_X^2} + \frac{1}{u-m_X^2} \right) + \dots$$

$$\tilde{\mathcal{T}}_{AA\to BB} = \quad + \cdots = -\frac{g_0' g_2'}{s-m_X^2} + \dots \tag{4.99b}$$

$$\tilde{\mathcal{T}}_{BB\to BB} = \quad + \quad + \quad + \cdots = \tag{4.99c}$$
$$= -|g_2'|^2 \left(\frac{1}{s-m_X^2} + \frac{1}{t-m_X^2} + \frac{1}{u-m_X^2} \right) + \dots$$

The vertex factor

$$= 0 \tag{4.99d}$$

vanishes, as the theory perturbed by the dilaton is diagonal in kinetic terms, so mixed terms involving two different matter fields and the dilaton cannot be constructed.

4.5 Numerical implementation

In practical computations, the amplitude is parametrized as linear combination of 'building blocks':

$$\mathcal{T}(s,t,u) = \sum \texttt{coeff}_i \cdot f_i(s,t,u) \tag{4.100}$$

Constructing an ansatz with analytic properties described in previous section, and imposing unitarity conditions on a set of matrices (4.91) derived from these amplitudes[11] allows to form the question about a-anomaly bounds as a semidefinite matrix problem (SDP), which allows using specialized solvers.

Therefore, using SDPB[14] to find a vector $\texttt{coeff}_i$ that minimizes a-anomaly given by (4.4), and describes amplitudes that obey unitarity bounds (4.91) can be done. However, besides including ρ series, described by (4.95a) (already a linear combination), the ansatz need to contain poles, and follow soft conditions described in previous section.

4.5.1 Poles

As mentioned previously, the terms in amplitude resulting from exchange of (4.97) are non-linear functions of coupling constants g_0, g_1, g_2. To be able to put the problem into semidefinite linear form, one shall define 'independent' linear coefficients

$$\begin{aligned} \texttt{ga} &\coloneqq g_0^2 \\ \texttt{gb} &\coloneqq g_1^2 \\ \texttt{gbb} &\coloneqq g_0 g_2 \\ \texttt{gdila} &\coloneqq g_2^2 \end{aligned} \tag{4.101}$$

For this parametrization to be equivalent, these parameters have to obey equation

$$\texttt{ga} \cdot \texttt{gdila} = \texttt{gbb} \cdot \texttt{gbb} \tag{4.102}$$

which may be written as a condition on matrix determinant

$$\begin{vmatrix} \texttt{ga} & \texttt{gbb} \\ \texttt{gbb} & \texttt{gdila} \end{vmatrix} = 0 \tag{4.103}$$

As $\texttt{ga} \geq 0$ and $\texttt{gdila} \geq 0$, the semidefinitness of such matrix

$$\begin{pmatrix} \texttt{ga} & \texttt{gbb} \\ \texttt{gbb} & \texttt{gdila} \end{pmatrix} \succeq 0 \tag{4.104}$$

does impose the inequality

$$\texttt{ga} \cdot \texttt{gdila} \geq \texttt{gbb} \cdot \texttt{gbb} \tag{4.105}$$

without any additional unwanted conditions.

As the term in amplitude $\tilde{\mathcal{T}}_{BB\to BB}$ related to parameter $\texttt{gdila}$, to be precise

$$\tilde{\mathcal{T}}_{BB\to BB} \supset -\texttt{gdila} \cdot \left(\frac{1}{s-1} + \frac{1}{t-1} + \frac{1}{u-1} \right) \quad , \tag{4.106}$$

is purely real, and the unitarity conditions (4.91) contain only $\operatorname{Im} \tilde{\mathcal{T}}_{BB\to BB}$, there is no additional bound on $\texttt{gdila}$ than imposed by (4.104). In later section it will be shown that to minimize a-anomaly $\texttt{gdila}$ is also to be minimized, and without any further constraints, that will lead to (4.104) being saturated, and (4.102) holding true.

[11] The matrices are therefore linear functions of $\texttt{coeff}_i$ as well.

4.5.2 Soft conditions

To impose soft conditions (4.77) around points $s = 0, t = 1, u = 1$, first, one fixes $\texttt{gb} = 2$ to match the residue, and then changes ansatz terms related to $\texttt{gbb}$. With $\rho(t;1) = \mathcal{O}(t-1)$, and $\rho(u;1) = \mathcal{O}(u-1)$ this is particularly simple:

$$\tilde{\mathcal{T}}_{AA\to BB} = -2\left(\frac{1}{t-1}+\frac{1}{u-1}\right) - \texttt{gbb}\left(1+\frac{1}{s-1}\right) + \tag{4.107}$$

$$+\sum_{a,b,c}\beta_{abc}\rho(s;0)^a\,\rho(t;1)^b\,\rho(u;1)^c \tag{4.108}$$

That guarantees the finite part of amplitude to be independent of value of $\texttt{gbb}$, therefore, all needed to impose correct soft condition is setting $\beta_{000} = -1$.

4.5.3 The goal: a-anomaly

To relate a-anomaly to coefficients of ansatz one needs to compare the relation

$$\tilde{\mathcal{T}}_{BB\to BB} = a\left(s^2+t^2+u^2\right)+\dots \tag{4.109}$$

to terms of the ansatz. Expanding the ansatz

$$\tilde{\mathcal{T}}_{BB\to BB} = -\texttt{gdila}\left(\frac{1}{s-1}+\frac{1}{t-1}+\frac{1}{u-1}\right) + \tag{4.110}$$

$$+\sum_{a,b,c}\gamma_{abc}\,\rho(s;0)^a\,\rho(t;0)^b\,\rho(u;0)^c \tag{4.111}$$

around $s = t = u = 0$ gives

$$\tilde{\mathcal{T}}_{BB\to BB} = (\text{const.}) + \left(\texttt{gdila}+\frac{\gamma_{001}}{128}+\frac{\gamma_{002}}{256}-\frac{\gamma_{011}}{512}\right)\left(s^2+t^2+u^2\right)+\dots \tag{4.112}$$

The constant term is purely real, so, in practice, as the unitarity matrices contain only $\operatorname{Im}\tilde{\mathcal{T}}_{BB\to BB}$, doesn't have to be explicitly fixed to 0.

4.5.4 Additional particles

The procedure of including another particles, as described by (4.99), follows very similarly. Again, one has to introduce 'independent' linear coefficients

$$\begin{aligned}\texttt{gaX} &\coloneqq g_0^2\\ \texttt{gbbX} &\coloneqq g_0 g_2\\ \texttt{gdilaX} &\coloneqq g_2^2\end{aligned} \tag{4.113}$$

with semidefinite condition

$$\begin{pmatrix}\texttt{gaX} & \texttt{gbbX}\\ \texttt{gbbX} & \texttt{gdilaX}\end{pmatrix} \succeq 0 \quad . \tag{4.114}$$

To keep the soft conditions on $\tilde{\mathcal{T}}_{AA\to BB}$ intact, the amplitude term related to `gbbX` is

$$\tilde{\mathcal{T}}_{AA\to BB} \supset -\texttt{gbb}\left(\frac{1}{m_X^2}+\frac{1}{s-m_X^2}\right) \tag{4.115}$$

which again, has no contribution to finite part of amplitude around $s=0, t=u=1$.

The contribution to a-anomaly from terms described in (4.99c), is derived as before, giving additional contribution of

$$\tilde{\mathcal{T}}_{BB\to BB} = \cdots + \frac{\texttt{gdilaX}}{m_X^6}\left(s^2+t^2+u^2\right)+\dots \tag{4.116}$$

Such construction can be repeated to include arbitrary many resonances resulting from exchange of particles of masses $1 < m_X < 2$. The condition (4.114) will again always be saturated when minimizing a-anomaly.

4.5.5 Improvement terms

Although, any amplitude of analytical properties described before can be reproduced by a linear combination of resonances, and (infinite) ρ series mentioned before, in practical computations one needs to limit the experiment to finite number of terms, usually with $\alpha_{abc}\neq 0$ only for some $a+b+c\leq \texttt{maxN}$. Given these limitations, it is often beneficial to include 'redundant' terms in the ansatz to improve convergence in such case.

The 'threshold singularity term', as introduced in [15] corresponds to bound state of two A particles, and is included in $AA\to AA$ amplitude ansatz as

$$\tilde{\mathcal{T}}_{AA\to AA} \supset \xi\cdot\left(\frac{1}{\rho\left(s;\frac{4}{3}\right)-1}+\frac{1}{\rho\left(t;\frac{4}{3}\right)-1}+\frac{1}{\rho\left(u;\frac{4}{3}\right)-1}\right) \tag{4.117}$$

with analytic bound on the related coefficient $\xi\in[\xi_{\min},0]$, with $\xi_{\min}=-32\sqrt{6}\pi$. The early trials (not plotted in this paper) showed better convergence with such addition, and its behavior in experimental data is discussed in the next section.

Along with improvement terms in amplitude $AA\to AA$, dilaton-to-dilaton scattering scattering amplitude can be expanded by including term proportional to $\tilde{\mathcal{T}}^{\text{free}}_{BB\to BB}$, corresponding amplitude in theory of free massive boson (so derived from $\tilde{\mathcal{T}}_{AA\to AA}=0$). Details of such derivation were described extensively in [9], and, quoting the relevant part,

$$\begin{aligned}\text{Im}[\widetilde{\mathcal{T}}^{\text{free}}_{BB\to BB}(s,t)] = {}& \frac{1}{32\pi}\sqrt{1-\frac{4}{s}}-\frac{1}{4\pi s}\ln\left(\frac{1+\sqrt{1-\frac{4}{s}}}{1-\sqrt{1-\frac{4}{s}}}\right)\\ &-\frac{1}{4\pi}\,\frac{1}{su}\frac{1}{\sqrt{1+\frac{4t}{su}}}\ln\left(\frac{\frac{1}{s}-\frac{u}{st}+\frac{u}{2t}\left[1+\sqrt{1-\frac{4}{s}}\sqrt{1+\frac{4t}{us}}\right]}{\frac{1}{s}-\frac{u}{st}+\frac{u}{2t}\left[1-\sqrt{1-\frac{4}{s}}\sqrt{1+\frac{4t}{us}}\right]}\right)\\ &-\frac{1}{4\pi}\,\frac{1}{st}\frac{1}{\sqrt{1+\frac{4u}{st}}}\ln\left(\frac{\frac{1}{s}-\frac{t}{su}+\frac{t}{2u}\left[1+\sqrt{1-\frac{4}{s}}\sqrt{1+\frac{4u}{ts}}\right]}{\frac{1}{s}-\frac{t}{su}+\frac{t}{2u}\left[1-\sqrt{1-\frac{4}{s}}\sqrt{1+\frac{4u}{ts}}\right]}\right)\end{aligned} \tag{4.118}$$

and

$$\tilde{\mathcal{T}}^{\text{free}}_{BB\to BB} = a_{\text{free}}\left(s^2+t^2+u^2\right)+\dots \tag{4.119}$$

with $a_{\text{free}} = \frac{1}{5760\pi^2}$.

Expanding ansatz with a term

$$\tilde{\mathcal{T}}_{BB\to BB} \supset \texttt{freeAmp}\cdot\frac{\tilde{\mathcal{T}}_{BB\to BB}}{a_{\text{free}}} \tag{4.120}$$

along with other contribution gives a goal for the optimization problem

$$a = \texttt{freeAmp} + \texttt{gdila} + \underbrace{\frac{\texttt{gdilaX}}{m_X^6}}_{\text{or sum of such terms for multiple resonances}} + \frac{\gamma_{001}}{128} + \frac{\gamma_{002}}{256} - \frac{\gamma_{011}}{512} \tag{4.121}$$

4.5.6 The grid, the limitations, the (CPU) time.

The unitarity condition (4.91) has to be imposed on every $s \in (4,\infty)$. In practice, SDP computations are limited to finite number of samples in s. The grid of values of s has to be chosen carefully to ensure convergence. As the most variation in $\mathcal{T}$'s occur around physical threshold $s \gtrsim 4$[12], and shall cover entire range from 4 to infinity somewhat uniformly (on log scale) for large energies.

The grid used for the computations is based on Chebyshev grid in ρ variables. With

$$\rho(4;0) = 1$$
$$\rho(\infty;0) = -1$$

we introduced grid of

$$\delta_k = \frac{1+\cos\left(\frac{2k-1}{2n}\pi\right)}{2}$$

for n grid points (and $\delta_i \in (0,1)$), which is used to construct a grid of values in s via relation

$$\rho(s_k;0) = e^{i\pi\delta_k}\ .$$

The resulting grid of points s_i has the desired properties mentioned before (large number of points around threshold, and rapidly increasing spacing between points for large s, allowing to *decently probe the infinity*).

With pilot computations to establish sufficient grid size, we found no difference between computations made for $n = 250$ and $n = 300$ grid points in s, and smaller sizes, like $n = 100$, $n = 150$ giving different, and explicitly wrong answers. All computations presented in following section were made using grid of 300 values in s, constructed using algorithm above.

The main building block of each amplitude is the ρ series,

$$\tilde{\mathcal{T}} = \sum_{a,b,c}\alpha_{abc}\rho(s;s_0)^a\,\rho(t;t_0)^b\,\rho(u;u_0)^c+\cdots \tag{4.122}$$

[12]This statement is intentionally broad, and comes from trials and errors. If an answer to SDP was computed on too small grid, the unitarity violations between grid points are usually found in vicinity of threshold.

that must be terminated for real computations. With time complexity of problem growing like $O\left(|\texttt{coeff}_i|^3\right)$ [14], the evaluation time sharply grows with number of terms in ρ series. Truncating each ρ series by imposing $\alpha_{abc} = 0$ for $a+b+c > \texttt{maxN}$ is how limiting the number of free coefficients is done. However, with overall time complexity $O(\texttt{maxN}^6)$, the line between *almost impossible* and *fast and inexpensive* SDPB computation is thin. This line, with hardware accessible for computations in this paper is around $\texttt{maxN} = 40$. The convergence with maxN is something that needs to be discussed separately for each experiment.

Other limitation is the number of spins included in (4.91). The computation time grows linearly with number of spins included, so pushing maxJ to the safe side is not computationally prohibitive. The experiment in this paper show that $\texttt{maxJ} = \texttt{maxN} + 12$ is a safe choice, and it is used for later numerics.

The precision of numerical values is another important topic in bootstrap computations. Many term cancelations in computations need large precision floating point numbers, and the experiments described later are no exception. 512 bits of mantissa precision was found to be (safely) more than enough and was used in the numerics for this paper.

4.6 Results

4.6.1 $\mathbb{Z}_2$-symmetric case

We start in section 4.6.1 by addressing the simplest possible question: what is the lowest value of the a-anomaly in the UV CFT which leads to a single $\mathbb{Z}_2$ odd asymptotic state given some relevant deformation. We will reconstruct the spin=0 partial amplitudes of our setup which lead to the absolute minimum of the a-anomaly. In section 4.6.1 we discuss several consistency checks of our numerical code. In section 4.6.1 we construct a lower bound on the a-anomaly as a function of λ_0, λ_2, Λ_0 and Λ_2. We reconstruct the spin=0 partial amplitudes of our setup corresponding to the maximally allowed value of λ_0.

Absolute minimum of the a-anomaly

Let us start by addressing the following question: what is the lowest value of the a-anomaly in the UV CFT which leads to a single $\mathbb{Z}_2$ odd asymptotic state given some relevant deformation. For running the numerics we have found the optimal size of the grid to be $N_{\text{grid}} = 300$. We have checked that $N_{\text{grid}} = 350$ and $N_{\text{grid}} = 400$ lead to the same solution. For $N_{\text{grid}} = 200$ the results differ significantly from the ones found with larger grids.

Let us fix the size of the ansatz to be $N_{max} = 20$. The minimum of the a-anomaly for various values of L_{max} is found to be

$$\begin{aligned}\{L_{max}, a/a_{\text{free}}\} = \{&(16, 0.4015), (18, 0.4074), (20, 0.4100),\\ &(22, 0.4115), (24, 0.4125), (26, 0.4133),\\ &(28, 0.4140), (30, 0.4146), (32, 0.4150), (34, 0.4154)\}.\end{aligned} \tag{4.123}$$

We see that the lower bound on the a-anomaly is stable under the change of L_{max} and gets stronger when L_{max} increases. In all the future numerical studies

we make the following conservative choice for

$$L_{max} = N_{max} + 10. \tag{4.124}$$

Let us now investigate the dependence of the numerical solution on N_{max}. We obtain the following values for the minimum of the a-anomaly for various values of N_{max}

$$\{N_{max}, a/a_{\text{free}}\} = \{(16, 0.4401), (18, 0.4223), (20, 0.4146), \\ (22, 0.4058), (24, 0.4001), (26, 0.3897)\}. \tag{4.125}$$

Using $N_{max} = 16$, 18, 20, 22, 24 and 26 we can extrapolate our data to $N_{max} = \infty$ with the following linear function

$$a/a_{\text{free}} = 0.316 + 1.969/N_{max}. \tag{4.126}$$

The dependence of the minimum of the a-anomaly on N_{max} and its extrapolation is given in figure 4.3. We conclude that the absolute minimum of the a-anomaly in our setup is

$$a/a_{\text{free}} \gtrsim 0.316 \pm 0.015. \tag{4.127}$$

Here we have also included the estimated extrapolation error.

At the absolute minimum of the a-anomaly we can actually reconstruct numerically scattering and partial amplitudes of all the process of our setup. In figures 4.4 - 4.6 we present the spin zero partial amplitudes of the $AA \to AA$ and $AA \to BB$ processes. In the left figure 4.5 we have plotted the real part of the spin zero phase shift of the $AA \to AA$ process. We recall that the spin ℓ phase shift δ^ℓ of the $AA \to AA$ process is defined via

$$\mathcal{S}^\ell_{AA\to AA}(s) = e^{2i\delta^\ell_{AA\to AA}(s)}. \tag{4.128}$$

From the right figure 4.5 we see that the amplitude is fully "elastic" up to very high energies.

In figure 4.7 we plot the integrand of the sum-rule (4.37) for various values of N_{max}. Numerical integration of these functions gives the values $a/a_{\text{free}} = 0.4146$, 0.4058, 0.4001 and 0.3897 which are in a perfect agreement with (4.125). In figure 4.8 we plot the integrand of the sum-rule (4.38) for spin 0, 2 and 4. Numerical integration of these functions gives the following value of the a-anomaly $a/a_{\text{free}} = 0.2396 + 0.1605 + 0.0105 + \ldots = 0.4106 + \ldots$, where the three entries correspond to spin 0, 2 and 4 respectively and the dots indicate the contribution due to higher spins..

Consistency checks

Before presenting more bounds let us perform several consistency checks.

First, we can set all the coefficients α and β in the ansatz (4.95a) to zero after. This situation corresponds to particle A being a free massive scalar, with the $AA \to BB$ scattering amplitude given by (4.165). As computed in appendix 4.B this inevitably leads to $a/a_{\text{free}} = 1$. We successfully reproduce this theoretical outcome numerically. It is important to notice that the ansatz (2.119) requires very large numbers N_{max} in order to reproduce the free theory

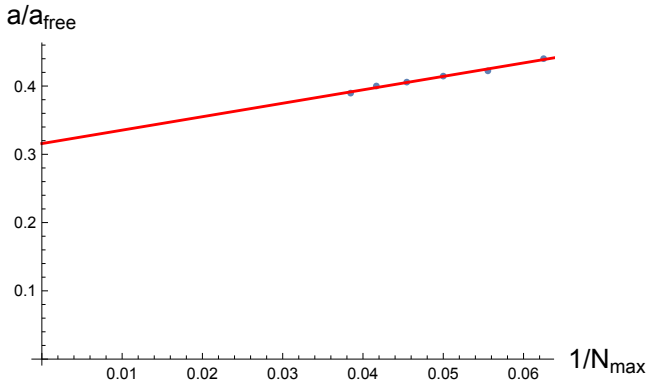

Figure 4.3: Minimum possible value of the a-anomaly without any further assumptions as a function of $1/N_{max}$ with $L_{max} = N_{max} + 10$. The numerical results are depicted by blue points. Linear extrapolation to $N_{max} \to \infty$ depicted by the red line gives 0.316 ± 0.015 for the minimum of a/a_{free}.

accurately. In practice it is very non-economical to work with such a big value of N_{max}. This was the motivation behind the introduction of the additional term (4.118) in the $BB \to BB$ ansatz which improves the convergence with N_{max} drastically in this particular situation.

Second, let us set all the α coefficients to zero and leave β coefficients to be completely free. One might expect the same outcome as before, however solving the optimization problem we obtain

$$a/a_{\text{free}} \approx 0.9071. \tag{4.129}$$

This result was obtained with $N_{max} = L_{max} = 20$. For comparison we get 0.9107 for $N_{max} = L_{max} = 10$. This result is very stable under the change of N_{max} and L_{max}. The solution of the optimization problem gives the coefficients of the ansatz such that only

$$\beta_{00n} \neq 0. \tag{4.130}$$

Under closer inspection of the unitarity conditions one observes that setting α to zero forces the imaginary part of the $\widetilde{\mathcal{T}}^{\ell}_{AA\to BB}(s)$ partial amplitude to be zero due to right-bottom minor of (4.91). However, the real part can still be non-zero. The solution (4.130) exactly reproduces such a situation. We, thus, conclude that the unitarity conditions we use do not fully constraint the behavior of the matter - dilaton scattering given the form of the matter scattering.

It is possible to guess analytically the $AA \to BB$ scattering amplitude which gives the solution (4.129), (4.130). Let us assume no discontinuity in the s-channel of the amplitude $AA \to BB$ (as follows from absence of $AA \to AA$ scattering), we can then write the general ansatz

$$\widetilde{\mathcal{T}}_{AA\to BB} = -m^2 - \frac{2m^4}{t-m^2} - \frac{2m^4}{u-m^2} + \\ - \int_{9m^2}^{\infty} \mathrm{d}w\, q(w) \left(\frac{m^2}{t-w} + \frac{m^2}{u-w} - \frac{2m^2}{m^2-w} \right), \tag{4.131}$$

where $q(w) \geq 0$ by unitarity. For the special case when $q(w) = Qm^2\delta(w - 9m^2)$ we obtain

$$\widetilde{\mathcal{T}}_{AA\to BB} = -m^2 - \frac{2m^4}{t-m^2} - \frac{2m^4}{u-m^2} + \\ - Qm^2\left(\frac{m^2}{t-9m^2} + \frac{m^2}{u-9m^2} + \frac{1}{4}\right). \quad (4.132)$$

Plugging it into (4.37) we obtain $a^{\text{UV}}/a_{\text{free}} \geq 0.905527$ for $Q = 2.07869$. The amplitude (4.132) matches precisely the one obtained numerically.

Finally, analogously to (4.37) one can write the following dispersion relation

$$\Lambda_2 = \frac{m^4}{8\pi^2}\int_{4m^2}^{\infty}\frac{\mathrm{d}s}{s^3}\,\mathrm{Im}\mathcal{T}_{AA\to AA}(s, 0, 4m^2 - s). \quad (4.133)$$

Setting Λ_2 to zero will force the imaginary part of the $AA \to AA$ process to be zero since the integrand is non-zero due to the semidefinitness of left-top minor in (4.91). Due to the same inequality we see that the imaginary part in turn forces the whole amplitude to be zero. In practice we indeed observe that by setting Λ_2 to zero the numerical solution leads to all the coefficients α being zero. In other words our numerics leads to (4.129) if $\Lambda_2 = 0$.

Lower bound on the a-anomaly as a function of couplings λ_0, λ_2, Λ_0 and Λ_2

The non-perturbative couplings, similarly to ones defined in [15, 40], are another physical observable worth investigating. At crossing-symmetric point one may define couplings

$$\lambda_0 \equiv \frac{1}{32\pi}\mathcal{T}_{AA\to AA}\left(\frac{4}{3}, \frac{4}{3}, \frac{4}{3}\right) \quad \lambda_2 \equiv \frac{1}{32\pi}\partial_s^2\mathcal{T}_{AA\to AA}\left(\frac{4}{3}, \frac{4}{3}, \frac{4}{3}\right) \quad (4.134)$$

and at the 'forward point' (as it lies on the line of forward scattering $t = 0$):

$$\Lambda_0 \equiv \frac{1}{32\pi}\mathcal{T}_{AA\to AA}(2, 0, 2) \quad \Lambda_2 \equiv \frac{1}{32\pi}\partial_s^2\mathcal{T}_{AA\to AA}(2, 0, 2) \quad (4.135)$$

Let us now construct a lower bound on the a-anomaly as a function of the coupling constants λ_0, λ_2, Λ_0 and Λ_2.

We begin by noticing that these couplings are bounded themselves. We can use our setup of section 4.3 to obtain upper and lower bounds which read as

$$\begin{aligned} -6.0253 \leq &\lambda_0 \leq +2.6613, \qquad 0 \leq \lambda_2 \leq +2.2568, \\ -2.8145 \leq &\Lambda_0 \leq +2.8086, \qquad 0 \leq \Lambda_2 \leq +0.6550. \end{aligned} \quad (4.136)$$

These are obtained by setting $a = 5a_{\text{free}}$ in the setup and using $N_{max} = 20$ and $L_{max} = 30$. Increasing the value of a does not change the result. Around $a/a_{\text{free}} \sim 1$ we get a non-trivial dependence of the bounds on a which will be better represented in the later plots. The dependence of these bounds on L_{max} is negligible. The dependence on N_{max} is non-trivial and should be taken into account. The correct bounds are obtained using the extrapolation to $N_{max} \to \infty$. The exception is the upper bound on λ_0, it is independent of N_{max} due to the

presence of the singularity term (4.117) which drastically improves the convergence of this particular bound. We do not perform $N_{max} \to \infty$ extrapolations in this section and instead we will always work at $N_{max} = 20$ and $L_{max} = 30$.

We can now pick value of λ_0, λ_2, Λ_0 and Λ_2 from the allowed ranges (4.136) and minimize the a-anomaly. The result is presented in figures 4.9 and 4.10. The allowed area is shaded in blue. The red dot represents the solution with the absolute minimum of the a-anomaly found in section 4.6.1. The right plots in figures 4.9 and 4.10 have a sharp peak around $\lambda_2 = 0$ and $\Lambda_2 = 0$. This point corresponds to a freely propagating particle A and gives the value of the a-anomaly quoted in (4.129). See the explanation below (4.129) why this value is not exactly one.

Another interesting point in these plots is the one with $\lambda_0 \approx 2.66$ and $a/a_{\text{free}} = 1.2$. As was done in section 4.6.1 we can plot spin zero partial amplitudes in our setup for this solution. They are given in figures 4.11 - 4.14.

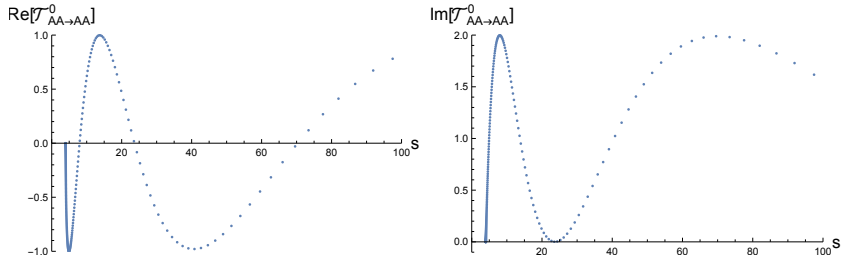

Figure 4.4: Real and imaginary parts of the spin 0 interacting part of the $AA \to AA$ partial amplitude leading to the absolute minimum of the a-anomaly. It is constructed at $N_{max} = 20$ and $L_{max} = 30$.

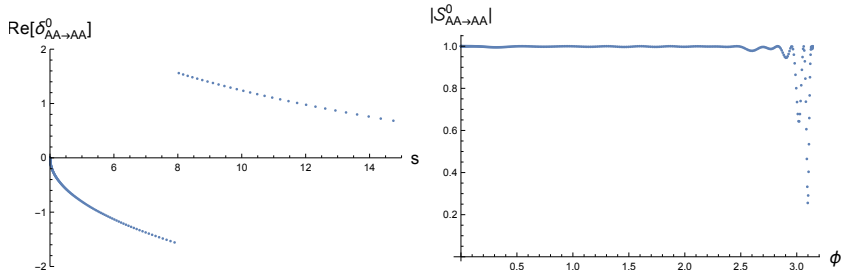

Figure 4.5: An alternative representation of the amplitude given in figure 4.4. Left plot represents the real part of the spin 0 phase shift of the $AA \to AA$ scattering defined in (4.128). The apparent jump around $s = 8$ is due to the periodicity $\delta \simeq \delta + \pi$. Right plot represents the absolute value of the spin 0 partial amplitude of the $AA \to AA$ scattering. On the real axis instead of the s variable we use the ϕ variable defined in (2.124). The amplitude is fully "elastic" up to very high energies.

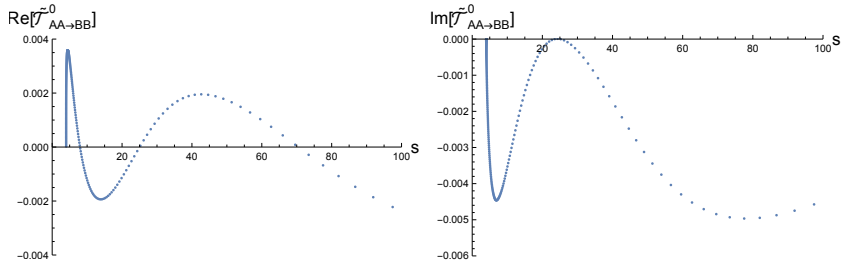

Figure 4.6: Real and imaginary parts of the spin 0 interacting part of the $AA \to BB$ partial amplitude leading to the absolute minimum of the a-anomaly. It is constructed at $N_{max} = 20$ and $L_{max} = 30$.

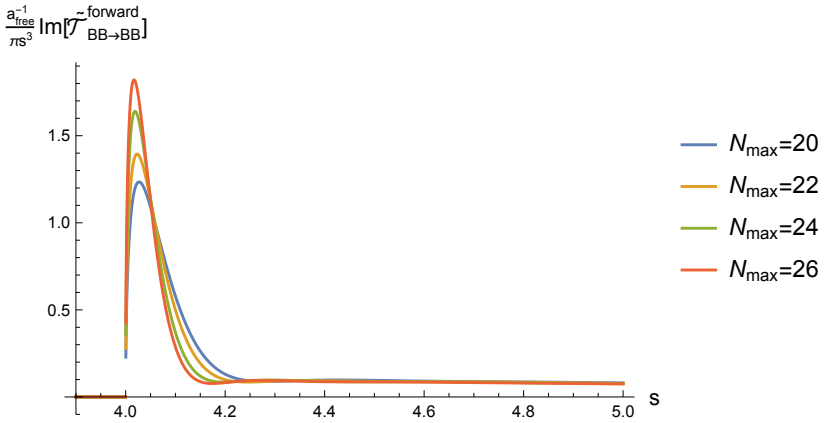

Figure 4.7: Integrand appearing in the sum-rule (4.37) for the absolute minimum of the a-anomaly. Different colors indicate different values of N_{max}. Numerical integration of these function leads to $a/a_{\text{free}} = 0.4146, 0.4058, 0.4001$ and 0.3896 in a perfect agreement with (4.125).

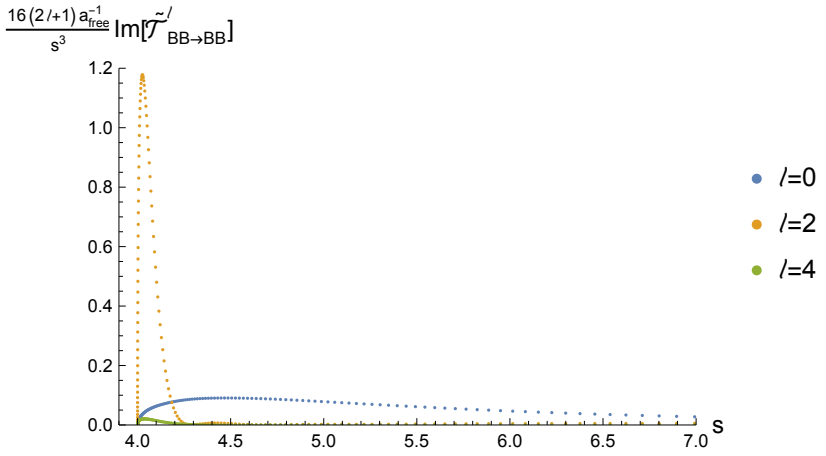

Figure 4.8: Integrand appearing in the sum-rule (4.37) for the absolute minimum of the a-anomaly for spin 0, 2 and 4. Numerical integration of this function leads to $a/a_{\text{free}} = 0.2396 + 0.1605 + 0.0105 + \ldots = 0.4106 + \ldots$, where the three entries correspond to spin 0, 2 and 4 respectively and the dots indicate the contribution due to higher spins. Plots are constructed at $N_{max} = 20$ and $L_{max} = 30$. Summing up these three contribution gives the $N_{max} = 20$ curve of figure 4.7.

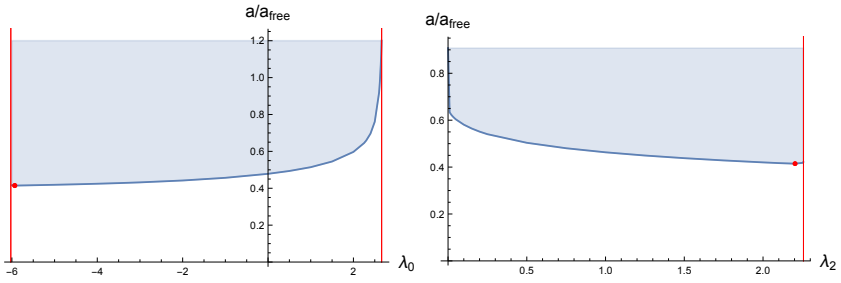

Figure 4.9: Lower bound on the a-anomaly as a function of λ_0 in the left plot and as a function of the λ_2 in the right plot. The allowed region is depicted in blue. Red dot represents the point with the lowest value of the a-anomaly. The red vertical lines indicate the boundaries of the allowed regions for λ_0 and λ_2 given in (4.136). The plots are built with $N_{max} = 20$ and $L_{max} = 30$.

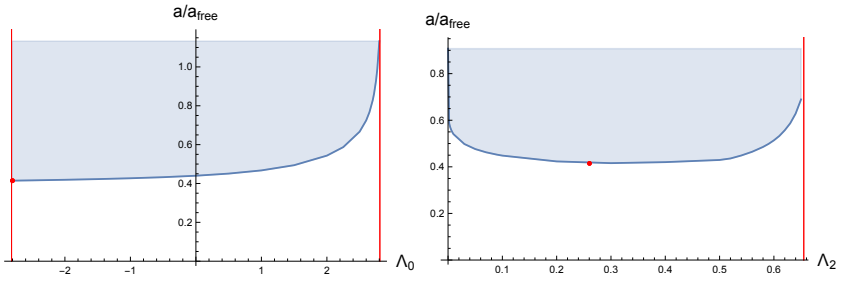

Figure 4.10: Lower bound on the a-anomaly as a function of Λ_0 in the left plot and as a function of the Λ_2 in the right plot. The allowed region is depicted in blue. Red dot represents the point with the lowest value of the a-anomaly. The red vertical lines indicate the boundaries of the allowed regions for Λ_0 and Λ_2 given in (4.136). The plots are built with $N_{max} = 20$ and $L_{max} = 30$.

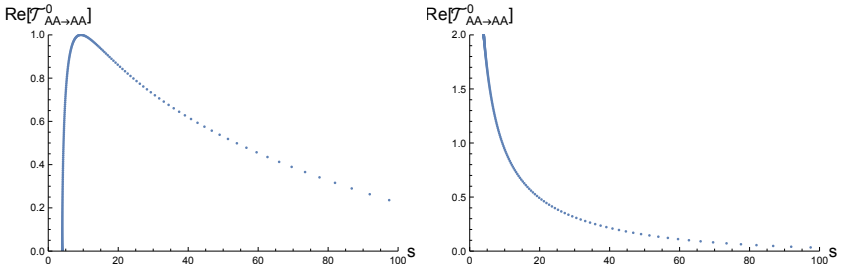

Figure 4.11: Real and imaginary parts of the spin 0 interacting part of the $AA \to AA$ partial amplitude for $\lambda_0 = 2.66$ which leads to $a/a_{\text{free}} = 1.2002$. It is constructed for $N_{max} = 20$ and $L_{max} = 30$.

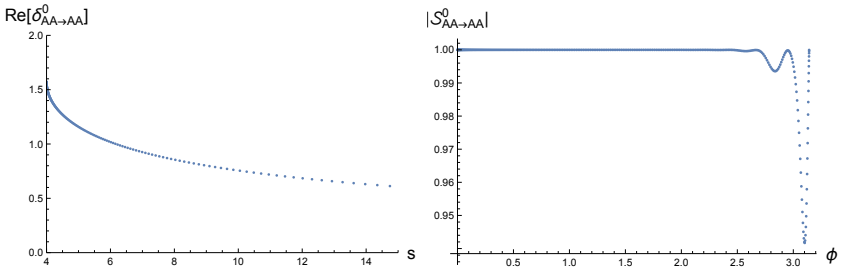

Figure 4.12: Left plot represents the real part of the spin 0 phase shift of the $AA \to AA$ scattering defined in (4.128). No resonances are present. Right plot represents the absolute value of the spin 0 partial amplitude of the $AA \to AA$ scattering. On the real axis instead of s variable we use ϕ variable defined in (2.124). The amplitude is fully "elastic" up to very high energies.

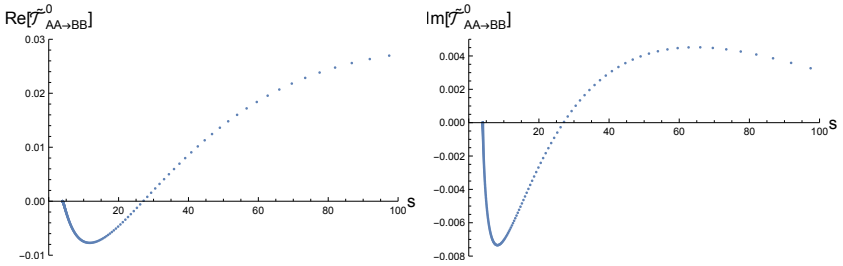

Figure 4.13: Real and imaginary parts of the spin 0 interacting part of the $AA \to BB$ partial amplitude for $\lambda_0 = 2.66$ which leads to $a/a_{\text{free}} = 1.2002$. It is constructed for $N_{max} = 20$ and $L_{max} = 30$.

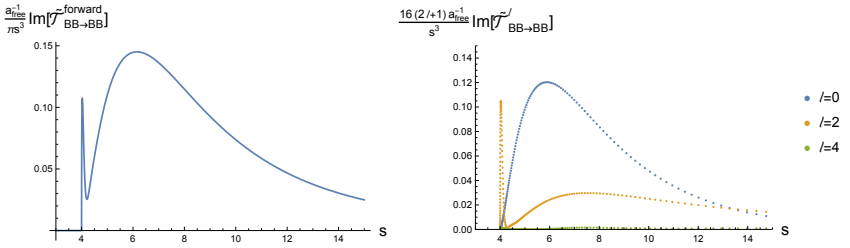

Figure 4.14: Left plot: integrand appearing in the sum-rule (4.37) for the absolute minimum of the a-anomaly. Numerical integration of this function leads to $a/a_{\text{free}} = 1.2002$. Right plot: integrand appearing in the sum-rule (4.37) for the absolute minimum of the a-anomaly. Numerical integration of this function leads to $a/a_{\text{free}} = 0.71146 + 0.45094 + 0.03238 + \ldots = 1.19477 + \ldots$, where the three entries correspond to spin 0, 2 and 4 respectively and the dots indicate higher spin contributions. The plots are constructed at $N_{max} = 20$ and $L_{max} = 30$.

4.6.2 Generalized case (no $\mathbb{Z}_2$ symmetry)

A story of one particle

The first performed experiment includes matter (particle A) and dilaton (particle B) without additional residues. The numerical data allowed to find a feasible range of ρ series size `maxN` and number of partial waves `maxJ` included in unitarity constraints, and the convergence pattern is shown on figure 4.15.

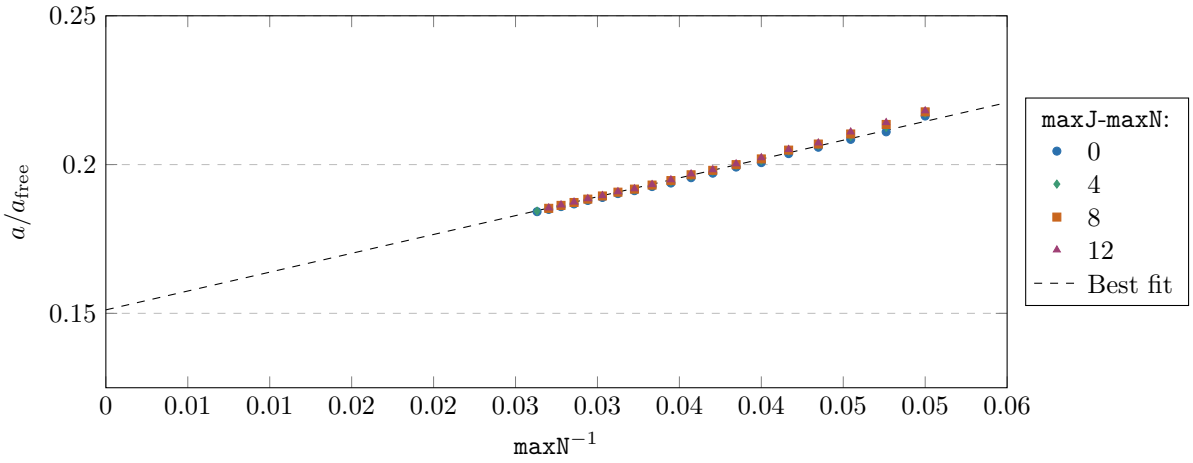

Figure 4.15: Absolute minimum of a as a fraction of a_{free}. A line fit to the best available data (highest `maxJ`) is marked. Comparing to figure 4.3 (with $\mathbb{Z}_2$ symmetry imposes), the bound is lower by roughly a factor of ½.

The close-to-linear behavior of $\frac{a}{a_{\text{free}}}$ as a function of $\frac{1}{\texttt{maxN}}$ allows to extrapolate the limit of $\texttt{maxN} \to \infty$, giving the answer of $a \gtrsim 0.1517 \cdot a_{\text{free}}$. This can be concluded to be absolute minimum a-anomaly of any theory with a single particle of spin 0.

As presented on a figure, the number of spins required for convergence depends on the ansatz size, however over entire range of feasible `maxN` (as time complexity grows approximately as $O(\texttt{maxN}^6)$ and experiments with $\texttt{maxN} > 40$ became prohibitively expensive), the difference between solutions found with $\texttt{maxJ} = \texttt{maxN} + 12$ and $\texttt{maxJ} = \texttt{maxN} + 8$ differed only marginally, proving $\texttt{maxJ} = \texttt{maxN} + 12$ is a safe choice for next experiments.

The strength of 3-point couplings may be extracted from data. The residue of pole in $\tilde{\mathcal{T}}_{AA\to AA}$ saturates the previously found bounds [15], however pole in $\tilde{\mathcal{T}}_{BB\to BB}$ does not contribute significantly to a-anomaly (see figure 4.16).

On the other hand, one would expect that the parameter associated with bound state at threshold, $\frac{1}{\rho(s;4/3)}$ would be saturating analytic bounds, as in scalar theories investigated in [15]. This is not the case, as optimized amplitude has associated parameter `boundState` converging to about 0.15 of minimal value of $-32\sqrt{6}\pi$, as shown on a plot. The second of improvement terms, `fAmp` doesn't appear to converge to any value, similarly to elements of γ_{abc}, as expected with having an ansatz that is (to some extent) redundant. Both patterns are shown on figure 4.17.

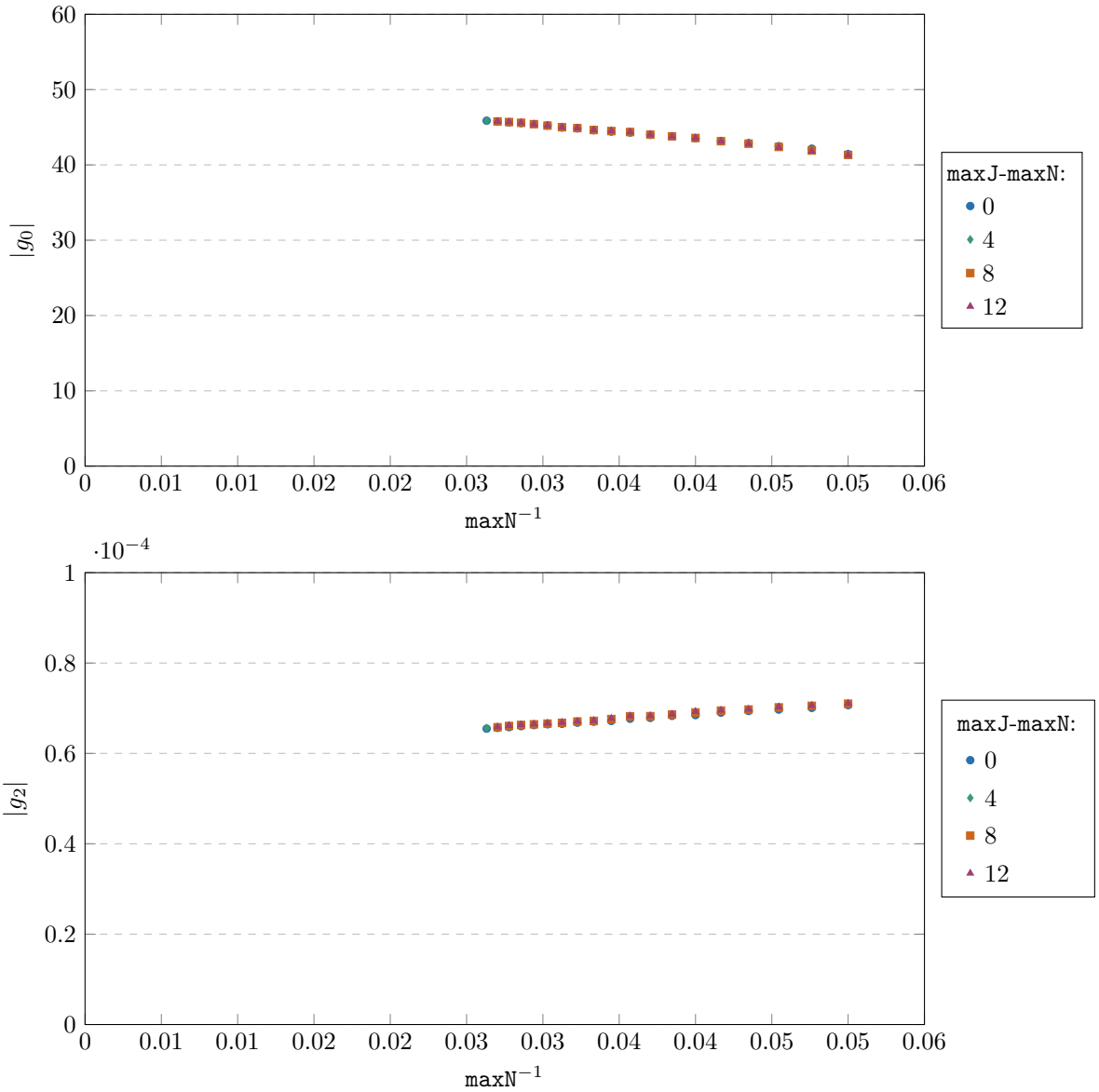

Figure 4.16: Size of 3-point couplings g_0 and g_2. Note difference in scales.

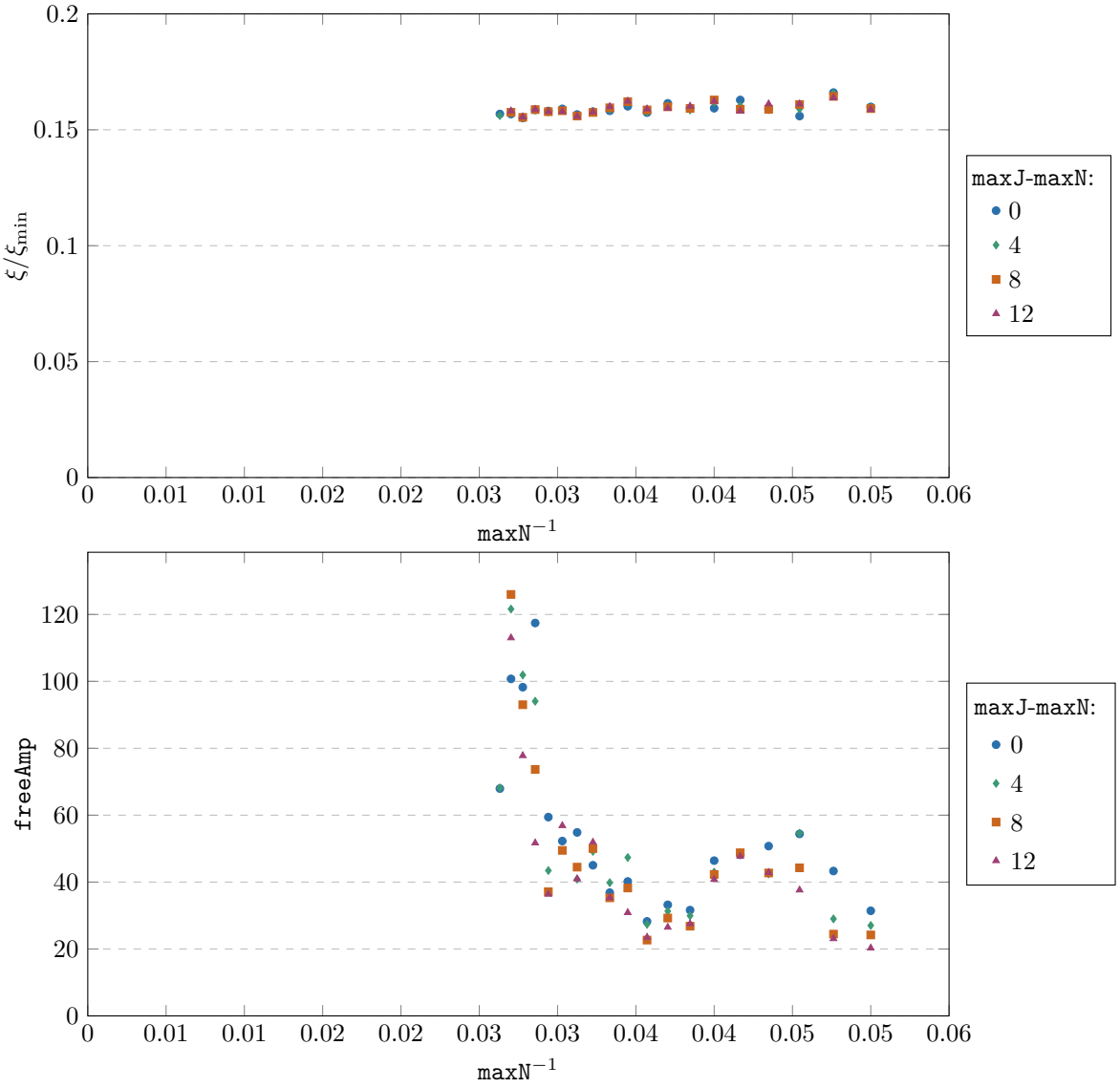

Figure 4.17: In contrast to amplitude maximizing 3-point coupling found in [15], the one minimizing a-anomaly doesn't saturate bounds on threshold term. The improvement term in $\tilde{\mathcal{T}}_{BB\to BB}$ doesn't show any convergence pattern.

A story of two particles

When considering resonances coming from exchange of massive particle X of mass $m_X^2 > 1$, the picture changes drastically. With square of mass m_X close to 1 or 4 the absolute minimum of a-anomaly is close to $0.15 \cdot a_{\text{free}}$ found which was expected, as these contributions are similar either to pole at $s = 1$ or to the threshold singularity. However, in between, the minimal value of anomaly dips at $a \approx 0.034 \cdot a_{\text{free}}$ for the mass $m_X^2 = 2.5 \pm 0.1$.

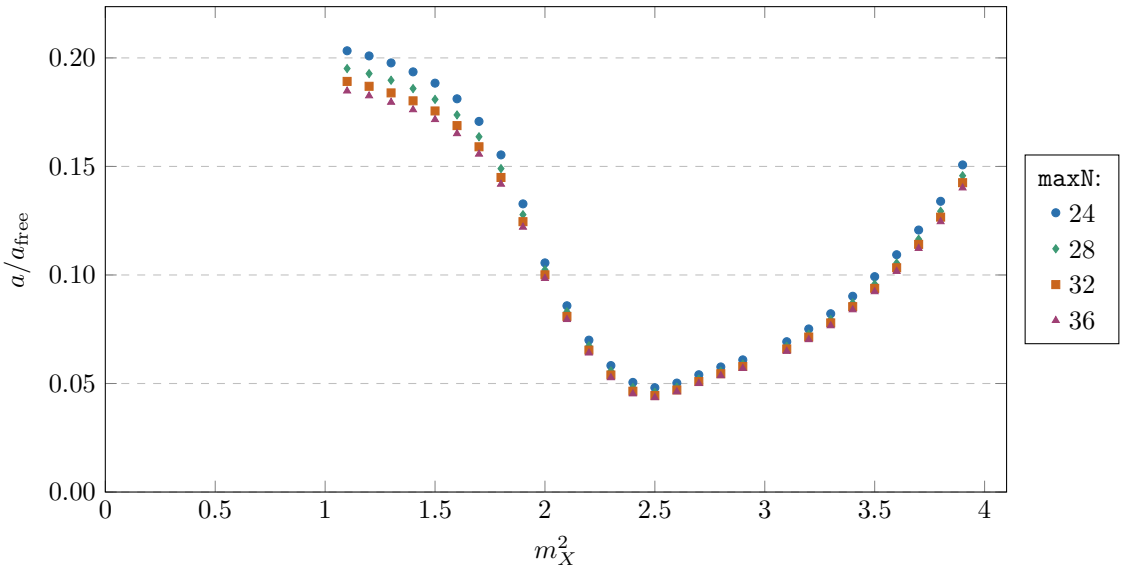

Figure 4.18: Absolute minimum of a-anomaly as a function of the mass square of the second particle. For each data point $\texttt{maxJ} = \texttt{maxN} + 12$

The behavior of three-point couplings (shown on figure 4.19) and threshold singularity term can be separated into two regions. For $m_X^2 \leq 2$ the value of g_0 is close to 0, and $|g_0'|$ (matter-matter-X) saturates the unitarity bound of 3-point coupling found in previous S-matrix bootstrap experiments[15]. Above $m_X^2 = 2$ the coupling $|g_0|$ starts to grow rapidly, maximizing around $m_X^2 = 2.5 \pm 0.1$. The opposite applies to threshold singularity term ξ - it decays quickly from ≈ 0.15 of minimal value coming from unitarity bounds ($\xi_{\text{min}} = -32\sqrt{6}\pi$) to decay to 0 at $m_X^2 = 2$. It looks like a pole below $m_X^2 = 2$ absolutely consumes pole at $m_A^2 = 1$, and pole above consumes threshold singularity, when it comes to minimization of a-anomaly.

Somewhat similar behavior (of disappearance of resonance at mass of A) is observed at dilaton-dilaton-matter and dilaton-dilaton-X couplings, as plotted in figure 4.20.

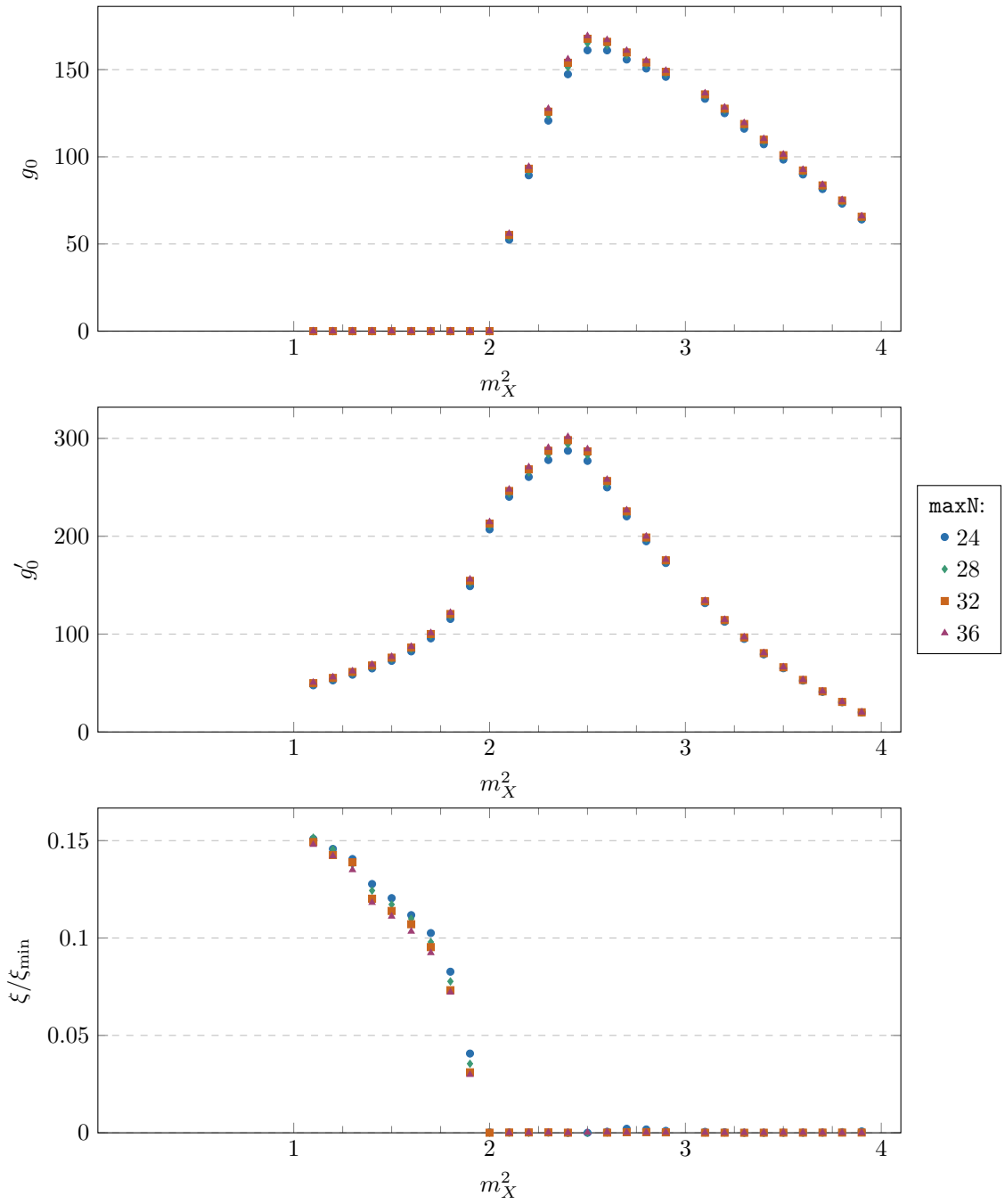

Figure 4.19: Size of 3-point couplings g_0 and g_0' and threshold singularity ξ with respect to additional particle mass m_X^2

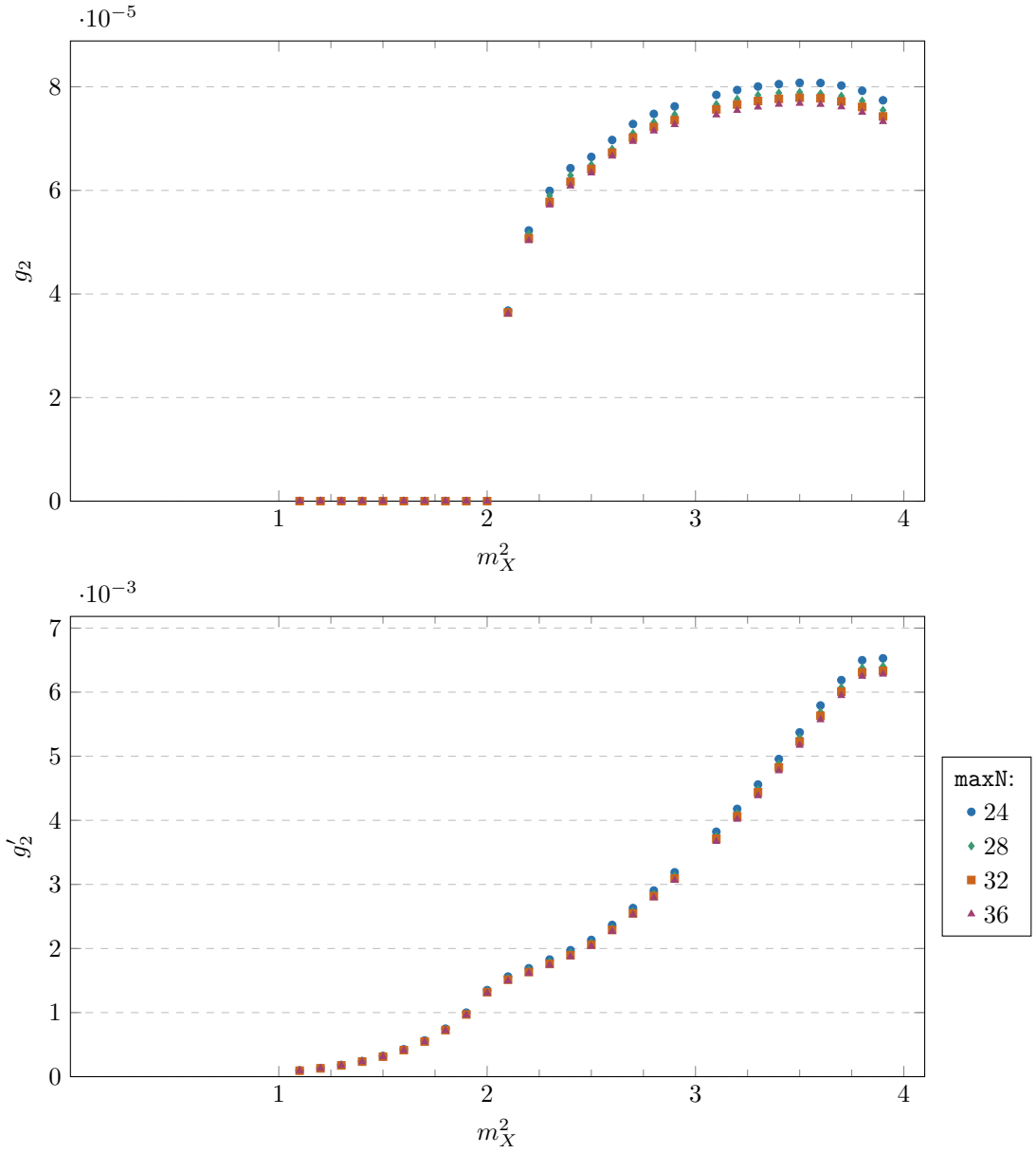

Figure 4.20: Size of 3-point couplings g_2 and g_2' with respect to additional particle mass m_X^2. Note the kink of g_2' around $m_X^2 = 2$ – it is very likely similar discontinuity applies to g_0', however it may be difficult to notice it due to low resolution in m_X^2.

A story of many particles

To approach a general theory containing *at least* a single particle of spin 0, a theory with many possible resonances is investigated. Instead of introducing single extra resonance of mass m_X, a set of them is included in the ansatz, with masses[13]

$$m_i^2 = 1.1, 1.2, \ldots, 3.8, 3.9 \tag{4.137}$$

with respective 3-point couplings $g_0(m_i)$ and $g_2(m_i)$, with A's and with dilatons respectively. Surprisingly, the absolute value of a-anomaly in such case can be extrapolated to

$$a_{\min} \approx 0.036 \cdot a_{\text{free}} \tag{4.138}$$

with convergence pattern presented on the figure 4.21.

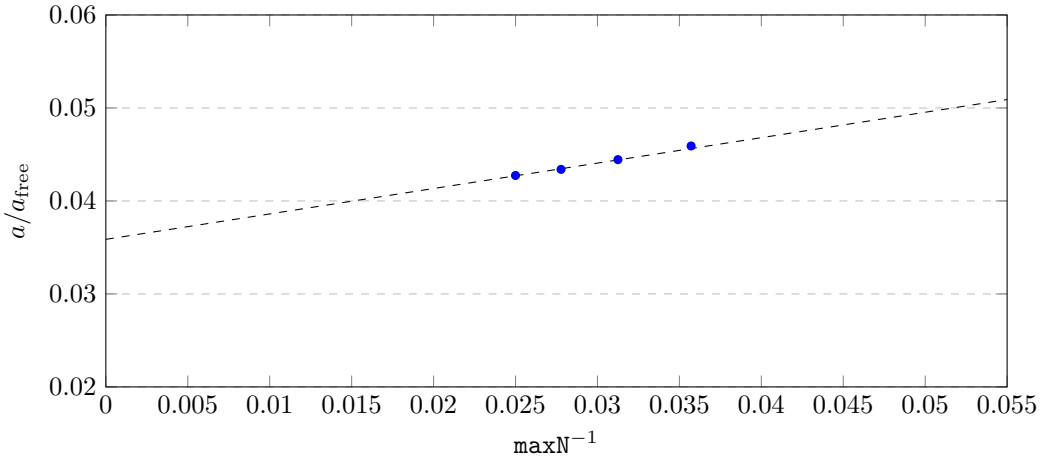

Figure 4.21: Convergence of a-anomaly bounds with multiple poles allowed. maxJ = maxN + 12 for all data points.

The exact numerical result shall be taken with a grain of salt, as little data points were evaluated due to high complexity of computations.

However, this value being so close to minimum of a-anomaly from previous section shall bring attention to 3-point couplings related to each of allowed intermediate particles.

When taking a closer look on figure 4.22, one can notice the only significant contribution to the amplitudes results from resonances at mass $m_i^2 = 2.4, m_i = 2.5$. The natural conjecture from this observation is that the non-trivial theory that really minimizes a-anomaly contains two stable particles, one of mass m_A (normalized to 1 in the experiment), and another with m_X^2 between 2.4 and 2.5. The further investigation, with more detailed grid of allowed resonances, shall eventually bring a definitive answer to question of minimal a-anomaly of non-trivial theory containing at least one spin-0 particle.

[13]The resonance at $m_i = 3.0$ is missing due to a numerical error.

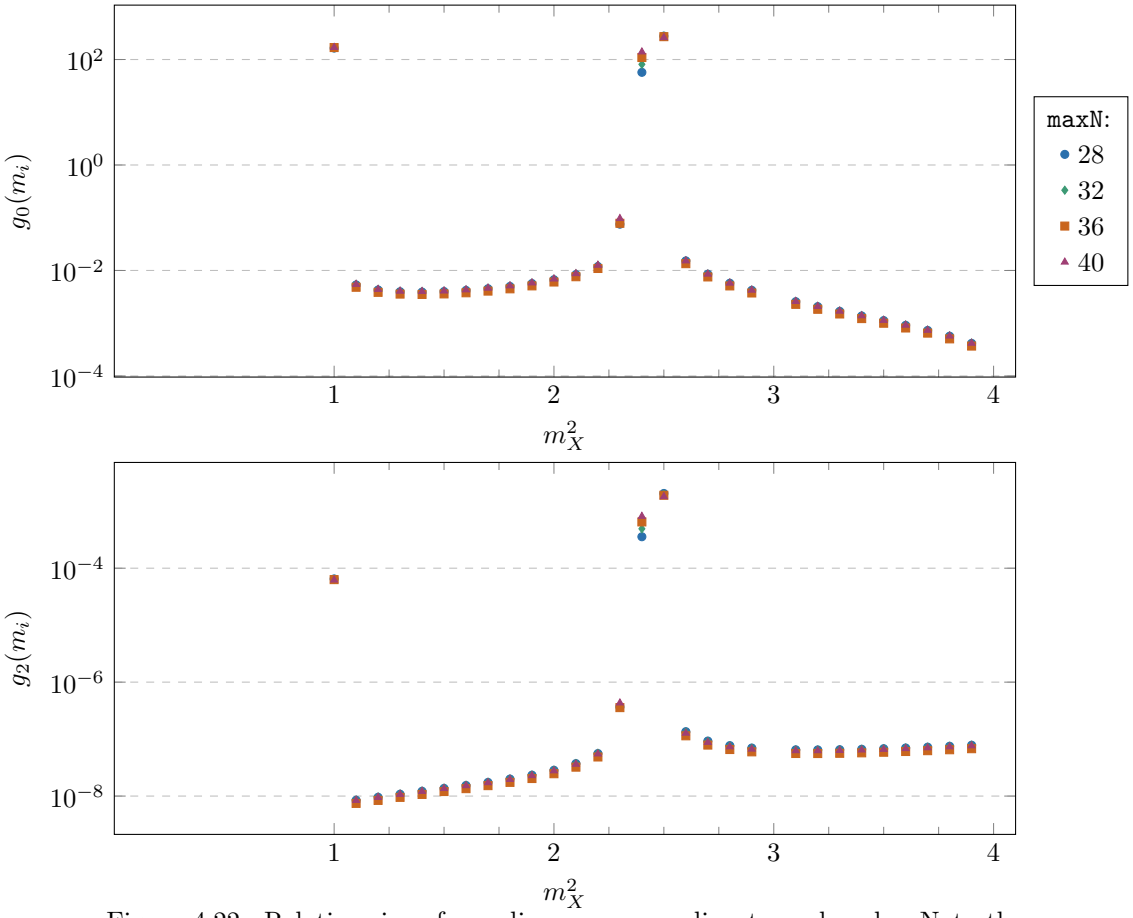

Figure 4.22: Relative size of couplings corresponding to each pole. Note the logarithmic scale.

4.A Correlation functions of the stress tensor

In this appendix we summarize results for the two- and three-point correlation functions of the stress-tensor in four spacetime dimension derived in a seminal paper [25] by Osborn and Petkou. Let us start by defining the short-hand notation

$$x_{ij}^{\mu} \equiv x_i^{\mu} - x_j^{\nu}. \tag{4.139}$$

All the tensor structures for the stress-tensor correlators are built out of these elementary tensors

$$\begin{aligned} I^{\mu\nu}(x) &\equiv \delta^{\mu\nu} - 2\,\frac{x^{\mu}x^{\nu}}{x^2}, \\ \mathcal{I}^{\mu\nu,\rho\sigma}(x) &\equiv \frac{1}{2}I^{\mu\rho}(x)I^{\nu\sigma}(x) + \frac{1}{2}I^{\mu\sigma}(x)I^{\nu\rho}(x) - \frac{1}{4}\eta^{\mu\nu}\eta^{\rho\sigma}, \\ X_{3,12}^{\mu} &\equiv \frac{x_{13}^{\mu}}{x_{13}^2} - \frac{x_{23}^{\mu}}{x_{23}^2}. \end{aligned} \tag{4.140}$$

According to [25] we have

$$\langle T^{\mu\nu}(x_1)T^{\rho\sigma}(x_2)\rangle = C_T\,\frac{1}{x_{12}^8}\,\mathbf{T}_0^{\mu\nu;\rho\sigma}, \tag{4.141}$$

$$\big\langle T^{\mu\nu}(x_1)T^{\rho\sigma}(x_2)T^{\alpha\beta}(x_3)\big\rangle = \frac{1}{x_{12}^4x_{23}^4x_{31}^4}\Big[\mathbb{A}\;\mathbf{T}_1^{\mu\nu;\rho\sigma;\alpha\beta} + \mathbb{B}\;\mathbf{T}_2^{\mu\nu;\rho\sigma;\alpha\beta} + \mathbb{C}\;\mathbf{T}_3^{\mu\nu;\rho\sigma;\alpha\beta}\Big]. \tag{4.142}$$

Here C_T is the central charge and $\mathbb{A}$, $\mathbb{B}$ and $\mathbb{C}$ are the stress-tensor OPE coefficients with itself. These obey the following relation

$$C_T \;=\; \frac{\pi^2}{3}\Big(14\mathbb{A} - 2\mathbb{B} - 5\mathbb{C}\Big). \tag{4.143}$$

The four tensor structures written above are defined as

$$\begin{aligned} \mathbf{T}_0^{\mu\nu;\rho\sigma} &\equiv \mathcal{I}_{\mu\nu,\rho\sigma}(x_{12}), \\ \mathbf{T}_1^{\mu\nu;\rho\sigma;\alpha\beta} &\equiv \mathcal{I}^{\mu\nu,\mu'\nu'}(x_{13})\mathcal{I}^{\rho\sigma,\rho'\sigma'}(x_{23})t^1_{\mu'\nu',\rho'\sigma'}{}^{\alpha\beta}(X_{3,12}), \\ \mathbf{T}_2^{\mu\nu;\rho\sigma;\alpha\beta} &\equiv \mathcal{I}^{\mu\nu,\mu'\nu'}(x_{13})\mathcal{I}^{\rho\sigma,\rho'\sigma'}(x_{23})t^2_{\mu'\nu',\rho'\sigma'}{}^{\alpha\beta}(X_{3,12}), \\ \mathbf{T}_3^{\mu\nu;\rho\sigma;\alpha\beta} &\equiv \mathcal{I}^{\mu\nu,\mu'\nu'}(x_{13})\mathcal{I}^{\rho\sigma,\rho'\sigma'}(x_{23})t^3_{\mu'\nu',\rho'\sigma'}{}^{\alpha\beta}(X_{3,12}), \end{aligned} \tag{4.144}$$

where

$$\begin{aligned} t^1_{\mu\nu,\rho\sigma,\alpha\beta}(X) \equiv& h^5_{\mu\nu,\rho\sigma,\alpha\beta}(X) - 2h^4_{\mu\nu,\rho\sigma,\alpha\beta}(X) - 2h^4_{\rho\sigma,\mu\nu,\alpha\beta}(X) + 24h^2_{\mu\nu,\rho\sigma}(X)h^1_{\alpha\beta}(X) \\ &- 16h^1_{\rho\sigma}(X)h^2_{\mu\nu,\alpha\beta}(X) - 16h^1_{\mu\nu}(X)h^2_{\rho\sigma,\alpha\beta}(X) + 64h^1_{\mu\nu}(X)h^1_{\rho\sigma}(X)h^1_{\alpha\beta}(X), \\ t^2_{\mu\nu,\rho\sigma,\alpha\beta}(X) \equiv& h^4_{\alpha\beta,\mu\nu,\rho\sigma}(X) - h^4_{\mu\nu,\rho\sigma,\alpha\beta}(X) - h^4_{\rho\sigma,\mu\nu,\alpha\beta}(X) + 6h^2_{\mu\nu,\rho\sigma}(X)h^1_{\alpha\beta}(X) \\ &- 2h^1_{\rho\sigma}(X)h^2_{\mu\nu,\alpha\beta}(X) - 2h^1_{\mu\nu}(X)h^2_{\rho\sigma,\alpha\beta}(X) + 32h^1_{\mu\nu}(X)h^1_{\rho\sigma}(X)h^1_{\alpha\beta}(X), \\ t^3_{\mu\nu,\rho\sigma,\alpha\beta}(X) \equiv& h^3_{\mu\nu,\rho\sigma}(X)h^1_{\alpha\beta}(X) + h^1_{\mu\nu}(X)h^3_{\rho\sigma,\alpha\beta}(X) + h^1_{\rho\sigma}(X)h^3_{\mu\nu,\alpha\beta}(X) \\ &- 6h^2_{\mu\nu,\rho\sigma}(X)h^1_{\alpha\beta}(X) + 4h^1_{\rho\sigma}(X)h^2_{\mu\nu,\alpha\beta}(X) + 4h^1_{\mu\nu}(X)h^2_{\rho\sigma,\alpha\beta}(X) \\ &- 16h^1_{\mu\nu}(X)h^1_{\rho\sigma}(X)h^1_{\alpha\beta}(X). \end{aligned} \tag{4.145}$$

and

$$\begin{aligned}
h^1_{\mu\nu}(X) \equiv& \frac{X_\mu X_\nu}{X^2} - \frac{1}{4}\eta_{\mu\nu},\\
h^2_{\mu\nu,\rho\sigma}(X) \equiv& \frac{1}{X^2}\Big[X_\mu X_\rho \eta_{\nu\sigma} + X_\mu X_\sigma \eta_{\nu\rho} + X_\nu X_\rho \eta_{\mu\sigma} + X_\nu X_\sigma \eta_{\mu\rho} - X_\mu X_\nu \eta_{\rho\sigma}\\
&- X_\rho X_\sigma \eta_{\mu\nu}\Big] + \frac{1}{4}\eta_{\mu\nu}\eta_{\rho\sigma},\\
h^3_{\mu\nu,\rho\sigma}(X) \equiv& \eta_{\mu\rho}\eta_{\nu\sigma} + \eta_{\mu\sigma}\eta_{\nu\rho} - \frac{1}{2}\eta_{\mu\nu}\eta_{\rho\sigma},\\
h^4_{\mu\nu,\rho\sigma,\alpha\beta}(X) \equiv& \frac{1}{X^2}\Big[h^3_{\mu\nu,\rho\alpha}X_\sigma X_\beta + h^3_{\mu\nu,\sigma\alpha}X_\rho X_\beta + h^3_{\mu\nu,\rho\beta}X_\sigma X_\alpha + h^3_{\mu\nu,\sigma\beta}X_\rho X_\alpha\Big]\\
&- \frac{1}{2}\eta_{\rho\sigma}h^2_{\mu\nu,\alpha\beta}(X) - \frac{1}{2}\eta_{\alpha\beta}h^2_{\mu\nu,\rho\sigma}(X) - \frac{1}{2}\eta_{\rho\sigma}\eta_{\alpha\beta}h^1_{\mu\nu}(X),\\
h^5_{\mu\nu,\rho\sigma,\alpha\beta}(X) \equiv& \eta_{\mu\rho}\eta_{\nu\alpha}\eta_{\sigma\beta} + \eta_{\nu\rho}\eta_{\mu\alpha}\eta_{\sigma\beta} + \eta_{\mu\sigma}\eta_{\nu\alpha}\eta_{\rho\beta} + \eta_{\nu\sigma}\eta_{\mu\alpha}\eta_{\rho\beta} + \eta_{\mu\rho}\eta_{\nu\beta}\eta_{\sigma\alpha}\\
&+ \eta_{\nu\rho}\eta_{\mu\beta}\eta_{\sigma\alpha} + \eta_{\mu\sigma}\eta_{\nu\beta}\eta_{\rho\alpha} + \eta_{\nu\sigma}\eta_{\mu\beta}\eta_{\rho\alpha} - \frac{1}{2}\eta_{\mu\nu}\eta_{\rho\sigma}\eta_{\alpha\beta}\\
&- \eta_{\mu\nu}h^3_{\rho\sigma,\alpha\beta}(X) - \eta_{\rho\sigma}h^3_{\mu\nu,\alpha\beta}(X) - \eta_{\alpha\beta}h^3_{\mu\nu,\rho\sigma}(X).
\end{aligned} \tag{4.146}$$

In curved spacetime one-point function of the trace of the stress-tensor is non-zero. It has the following form

$$\left\langle T^\mu_\mu \right\rangle_g = -a \times \ E_4 \ + \times \ c \ W^2, \tag{4.147}$$

where E_4 is the Eular density and W^2 is the square of the Weyl tensor. They have the following expressions in $4d$,

$$E_4 = R^{\alpha\beta\gamma\delta}R_{\alpha\beta\gamma\delta} - 4R^{\alpha\beta}R_{\alpha\beta} + R^2, \tag{4.148}$$

$$W^2 = R^{\alpha\beta\gamma\delta}R_{\alpha\beta\gamma\delta} - 2R^{\alpha\beta}R_{\alpha\beta} + \frac{1}{3}R^2. \tag{4.149}$$

The coefficients a and c are called the Weyl anomalies. They are related to the OPE coefficients $\mathbb{A}$, $\mathbb{B}$ and $\mathbb{C}$ as

$$a \ = \ \frac{\pi^4}{64\times 90}\Big(9\mathbb{A} - 2\mathbb{B} - 10\mathbb{C}\Big), \quad c \ = \ \frac{\pi^4}{64\times 30}\Big(14\mathbb{A} - 2\mathbb{B} - 5\mathbb{C}\Big). \tag{4.150}$$

As an example let us consider a theory of a free massless (conformally coupled) scalar $\Phi(x)$ which is described by the free CFT. According to [41] it has the following stress-tensor

$$T_{\mu\nu} = p_\mu\Phi p_\nu\Phi - \frac{1}{12}\Big[2p_\mu p_\nu\Phi^2 + \eta_{\mu\nu}p^2\Phi^2\Big]. \tag{4.151}$$

Such a CFT has the following parameters

$$\mathbb{A} = \frac{1}{27\pi^6}, \quad \mathbb{B} = -\frac{4}{27\pi^6}, \quad \mathbb{C} = -\frac{1}{27\pi^6}, \quad C_T = \frac{1}{3\pi^4}, \tag{4.152}$$

$$a = \frac{1}{5760\pi^2}, \quad c = \frac{1}{1920\pi^2}. \tag{4.153}$$

4.B Example of the free scalar theory

In this appendix we consider the theory of a free massive scalar field $\Phi(x)$ which has the following action

$$A_{\text{free}}(m) = \int \mathrm{d}^4x \Big[-\frac{1}{2}\partial_\mu\Phi\partial^\mu\Phi - \frac{1}{2}m^2\Phi^2\Big]. \tag{4.154}$$

It can be interpreted as a free massless CFT in the UV deformed by the mass term. As reviewed in sections 4.1.2 and 4.1.3 one can define the following modified action

$$A'_{\text{free}}(m) = \int \mathrm{d}^4x \Big[-\frac{1}{2}\partial_\mu\Phi\partial^\mu\Phi - \frac{1}{2}m^2\Phi^2 - \frac{1}{2}\partial_\mu\varphi\partial^\mu\varphi + \frac{m^2}{\sqrt{2}f}\,\varphi\Phi^2 - \frac{m^2}{4f^2}\varphi^2\Phi^2\Big]. \tag{4.155}$$

In what follows using this action we will compute the $BB \to BB$ scattering amplitude, where B is the dilaton particle created by the dilaton field $\varphi(x)$ from the vacuum. We will show that in this particular model this amplitude at low energy is given by equation (4.44). The particle created by the field $\Phi(x)$ from the vacuum is referred to as the particle A. We will do the computation in two different ways.

All the Feynman rules needed for the computation of scattering amplitudes in the model (4.155) read as

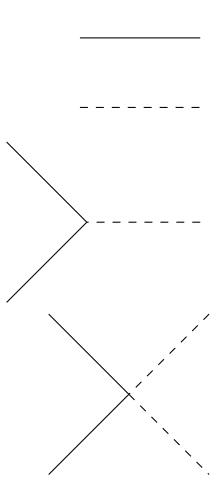

$$= \frac{-i}{p^2 + m^2 - i\epsilon} \tag{4.156}$$

$$= \frac{-i}{p^2 - i\epsilon} \tag{4.157}$$

$$= \frac{i\sqrt{2}m^2}{f} \tag{4.158}$$

$$= -\frac{im^2}{f^2} \tag{4.159}$$

Here solid lines represent the field $\Phi(x)$ and dashed lines represent the dilaton field $\varphi(x)$.

Direct computation The $BB \to BB$ dilaton scattering at the order $\mathcal{O}(f^{-4})$ is described by the Feynman diagram depicted in figure 4.23. We compute these diagrams one by one using the standard Feynman parametrization. We will then expand these expressions at the leading order in energy and the perform the Feynman integrals.

The amplitude described by the first diagram in figure 4.23 together with

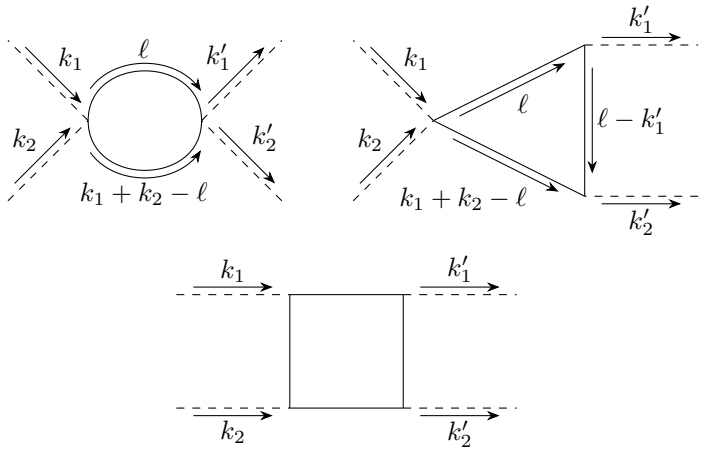

Figure 4.23: We consider the momenta of incoming dilatons be k_1 and k_2 and the momenta of outgoing dilatons be k_1' and k_2'. In the total amplitude contribution we also need to add the contributions of two topologically in-equivalent diagrams for the above individuals which we can easily read off using crossing symmetry.

the ones obtained from it by using crossing symmetry has the following form

$$\begin{aligned} & i\mathcal{A}_I(s,t) \\ &= \frac{m^4}{2f^4}\int \frac{\mathrm{d}^4\ell}{(2\pi)^4}\frac{1}{\ell^2+m^2-i\epsilon}\,\frac{1}{(k_1+k_2-\ell)^2+m^2-i\epsilon} + (\text{cross-sym}) \\ &= -\frac{im^4}{32\pi^2 f^4}\int_0^1 dx\,\left[\ln\left(\frac{m^2-sx(1-x)}{\Lambda^2}\right)+\right. \\ &\qquad\qquad + \ln\left(\frac{m^2-tx(1-x)}{\Lambda^2}\right)+ \\ &\qquad\qquad\left. + \ln\left(\frac{m^2-ux(1-x)}{\Lambda^2}\right)\right]. \end{aligned} \tag{4.160a}$$

Here Λ is the Pauli-Villars regularisation parameter representing the UV cut-off. Contribution from the second diagram in figure 4.23 together the ones obtained from it by corssing symmetry has the form

$$\begin{aligned} & i\mathcal{A}_{II}(s,t) \\ &= -\frac{2m^6}{f^4}\int \frac{\mathrm{d}^4\ell}{(2\pi)^4}\frac{1}{\ell^2+m^2-i\epsilon}\,\frac{1}{(\ell-k_1')^2+m^2-i\epsilon} \\ &\qquad\qquad \frac{1}{(k_1+k_2-\ell)^2+m^2-i\epsilon} + (\text{cross-sym}) \\ &= -\frac{im^6}{4\pi^2 f^4}\int_0^1 \mathrm{d}x\,\mathrm{d}y\,\mathrm{d}z\,\delta(x+y+z-1)\cdot \\ &\qquad\qquad \cdot\left[\frac{1}{m^2-sxy}+\frac{1}{m^2-txy}+\frac{1}{m^2-uxy}\right]. \end{aligned} \tag{4.160b}$$

Contribution from the third diagram in figure 4.23 together the ones obtained from it by corssing symmetry has the form

$$\begin{aligned} i\mathcal{A}_{III}(s,t) =& \frac{im^8}{4\pi^2 f^4}\int_0^1 \mathrm{d}x\,\mathrm{d}y\,\mathrm{d}z\,\mathrm{d}w\,\delta(x+y+z+w-1)\times \\ &\times\Bigg[\frac{1}{\big[m^2-\{sy(z+w)+tyz+uz(1-z-w)\}\big]^2} \\ &+\frac{1}{\big[m^2-\{ty(z+w)+uyz+sz(1-z-w)\}\big]^2} \\ &+\frac{1}{\big[m^2-\{uy(z+w)+syz+tz(1-z-w)\}\big]^2}\Bigg]. \end{aligned} \tag{4.160c}$$

Above the Mandelstam variables are defined as $s=-(k_1+k_2)^2$, $t=-(k_1-k_1')^2$, $u=-(k_1-k_2')^2$ with $s+t+u=0$. Summing all the above contributions we get the four dilaton scattering amplitude

$$\mathcal{T}_{BB\to BB}(s,t,u)=\mathcal{A}_I(s,t)+\mathcal{A}_{II}(s,t)+\mathcal{A}_{III}(s,t)+O(f^{-5}) \tag{4.161}$$

Let us for simplicity work in the forward limit and focus on low energies when $s << m^2$. Up to the order $O(s^2)$ we obtain

$$\begin{aligned} \mathcal{T}_{BB\to BB}(s,0,-s) =& \frac{3m^4}{16\pi^2 f^4}\ln\Big(\frac{\Lambda}{m}\Big)+ \\ &+\frac{s^2}{32\pi^2 f^4}\int_0^1 \mathrm{d}x\,x^2(1-x)^2+ \\ &-\frac{s^2}{4\pi^2 f^4}\int_0^1 \mathrm{d}x\int_0^{1-x}\mathrm{d}y\,2x^2y^2+ \\ &+\frac{3s^2}{4\pi^2 f^4}\int_0^1 \mathrm{d}y\int_0^{1-y}\mathrm{d}z\int_0^{1-y-z}\mathrm{d}w\,\Big[\\ &\qquad (yz+yw-z+z^2+zw)^2 \\ &\qquad +(-yz+z-z^2-wz)^2+(yw)^2\Big] \\ &+O(s^3) \\ =& \frac{3m^4}{16\pi^2 f^4}\ln\Big(\frac{\Lambda}{m}\Big)+\frac{s^2}{960\pi^2 f^4}-\frac{s^2}{360\pi^2 f^4}+\frac{s^2}{480\pi^2 f^4}+O(s^3) \\ =& \frac{3m^4}{16\pi^2 f^4}\ln\Big(\frac{\Lambda}{m}\Big)+\frac{s^2}{2880\pi^2 f^4}+O(s^3). \end{aligned} \tag{4.162}$$

The amplitude away from the forward limit at the order $O(s^2)$ can be obtained from (4.162) by using crossing symmetry, then it reads

$$\mathcal{T}_{BB\to BB}(s,t,u)=\frac{3m^4}{16\pi^2 f^4}\ln\Big(\frac{\Lambda}{m}\Big)+\frac{1}{5760\pi^2 f^4}\times(s^2+t^2+u^2)+O(s^3). \tag{4.163}$$

It is obvious that (4.163) reduces to (4.162) in the forward limit. The equation (4.163) is precisely (4.44) quoted in the main text once we set $\Lambda=m$ to make the cosmological constant equals to zero.

Indirect computation The imaginary part of the $BB \to BB$ scattering amplitude at one loop is related to the tree level scattering amplitude $BB \to AA$ via the optical theorem which can be written as

$$\begin{aligned}\mathrm{Im}\mathcal{T}_{BB\to BB}(s,0,-s) = \frac{1}{2}\left[\frac{1}{2}\int \frac{\mathrm{d}^3\vec{p}_1}{(2\pi)^3 2E_{\vec{p}_1}}\frac{\mathrm{d}^3\vec{p}_2}{(2\pi)^3 2E_{\vec{p}_2}}\right](2\pi)^4\times \\ \times\,\delta^{(4)}(k_1+k_2-p_1-p_2)\times\left|\mathcal{T}_{BB\to AA}(s,t,u)\right|^2. \quad (4.164)\end{aligned}$$

The terms within the square bracket is the two identical particle phase space integral. To derive the above relation we considered only two massive particle exchange in the unitarity cut, which is the leading order contribution in large f. Above we can use crossing symmetry to write $\mathcal{T}_{BB\to AA}(s,t,u) = \mathcal{T}_{AA\to BB}(s,t,u)$. The tree level Feynman diagrams describing the $AA \to BB$ scattering process are depicted in figure 4.24. This leads to the following explicit

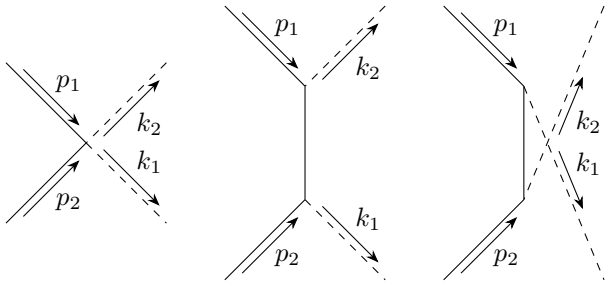

Figure 4.24: Tree level Feynman diagrams describing the $AA \to BB$ scattering amplitude.

expression for the amplitude

$$i\mathcal{T}_{AA\to BB}(s,t,u) = -\frac{im^2}{f^2}\left[1 + \frac{2m^2}{t-m^2} + \frac{2m^2}{u-m^2}\right], \quad (4.165)$$

where $s=-(p_1+p_2)^2$, $t=-(p_1-k_1)^2$, $u=-(p_1-k_2)^2$ with $s+t+u=2m^2$. We recall that in the center of mass frame the t and u variables can be expressed in terms of total energy squared s and the scattering angle θ according to the second entry in (2.34). We write this relation here again for convenience

$$\begin{aligned}t &= m^2 - \frac{s}{2} + \frac{1}{2}\sqrt{s(s-4m^2)}\cos\theta, \\ u &= m^2 - \frac{s}{2} - \frac{1}{2}\sqrt{s(s-4m^2)}\cos\theta.\end{aligned} \quad (4.166)$$

Plugging (4.165) into (4.164) we obtain

$$\begin{aligned}
&\mathrm{Im}\mathcal{T}_{BB\to BB}(s,0,-s)\\
&=\frac{1}{64\pi}\,\frac{\sqrt{s-4m^2}}{\sqrt{s}}\,\frac{m^4}{f^4}\int_{-1}^{1}\mathrm{d}(\cos\theta)\,\left[1+\frac{2m^2}{t-m^2}+\frac{2m^2}{u-m^2}\right]^2\\
&=\frac{1}{64\pi}\frac{\sqrt{s-4m^2}}{\sqrt{s}}\,\frac{m^4}{f^4}\int_{-1}^{1}\mathrm{d}x\left[1-\frac{8s\,m^2}{s^2-s(s-4m^2)x^2}\right]^2\\
&=\frac{1}{64\pi}\frac{\sqrt{s-4m^2}}{\sqrt{s}}\,\frac{m^4}{f^4}\Bigg[2+\frac{16m^2}{s}+\\
&\quad-\frac{16m^2(s-2m^2)}{s\sqrt{s(s-4m^2)}}\ln\left(\frac{s+\sqrt{s(s-4m^2)}}{s-\sqrt{s(s-4m^2)}}\right)\Bigg].
\end{aligned}\tag{4.167}$$

At low energy the $BB\to BB$ amplitude will have the form (4.36). We remind that for the QFT under consideration $a^{\mathrm{IR}}=0$. The a^{UV} is given by the sum rule (4.37) which is completely determined by the imaginary part (4.167). Plugging (4.167) into (4.37) we conclude that

$$\begin{aligned}
a^{\mathrm{UV}}&=\frac{m^4}{64\pi^2}\int_{4m^2}^{\infty}\frac{ds}{s^3}\,\frac{\sqrt{s-4m^2}}{\sqrt{s}}\Bigg[2+\frac{16m^2}{s}+\\
&\qquad-\frac{16m^2(s-2m^2)}{s\sqrt{s(s-4m^2)}}\ln\left(\frac{s+\sqrt{s(s-4m^2)}}{s-\sqrt{s(s-4m^2)}}\right)\Bigg]\\
&=\frac{m^4}{64\pi^2}\Big[\frac{1}{30m^4}+\frac{4}{105m^4}-\frac{19}{315m^4}\Big]\\
&=\frac{1}{(64\times 90)\pi^2}\;=\;\frac{1}{5760\pi^2}.
\end{aligned}\tag{4.168}$$

This together with (4.36) is in a perfect agreement with (4.163).

One can obtain the imaginary part of the $BB\to BB$ amplitude away from the forward limit away using (4.161). It reads

$$\begin{aligned}
\mathrm{Im}[\widetilde{\mathcal{T}}_{BB\to BB}(s,t)]=\;&\frac{1}{32\pi}\sqrt{1-\frac{4}{s}}-\frac{1}{4\pi s}\ln\left(\frac{1+\sqrt{1-\frac{4}{s}}}{1-\sqrt{1-\frac{4}{s}}}\right)\\
&-\frac{1}{4\pi}\,\frac{1}{su}\frac{1}{\sqrt{1+\frac{4t}{su}}}\ln\left(\frac{\frac{1}{s}-\frac{u}{st}+\frac{u}{2t}\left[1+\sqrt{1-\frac{4}{s}}\sqrt{1+\frac{4t}{us}}\right]}{\frac{1}{s}-\frac{u}{st}+\frac{u}{2t}\left[1-\sqrt{1-\frac{4}{s}}\sqrt{1+\frac{4t}{us}}\right]}\right)\\
&-\frac{1}{4\pi}\,\frac{1}{st}\frac{1}{\sqrt{1+\frac{4u}{st}}}\ln\left(\frac{\frac{1}{s}-\frac{t}{su}+\frac{t}{2u}\left[1+\sqrt{1-\frac{4}{s}}\sqrt{1+\frac{4u}{ts}}\right]}{\frac{1}{s}-\frac{t}{su}+\frac{t}{2u}\left[1-\sqrt{1-\frac{4}{s}}\sqrt{1+\frac{4u}{ts}}\right]}\right).
\end{aligned}\tag{4.169}$$

We can check that this expression in the forward limit $t=0$ reproduces (4.167).

Partial amplitudes and unitarity Using the definitions (2.99) and the explicit expressions (4.165) and (4.169) in free theory we obtain the following spin

0 and 2 partial amplitudes

$$\widetilde{\mathcal{T}}^{0}_{AA\to BB}(s) = -\frac{1}{32\pi}\Big(1-4/s\Big)^{1/4}\left[2-\frac{8}{s\sqrt{1-4/s}}\ln\left(\frac{1+\sqrt{1-4/s}}{1-\sqrt{1-4/s}}\right)\right], \tag{4.170}$$

$$\widetilde{\mathcal{T}}^{2}_{AA\to BB}(s) = -\frac{1}{4\pi}\Big(1-4/s\Big)^{1/4}\left[\frac{3}{s-4}-\frac{1+2/s}{s\Big(1-4/s\Big)^{3/2}}\ln\left(\frac{1+\sqrt{1-4/s}}{1-\sqrt{1-4/s}}\right)\right] \tag{4.171}$$

$$\begin{aligned}\mathrm{Im}\Big[\widetilde{\mathcal{T}}^{0}_{BB\to BB}(s)\Big] &= \frac{1}{2(16\pi)^2}\sqrt{1-4/s} \;-\; \frac{1}{64\pi^2 s}\ln\left(\frac{1+\sqrt{1-4/s}}{1-\sqrt{1-4/s}}\right)\\ &\quad+\frac{1}{32\pi^2 s^2}\frac{1}{\sqrt{1-4/s}}\left[\ln\left(\frac{1+\sqrt{1-4/s}}{1-\sqrt{1-4/s}}\right)\right]^2,\end{aligned} \tag{4.172}$$

$$\begin{aligned}\mathrm{Im}\Big[\widetilde{\mathcal{T}}^{2}_{BB\to BB}(s)\Big] &= \frac{9}{32\pi^2}\,\frac{1}{s^2\Big(1-4/s\Big)^{3/2}}-\frac{3}{16\pi^2}\frac{s+2}{s^3\Big(1-4/s\Big)^{2}}\ln\left(\frac{1+\sqrt{1-4/s}}{1-\sqrt{1-4/s}}\right)\\ &\quad+\frac{1}{32\pi^2}\frac{(s+2)^2}{s^4\Big(1-4/s\Big)^{5/2}}\left[\ln\left(\frac{1+\sqrt{1-4/s}}{1-\sqrt{1-4/s}}\right)\right]^2.\end{aligned} \tag{4.173}$$

For the free scalar theory the unitarity condition (4.91) simplifies to the following expression

$$\begin{matrix}\forall \ell = 0,2,4,\dots\\ \forall s\in[4m^2,\infty)\end{matrix}: \qquad \begin{pmatrix} 1 & \widetilde{\mathcal{T}}^{*\ell}_{AA\to BB}(s)\\ \widetilde{\mathcal{T}}^{\ell}_{AA\to BB}(s) & 2\mathrm{Im}\widetilde{\mathcal{T}}^{\ell}_{BB\to BB}(s)\end{pmatrix}\succeq 0. \tag{4.174}$$

One explicitly check that the expressions obtained for spin 0 and 2 partial amplitude saturate this matrix inequality as expected.

4.C Derivation of poles

Let us consider the scattering amplitude $AB\to AB$ defined in previous sections. Unitarity allows to determine part of this amplitude non-perturbatively. This is explained for example in section 2.5.1 in [42]. One can argue that the amplitude $AB\to AB$ has a pole in the s-channel due to the presence of one-particle states A, namely

$$\mathcal{T}_{AB\to AB}(s,t,u) = -\frac{|g|^2}{s-m^2}+\dots, \tag{4.175}$$

where the residue g is given as the limit

$$g \equiv \lim_{s\to m^2} g(s). \tag{4.176}$$

The function $g(s)$ is defined as the following matrix element

$$g(s)\times(2\pi^4)\delta^4(p-p_1-p_2) = \big\langle p^0,\vec{p}\big|T\big|m_A,\vec{p}_1;m_B,\vec{p}_2\big\rangle, \tag{4.177}$$

where T is the interacting part of the scattering operator and the total energy squared s reads as

$$s \equiv -p^2 = -(p_1 + p_2)^2. \tag{4.178}$$

The ... in (4.175) denote al the finite contributions at $s = m^2$. The physical range of energies in (4.178) is $s \in [m^2, \infty)$. The masses of particles A and B are, as in the rest of given by $m_A = m$ and $m_B = 0$. Due to the presence of the $\mathbb{Z}_2$ symmetry, the bra-state in the right-hand side of (4.177) is $\mathbb{Z}_2$ odd.

From the explicit expression of the modified action (4.26) one can conclude that the interacting part of the scattering operator has the form

$$T = -\frac{i}{\sqrt{2}f} \int d^4x \, \Theta(x)\varphi(x) + O\left(f^{-2}\right), \tag{4.179}$$

where $\Theta(x)$ is the trace of the stress-tensor. Plugging this expression into (4.177) we obtain

$$g(s) \times (2\pi^4)\delta^4(p - p_1 - p_2) = -\frac{i}{\sqrt{2}f} \int d^4x \, e^{ip_2 \cdot x} \left\langle p^0, \vec{p} \middle| \Theta(x) \middle| m_A, \vec{p}_1 \right\rangle + O(f^{-2}). \tag{4.180}$$

Here we have used the contraction between the dilaton field $\varphi(x)$ and the dilaton state $|m_B, \vec{p}_2\,\rangle$. The translation symmetry allows us to write

$$\Theta(x) = e^{-iP \cdot x} \Theta(0) e^{+iP \cdot x}. \tag{4.181}$$

Here P^μ are the generators of translation. Using (4.181) and taking into account the fact that the states in (4.180) are eigenstates of P^μ, writing the integral over x as a δ-function we get the final expression for the function $g(s)$ which reads

$$g(s) = -\frac{i}{\sqrt{2}f} \left\langle p^0, \vec{p} \middle| \Theta(0) \middle| m_A, \vec{p}_1 \right\rangle + O(f^{-2}). \tag{4.182}$$

We remind that the total energy squared s was defined in (4.178), as a result we have

$$p^0 = |\vec{p}_2| + \sqrt{m_A^2 + \vec{p}_1^{\,2}}, \quad \vec{p} = \vec{p}_1 + \vec{p}_2. \tag{4.183}$$

Let us now take the limit (4.176). This limit is achieved by setting $\vec{p}_2 \to 0$. Hence we get,

$$g = -\frac{i}{\sqrt{2}f} \langle m, \vec{p}_1 | \Theta(0) | m, \vec{p}_1 \rangle + O(f^{-2}) \tag{4.184}$$

As derived in [42, 43], in particular see appendix G of [43], the following normalization condition holds

$$\lim_{\vec{p}_2 \to \vec{p}_1} \langle m, \vec{p}_1 | \Theta(0) | m, \vec{p}_2 \rangle = -2m^2. \tag{4.185}$$

Plugging it into (4.184) we conclude that

$$|g|^2 = \frac{2m^4}{f^2}. \tag{4.186}$$

In turn, plugging this into (4.175), using crossing symmetry (2.40) and the definitions (4.87) we finally obtain

$$\widetilde{\mathcal{T}}_{AB \to AB}(s, t, u) = -\frac{2m^4}{s - m^2} - \frac{2m^4}{u - m^2} + \dots \tag{4.187}$$

4.D Worldline action in dilaton background

In this appendix, the effective worldline action for a massive particle moving in a background geometry with metric $g_{\mu\nu} = e^{-2\tau(x)}\eta_{\mu\nu}$ is considered. Writing $e^{-\tau(x)} = 1 - \frac{1}{\sqrt{2}f}\varphi(x)$, we shall show that the worldline action is universal up to two derivatives and quadratic order in the dilaton field $\varphi(x)$.

The most general coordinate invariant worldline action is

$$S = -m \int dt \, [1 + c_1 \ddot{x}^\mu \ddot{x}^\nu g_{\mu\nu} + c_2 R + c_3 \dot{x}^\mu \dot{x}^\nu R_{\mu\nu} + \dots] \tag{4.188}$$

where m is the mass of the particle and c_i are non-universal Wilson coefficients. The 4-vector $\dot{x}^\mu$ is equal to $\frac{dx^\mu}{dt}$ with t the proper time defined by

$$dt^2 = -g_{\mu\nu} dx^\mu dx^\nu \, . \tag{4.189}$$

R ($R_{\mu\nu}$) stands for the Ricci scalar (tensor) of the background metric evaluated on the worldline, and the dots represent higher derivative terms. Notice that the extrinsic curvature of a worldline is simply given in terms of $\dot{x}^\mu$ and $\ddot{x}^\mu$.

For the conformally flat metric $g_{\mu\nu} = e^{-2\tau}\eta_{\mu\nu}$, the Riemann curvature tensor is

$$R_{\alpha\beta\gamma\delta} = e^{-2\tau}(\eta_{\alpha\gamma}T_{\beta\delta} + \eta_{\beta\delta}T_{\alpha\gamma} - \eta_{\alpha\delta}T_{\beta\gamma} - \eta_{\beta\gamma}T_{\alpha\delta}) \, , \tag{4.190}$$

with

$$T_{\alpha\beta} = \partial_\alpha\partial_\beta\tau + \partial_\alpha\tau\partial_\beta\tau - \frac{1}{2}(\partial\tau)^2\eta_{\alpha\beta} \, . \tag{4.191}$$

Therefore, up to quadratic order in the dilaton field, both R and $R_{\mu\nu}$ are of order $O(\partial^2\varphi, (\partial\varphi)^2)$. Clearly, higher derivative terms will contain more derivatives (and more powers of φ in some cases). Notice that $\ddot{x}^\mu = 0$ is the leading order equation of motion, thus we can neglect the second term in (4.188). We conclude that non-universal terms contribute to the scattering amplitude $\widetilde{T}_{AB\to AB}$ at order at least p^2 where p is dilaton 4-momentum. This confirms the universality of the result (4.77).

4.E Identities for Fourier transforms

In this appendix we derive a set of identities used in section 4.2.1.

Let us start with the following Fourier transform

$$\sum_{n=0}^{\infty} c_n^{\mu_1\mu_2\dots\mu_n} \, n p_{\mu_1} p_{\mu_2} \cdots p_{\mu_n} \Phi(x) \longrightarrow H_1(q) \equiv \sum_{n=0}^{\infty} (i)^n c_n^{\mu_1\cdots\mu_n} \, n \, q_{\mu_1} q_{\mu_2} \cdots q_{\mu_n} \Phi(q). \tag{4.192}$$

Recall that in section 4.2.1 we introduced the object $\mathcal{K}(q)$, it was defined in (4.57). Let us reproduce this definition here for the readers convenience

$$\mathcal{K}(q) \equiv \sum_{n=0}^{\infty} (i)^n \, c_n^{a_1 a_2 \dots a_n} q_{a_1} q_{a_2} \dots q_{a_n}. \tag{4.193}$$

Using the obvious fact that the object $\mathcal{K}(q)$ is homogeneous in q_μ we conclude that

$$H_1(q) = q^\mu \frac{\partial \mathcal{K}(q)}{\partial q^\mu} \Phi(q). \tag{4.194}$$

Let us denote arbitrary tensors of rank 1 and 3 by $\mathcal{E}$ and $\mathcal{F}$ respectively. In section 4.2.1 we had another three Fourier transforms which are

$$\sum_{n=0}^{\infty} c_n^{\mu_1\mu_2\cdots\mu_n}\ \frac{n(n+1)}{2} p_{\mu_1}p_{\mu_2}\cdots p_{\mu_n}\Phi(x) \longrightarrow$$
$$H_2(q) \equiv \sum_{n=0}^{\infty}(i)^n c_n^{\mu_1\cdots\mu_n}\ \frac{n(n+1)}{2}\ q_{\mu_1}q_{\mu_2}\cdots q_{\mu_n}\Phi(q), \quad (4.195)$$

$$\sum_{n=1}^{\infty} c_n^{\mu_1\cdots\mu_n}\sum_{i=1}^{n}\mathcal{E}_{\mu_i}\ p_{\mu_1}\cdots p_{\mu_{i-1}}p_{\mu_{i+1}}\cdots p_{\mu_n}\Phi(x) \longrightarrow$$
$$H_3(q) \equiv \sum_{n=1}^{\infty}(i)^{n-1} c_n^{\mu_1\cdots\mu_n}\sum_{i=1}^{n}\mathcal{E}_{\mu_i}\ q_{\mu_1}\cdots q_{\mu_{i-1}}q_{\mu_{i+1}}\cdots q_{\mu_n}\Phi(q), \quad (4.196)$$

$$\sum_{n=2}^{\infty} c_n^{\mu_1\cdots\mu_n}\sum_{\substack{i,j=1\\ i<j}}^{n}\mathcal{F}^{\nu}_{\mu_i\mu_j}p_{\mu_1}\cdots p_{\mu_{i-1}}p_{\mu_{i+1}}\cdots p_{\mu_{j-1}}p_{\mu_{j+1}}\cdots p_{\mu_n}p_{\nu}\Phi(x) \longrightarrow$$
$$H_4(q) \equiv \frac{1}{2}\sum_{n=2}^{\infty}(i)^{n-1} c_n^{\mu_1\cdots\mu_n}\sum_{\substack{i,j=1\\ i\neq j}}^{n}\mathcal{F}^{\nu}_{\mu_i\mu_j}q_{\mu_1}\cdots q_{\mu_{i-1}}q_{\mu_{i+1}}\cdots q_{\mu_{j-1}}q_{\mu_{j+1}}\cdots q_{\mu_n}q_{\nu}\Phi(q). \quad (4.197)$$

Analogously to (4.194) we can write

$$H_2(q) = \frac{1}{2}q^{\mu}q^{\nu}\frac{\partial^2\mathcal{K}(q)}{\partial q^{\mu}pq^{\nu}}\Phi(q) + q^{\mu}\frac{p\mathcal{K}(q)}{\partial q^{\mu}}\Phi(q), \quad (4.198)$$

$$H_3(q) = -i\ \mathcal{E}_{\mu}\frac{p\mathcal{K}(q)}{pq_{\mu}}\Phi(q), \quad (4.199)$$

$$H_4(q) = -\frac{i}{2}\mathcal{F}^{\nu}_{\mu\rho}q_{\nu}\frac{p^2\mathcal{K}(q)}{pq_{\mu}pq_{\rho}}\Phi(q). \quad (4.200)$$

Chapter 5

Future

As common with research, each question answered creates yet more questions, each tool developed provides more problems to solve, and each method developed asks for new applications and new techniques. Bootstrapping S-matrix provides a powerful technique of ruling out inconsistent theories, and its use in analyzing the space of 4d CFTs gives a promising insight. The existence of CFTs of $a < 1$ is not ruled out, and the lower bound on a has been found in investigated setup, but to answer what those CFTs are, what properties do they have and how they can be realized – this is still an open question, and one day in the future, it will be answered.

Hopefully, with new bootstrapping techniques, more useful tools developed, and just more effort put into researching the topic, we, as the scientists, will make yet another step into understanding physics.

`SMatrixToolkit`, the package developed for these computations, is (as author believes) a good step forward in helping next scientists develop their own S-matrix experiments, but its use is so far limited to scattering of scalar particles in 4d. However, the effort was put into making the code expandable. By generalizing the function for partial wave expansion one can adapt it to $d \geq 3$ number of dimensions, by expanding the crossing equations (and partial wave expansion), one can generalize the toolkit to spinning particles. Hopefully, the future for the toolkit exists.

As a being with finite lifetime in this world, it's likely I won't see if the dream of bootstrapper will come true – if we can solve physics just by making it self-consistent, limiting the vast space of possible theories to a single point corresponding to our world. However, this enormous island is shrinking with every conclusion we, the scientist, make, and even the minor ones take us closer to understanding the world.

I started this thesis with a cliché, and some overly grand statements about science, so it feels justified to end with the same. This thesis doesn't solve the physics, neither any book nor paper published in the history of the universe, but even the smallest step towards understanding science is a step in the right direction. And there is a beauty in fact that number of these steps one can take in the future seems to be limitless, even if it means the goal of understanding is very, very far.

Bibliography

[1]Aristotle, *Physics, Volume I: Books 1-4*, Loeb Classical Library (Harvard University Press, Cambridge, MA, Jan. 1, 1957), 528 pp.

[2]Aristotle, *Physics, Volume II: Books 5-8*, Loeb Classical Library (Harvard University Press, Cambridge, MA, Jan. 1, 1934), 464 pp.

[3]I. Newton, *Philosophiæ Naturalis Principia Mathematica* (Jussu Societatis Regiæ ac Typis Joseph Streater, Londini, 1687).

[4]T. Howard, *The Elder Scrolls V: Skyrim*, [PC DVD-ROM], Bethesda Game Studios, 2011.

[5]A. L. Guerrieri, J. Penedones, and P. Vieira, "Bootstrapping QCD Using Pion Scattering Amplitudes", Phys. Rev. Lett. **122**, 241604 (2019).

[6]J. Albert and L. Rastelli, "Bootstrapping Pions at Large N", JHEP **08**, 151 (2022).

[7]J. Albert and L. Rastelli, "Bootstrapping Pions at Large N. Part II: Background Gauge Fields and the Chiral Anomaly", arXiv:2307.01246 [hep-th], 10.48550/arXiv.2307.01246 (2023).

[8]K. Häring, A. Hebbar, D. Karateev, M. Meineri, and J. Penedones, "Bounds on photon scattering", arXiv:2211.05795 [hep-th], 10.48550/arXiv.2211.05795 (2022).

[9]D. Karateev, J. Marucha, J. Penedones, and B. Sahoo, "Bootstrapping the a-anomaly in $4d$ QFTs", JHEP **12**, 136 (2022).

[10]J. K. Marucha, *Bootstrapping the a-anomaly in 4d QFTs: Episode II*, arXiv.org, (July 5, 2023) https://arxiv.org/abs/2307.02305v2 (visited on 10/09/2023).

[11]D. Karateev, Z. Komargodski, J. Penedones, and B. Sahoo, "Probing the c-anomaly in 4d QFTs",

[12]A. Guerrieri, H. Murali, J. Penedones, and P. Vieira, *Where is M-theory in the space of scattering amplitudes?*, arXiv.org, (Nov. 30, 2022) https://arxiv.org/abs/2212.00151v1 (visited on 10/09/2023).

[13]R. J. Eden, P. V. Landshoff, and D. I. Olive, *The Analytic S-Matrix* (Cambridge, Apr. 17, 2002).

[14]D. Simmons-Duffin, "A semidefinite program solver for the conformal bootstrap", JHEP **06**, 174 (2015).

[15]M. F. Paulos, J. Penedones, J. Toledo, B. C. van Rees, and P. Vieira, "The S-matrix bootstrap III: higher dimensional amplitudes", JHEP **12**, 040 (2019).

[16]M. Correia, A. Sever, and A. Zhiboedov, "An Analytical Toolkit for the S-matrix Bootstrap", JHEP **03**, 013 (2021).

[17]G. Sommer, "Present State of Rigorous Analytic Properties of Scattering Amplitudes", Fortsch. Phys. **18**, 577–688 (1970).

[18]H. Lehmann, "Analytic properties of scattering amplitudes as functions of momentum transfer", Nuovo Cim. **10**, 579–589 (1958).

[19]J. Bros, H. Epstein, and V. Glaser, "A proof of the crossing property for two-particle amplitudes in general quantum field theory", Commun. Math. Phys. **1**, 240–264 (1965).

[20]M. Srednicki, *Quantum Field Theory* (Cambridge Univ. Press, Cambridge, 2007).

[21]D. Simmons-Duffin, *SDPB Manual*, GitHub, `https://github.com/davidsd/sdpb/blob/master/docs/SDPB-Manual.pdf` (visited on 10/03/2023).

[22]S. Reymond, "S-matrix Bootstrap Explorations in 4D" ().

[23]J. Penedones, "The Non-perturbative S-matrix Bootstrap" (CERN), Aug. 11, 2023.

[24]Z. Komargodski and A. Schwimmer, "On Renormalization Group Flows in Four Dimensions", JHEP **12**, 099 (2011).

[25]H. Osborn and A. Petkou, "Implications of Conformal Invariance in Field Theories for General Dimensions", Annals of Physics **231**, 311–362 (1994).

[26]J. L. Cardy, "Is there a c-theorem in four dimensions?", Phys. Lett. B **215**, 749–752 (1988).

[27]H. Osborn, "Derivation of a four dimensional c-theorem for renormaliseable quantum field theories", Phys. Lett. B **222**, 97–102 (1989).

[28]I. Jack and H. Osborn, "Analogs of the c-theorem for four-dimensional renormalisable field theories", Nucl. Phys. B **343**, 647–688 (1990).

[29]Z. Komargodski, "The Constraints of Conformal Symmetry on RG Flows", JHEP **07**, 069 (2012).

[30]M. A. Luty, J. Polchinski, and R. Rattazzi, "The a-theorem and the Asymptotics of 4D Quantum Field Theory", JHEP **01**, 152 (2013).

[31]Z. Komargodski, "Renormalization group flows and anomalies", in *Les Houches Lect. Notes*, Vol. 97, edited by L. Baulieu, K. Benakli, M. R. Douglas, B. Mansoulie, E. Rabinovici, and L. F. Cugliandolo (Oxford University Press, 2015), pp. 255–271.

[32]V. Niarchos, C. Papageorgakis, A. Pini, and E. Pomoni, "(Mis-)Matching Type-B Anomalies on the Higgs Branch", JHEP **01**, 106 (2021).

[33]A. Schwimmer and S. Theisen, "Spontaneous Breaking of Conformal Invariance and Trace Anomaly Matching", Nucl. Phys. B **847**, 590–611 (2011).

[34]A. Sen, "Subleading Soft Graviton Theorem for Loop Amplitudes", JHEP **11**, 123 (2017).

[35]S. Chakrabarti, S. P. Kashyap, B. Sahoo, A. Sen, and M. Verma, "Subleading Soft Theorem for Multiple Soft Gravitons", JHEP **12**, 150 (2017).

[36]A. Laddha and A. Sen, "Sub-subleading Soft Graviton Theorem in Generic Theories of Quantum Gravity", JHEP **10**, 065 (2017).

[37]P. Di Vecchia, R. Marotta, M. Mojaza, and J. Nohle, "New soft theorems for the gravity dilaton and the Nambu-Goldstone dilaton at subsubleading order", Phys. Rev. D **93**, 085015 (2016).

[38]P. Di Vecchia, R. Marotta, and M. Mojaza, "Double-soft behavior of the dilaton of spontaneously broken conformal invariance", JHEP **09**, 001 (2017).

[39]A. L. Guerrieri, Y.-t. Huang, Z.-Z. Li, and C. Wen, "On the exactness of soft theorems", JHEP **12**, 052 (2017).

[40]A. Homrich, J. Penedones, J. Toledo, B. C. Van Rees, and P. Vieira, "The S-matrix bootstrap IV: multiple amplitudes", JHEP **11**, 076 (2019).

[41]C. G. Callan, S. Coleman, and R. Jackiw, "A new improved energy-momentum tensor", Annals Phys. **59**, 42–73 (1970).

[42]D. Karateev, S. Kuhn, and J. Penedones, "Bootstrapping Massive Quantum Field Theories", JHEP **07**, 035 (2020).

[43]A. Hebbar, D. Karateev, and J. Penedones, "Spinning S-matrix Bootstrap in 4d", JHEP **01**, 060 (2022).